Dissertation der Fakultät für Biologie der Ludwig-Maximilians-Universität München

Transient tetraploidy as a route to chromosomal instability

vorgelegt von

Anastasia Yurievna Kuznetsova

aus Moskau, Russland

2013

Erklärung

Die vorliegende Arbeit wurde zwischen October 2008 und Mai 2013 unter Anleitung von Frau. Dr. Zuzana Storchova am Max-Planck-Institut für Biochemie in Martinsried durchgeführt.

Wesentliche Teile dieser Arbeit sind in folgenden Publikationen veröffentlicht:

Abnormal mitosis triggers p53-dependent cell cycle arrest in human tetraploid cells

Kuffer C, Kuznetsova AY, Zuzana Storchova. *Chromosoma*.

DOI 10.1007/s00412-013-0414-0

Eidestattliche Erklärung

Diese Dissertation wurde selbstständig, ohne unerlaubte Hilfe erarbeitet.

Martinsried, am 23.05.13

Anastasia Kuznetsova

Dissertation eingereicht am: 23.05.13

1. Gutachter: Herr Prof. Dr. Stefan Jentsch

2. Gutachter: Herr Prof. Dr. Peter Becker

Mündliche Prüfung am: 06.09.13

Table of Contents

Summary

Aneuploidy, defined as alterations in both chromosome number and structure, along with chromosomal instability (CIN) are common hallmarks of cancer. Growing evidence suggests that aneuploidy and CIN facilitate carcinogenesis in both mice and humans. One of the routes to CIN can be via an unstable tetraploid intermediate. However, the mechanisms contributing to the development of CIN in the post-tetraploid progeny remain elusive.

I examined the progress of human cells after tetraploidization induced by cytokinesis failure in otherwise chromosomally stable and p53-proficient human cells. The post-tetraploid progeny displayed both complex aneuploidy and CIN manifested by the increased frequency of mitotic errors, in particular lagging chromosomes and anaphase bridges. I could rule out the presence of multiple centrosomes as the sole source of CIN, as the doubled centrosome numbers reduced soon after tetraploidization. Instead, I identified downregulation of several mitotic kinesins, in particular the kinesin-8 family motor protein Kif18A. Accordingly, the post-tetraploid progeny show an altered spindle geometry, which likely allows segregation larger DNA amounts and reflects changes in microtubule dynamics. Furthermore, I found that the post-tetraploid cells divide in the presence of tensionless attachments. This suggests an altered spindle assembly checkpoint response, possibly accompanied by a defective mitotic error correction. Finally, posttetraploids arrest less frequently after defective mitosis than the progenitor diploid and tetraploid cells. The present work shows for the first time that a single tetraploidization event is sufficient to cause CIN even in p53-proficient human cells. Importantly, the results outline the possible mechanisms that can lead to CIN in the progeny of human tetraploid cells.

Introduction

1. Tetraploidy: causes and proliferation control.

A whole genome multiplication or polyploidy (for example, three fold – triploidy, four fold – tetraploidy, etc.) is currently regarded as one of the driving forces of biological diversity. Polyploidization, or paleopolyploidy, was proposed to occur in plant evolution (Masterson, 1994) and early in the vertebrate evolution (Van de Peer et al., 2009). It can provide organisms and their cells with additional genetic material for adaptation to changes in the environment (Aleza et al., 2011; Otto and Whitton, 2000), as well as robustness against lethal mutations and loss of chromosomes. To date, polyploidy has been described to frequently occur in plants and fungi (Albertin and Marullo, 2012). In animals, polyploidy occurs predominantly in lower forms, such as flatworms. However, polyploidy was also reported in some higher forms of Animalia, such as African clawed frog (*Xenopus laevis*), salamanders, salmon; at the same time, so far in only one mammalian species red vizcacha rat (*Tympanoctomys barrerae*) and related species (Gallardo et al., 1999).

Polyploidy can also occur in the tissues of otherwise diploid organisms. For example, polyploidization frequently takes place as a part of a developmental and differentiation program in human organisms. Prominent examples are human heart muscle cells and megakaryocytes, where a single polyploid cell can give rise to many thrombocytes. A programmed cytokinesis failure results in polyploidization in liver hepatocytes (Guidotti et al., 2003). A large body of evidence suggests that polyploidy occurs through endoreplication (i.e. duplication of the genome without subsequent cell division) as a stress response mechanism (Lee et al., 2009a).

In contrast to programmed polyploidization, a duplication of the genome can occur aberrantly. Unscheduled polypoidy is, however, poorly tolerated by mammalian organisms. In humans, polyploidy is lethal at early embryonic stages and comprises around 20% of miscarriages due to chromosomal abnormalities (Storchova and Kuffer, 2008), although a few cases of tetraploid live births in humans were reported (Nakamura et al., 2003; Stefanova et al., 2010).

Three major routes to aberrant polyploidization, well documented for tetraploidy, are described up to date, namely, cytokinesis failure, cell-cell fusion and mitotic slippage (Figure 1).

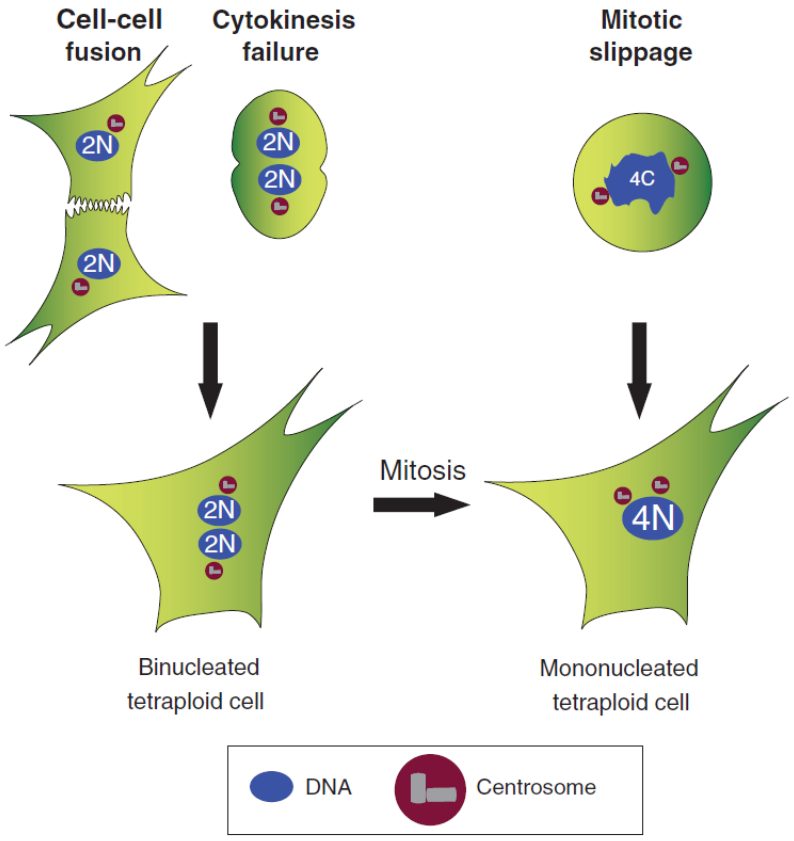

Figure 1. Three main routes to aberrant tetraploidy (from Storchova and Kuffer, 2008)

Cytokinesis failure occurs when the final step in the cell division fails to execute properly. This can happen due to perturbations of the spindle elongation or spindle positioning (Normand and King, 2010), mutations in the APC (Adenomatous Polyposis Coli) tumor suppressor (Caldwell et al., 2007), or telomere dysfunction (Pampalona et al., 2012). Another pervasive reason of the cytokinesis failure is lagging chromosomes in anaphase that are trapped in a cleavage furrow, thus inhibiting furrow progression (Shi and King, 2005). The resulting binucleated tetraploid cell contains not only a doubled complement of chromosomes, but also doubled number of centrosomes. Similar binucleated cells can be formed after cell-cell fusion, often as a consequence of virus infections, such as SV40, SARS coronavirus, Hepatitis B and C, and other viruses (Duelli and Lazebnik, 2007; Ornitz et al., 1987; Storchova and Kuffer, 2008). The slippage from mitosis, caused by premature exit from mitosis and G1-phase entry despite uncorrected mitotic errors,

can also lead to tetraploidization (Rieder and Maiato, 2004; Storchova and Kuffer, 2008). In contrast to the first two mechanisms, mitotic slippage results in a mononucleated tetraploid cell. Thus, tetraploidization can occur due to various mechanisms, such as different types of abortive cell division as well as virus-induced cell-cell fusion.

Since aberrant tetraploidization is poorly tolerated by human organism, it suggests the existence of mechanisms restricting further proliferation of spontaneously formed tetraploids (Ganem and Pellman, 2007). Initially, tetraploidy was proposed to trigger a so-called “tetraploidy checkpoint”, blocking subsequent mitotic entry after cytokinesis failure in a p53-dependent manner in mammalian cells (Andreassen et al., 2001; Margolis et al., 2003). However, follow-up studies using lower, less toxic concentrations of dihydrocytochalasin B (DCB) to induce tetraploidization, proved that DNA replication and mitotic entry takes place in tetraploid RPE1-hTERT (retinal pigment epithelium cell line) and HDF (human diploid fibroblasts) (Uetake and Sluder, 2004; Wong and Stearns, 2005).

The p53 pathway plays an essential role in the proliferation inhibition of tetraploid cells after mitotic slippage (Rieder and Maiato, 2004). In addition, p53-proficient DCB-treated and sorted newly formed tetraploid murine cells did not proliferate in culture, whereas p53-deficient cells did (Fujiwara et al., 2005). Similarly, absence of p53 in the tetraploids was shown to promote subtetraploid aneuploidy (Vitale et al., 2010). The fact that tetraploid cells, formed through different mechanisms, arrest in a p53-dependent manner raised a question of the nature of *upstream* triggers of this arrest.

Several cellular stresses were proposed to cause p53 activation and cell cycle arrest in tetraploids. For example, DNA damage might serve as an *upstream* activator of p53 pathway. In this scenario, lagging chromosomes, frequently produced in mitosis in tetraploids, can be damaged during cytokinesis by cleavage furrow-generated forces (Janssen et al., 2011) or can be exposed to conflicting forces generated by microtubules, emanating from multiple poles and form DNA double-strand breaks (DSBs) (Guerrero et al., 2010). Alternatively, defective mitosis in the presence of multiple centrosomes can change the cytoskeleton, organization of mitotic spindle and centrosome integrity. Presence of multiple centrosomes is often associated with centrosomal stress. The stress was shown to trigger p53 activation mediated by

p38/MAP stress kinase pathway; the role of p38/MAP pathway in proliferation restriction of tetraploids was shown in at least two independent studies (Mikule et al., 2007; Vitale et al., 2008). Defective spindle assembly checkpoint (SAC) can lead to chromosome missegregation and further cause p53-dependent cell cycle arrest and/or death, as reported for defects in some of key SAC proteins Bub1 (Budding uninhibited by benzimidazoles 1), BubR1 (Budding uninhibited by benzimidazoles-related 1) and TTK/hMps1 kinase (Huang et al., 2009b; Jeganathan et al., 2007; Shin et al., 2003). It is also possible that chromosome missegregation after multipolar mitosis that leads to imbalanced gene copy number and protein abundance, in turn might cause proteotoxic stress. The proteotoxic stress was shown in budding yeast with few additional copies of chromosomes; however, these changes were not associated with cell cycle arrest (Oromendia et al., 2012). Since the protein imbalance after chromosome missegregation in multipolar mitosis is substantially higher than described in aneuploid yeast, this imbalance can potentially impair cell proliferation.

Complex mitotic spindle organization of tetraploids, i.e. the increased amount of chromosomes and centrosomes, impedes the identification of the arrest triggers. Moreover, multiple factors functioning either together or independently might cause cell cycle arrest. Therefore, the pathways restricting the proliferation of tetraploids, as well as the consequences of the escape from the restriction control remain enigmatic.

2. Tetraploid state as an intermediate to aneuploidy, chromosomal instability and tumorigenesis.

The fact that living organisms developed a robust arrest response to erroneous tetraploidy suggests that proliferation after tetraploidization can have deleterious consequences. In recent years, big attention has been drawn to a role of tetraploidy as a potential route to aneuploidy – numerical and structural chromosomal abnormalities. Aneuploidy, in turn, shows a strong correlation with tumorigenesis, however, the causal relationship is unclear (Gordon et al., 2012; Lengauer et al., 1998; Matzke et al., 2003; Ricke et al., 2008). The evidence that many tumors display near-triploid or near-tetraploid (complex hyperdiploid) aneuploidy suggests, that the potential route to the aneuploidy observed in tumors can be a tetraploid

intermediate formation followed by chromosome missegregation (Nigg, 2002; Shackney et al., 1989; Storchova and Pellman, 2004) (Figure 2).

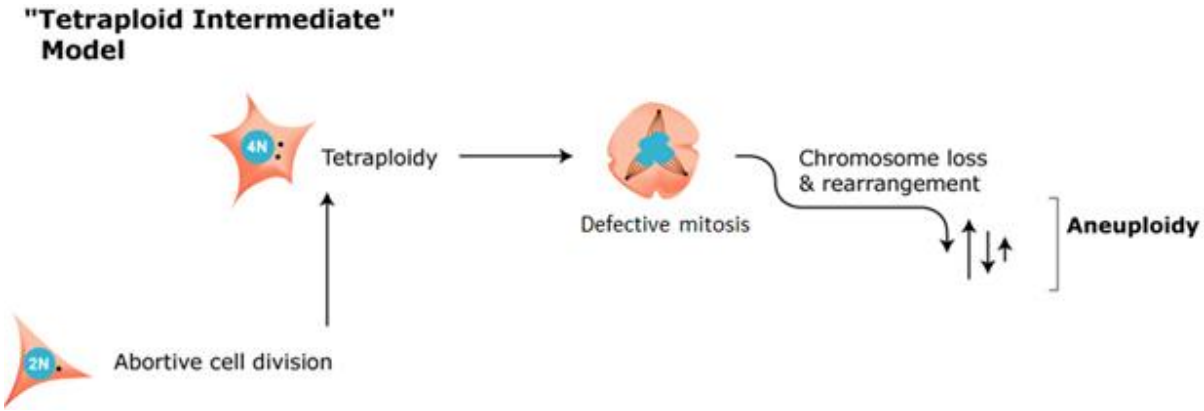

Figure 2. Tetraploid state as an intermediate to complex numerical aneuploidy.

The hypothesis is further supported by an important characteristic of aneuploid tumors – a frequent presence of multiple centrosomes that can originate after cytokinesis failures during tetraploidization. Multiple centrosomes were proposed to be a major source of chromosome missegregation and tumorigenesis by Theodor Boveri at the beginning of the last century (Boveri, 2008). Subsequent studies showed a strong correlation between amplification of centrosome numbers and tumorigenesis in majority of cancers (Nigg, 2002). Moreover, tetraploid cells were identified in early stages of cervical cancer (Kirkland et al., 1967; Olaharski et al., 2006). In addition, tetraploid cells in the Barrett's oesophagus were shown to give rise to aneuploids upon p53 inactivation (Galipeau et al., 1996). A mutation in APC gene frequently found in colorectal tumors leads to cytokinesis failure followed by aneuploidy *in vivo* (Caldwell et al., 2007). Other described cases providing the evidence for tetraploidization in tumors are bladder- (Shackney et al., 1995), breast- (Dutrillaux et al., 1991; Shackney and Silverman, 2003) and prostate cancers (Deitch et al., 1993; Montgomery et al., 1990), and hyperplastic lesions in the pancreatic cancers (Tanaka et al., 1984). Thus, tetraploidy can frequently occur in different tumors, in particular during early stages of tumorigenesis. According to the tetraploid intermediate model, tetraploidization leading to aneuploidy might eventually facilitate tumorigenesis (Storchova and Pellman, 2004).

Can aneuploid state stemming from tetraploidy *per se* cause tumor formation? Mounting evidence suggests that not every type of aneuploidy can be associated

with cell transformation; *de novo* aneuploidy is more likely to trigger tumorigenesis. Trisomic and tetrasomic aneuploids, generated by chromosome transfer, display rather an antiproliferative response, manifesting in a slower growth rate and a slow growth-related changes in gene expression (Lengauer et al., 1997; Pfau and Amon, 2012; Sheltzer et al., 2012; Stingele et al., 2012; Williams et al., 2008). Furthermore, chromosome gains, occuring during chronic inflammatory processes, such as osteoarthritis and Dupuytren's contracture, do not lead to malignancies (Gisselsson, 2011). Down syndrome (trisomy of chromosome 21) patients, on one hand display increased risk of leukaemia, but on the other hand a remarkably lower frequency of solid tumors in comparison to the general population (Satge et al., 1998).

Overall, the trisomic and tetrasomic aneuploids frequently (but not necessarily) maintain stable karyotypes, in a stark contrast to karyotypically divergent near-tetraploid cells observed in most aneuploid cancers. These complex aneuploidies are likely linked to tumor formation, hence supporting a role of tetraploidization prior to aneuploidy in cell transformation.

Complex aneuploidy is usually a steady-state manifestation of CIN – dynamic changes in the number of the chromosomes during propagation. CIN is the hallmark of the majority of solid tumors (Haruki et al., 2001; Lengauer et al., 1997; Yoon et al., 2002). Clinical studies show that CIN in cancer is associated with resistance to drug treatment and poor prognosis (Carter et al., 2006; Duesberg et al., 2000; Walther et al., 2008). This can be explained by inherent ability of CIN cells to easily adapt to changes in their growth environment (Bakhoum and Compton, 2012). Interestingly, the frequency of CIN in non-diploid (near-triploid and near-tetraploid) tumors is substantially higher than in near-diploid tumors (Storchova and Kuffer, 2008). A possible explanation is that increased ploidy can provide reserves in chromosome copy number and decrease a probability of lethal nullisomies (loss of both chromosome copies) after chromosome missegregation in CIN cells. Taken together, tetraploidization is associated with CIN and tumorigenesis. However, it remains unclear what are the mechanisms causing CIN and development of cancer in tetraploid cells.

The role of polyploidization in triggering CIN was shown in budding yeast *Saccharomyces cerevisiae* (Mayer and Aguilera, 1990; Storchova et al., 2006) as well as in mammalian cells (Ho et al., 2010; Vitale et al., 2010). In particular, the first

direct evidence of the role of unstable tetraploid intermediates in CIN and tumorigenesis was demonstrated upon injection of tetraploid p53-deficient murine mammary epithelial cells (MMEC) into nude mice (Fujiwara et al., 2005). Remarkably, only tetraploid cell injections led to tumors, in contrast to control diploid cell injections. The resulting tumors displayed near-tetraploid aneuploidy with chromosome gains and losses as well as structural chromosome rearrangements, suggesting ongoing CIN (Figure 3).

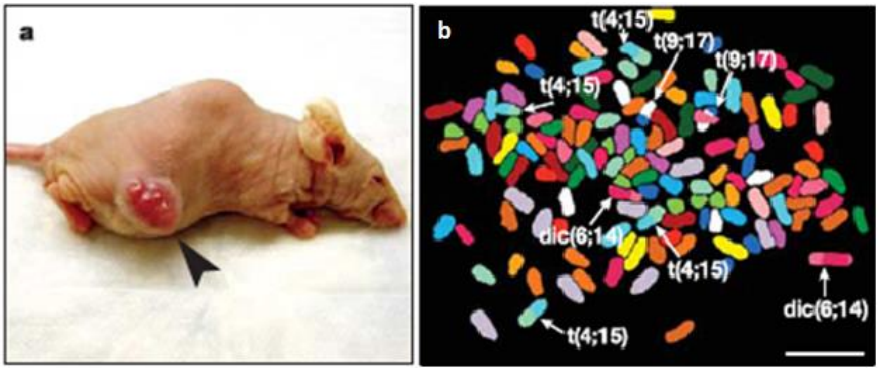

Figure 3. Tetraploidy facilitates tumorigenesis and CIN (adapted from Fujiwara et al., 2005).
(a) Tumor indicated by an arrowhead in a nude mouse at the site of injection of tetraploid p53-deficient MMECs; (b) Representative spectral karyotyping data from one tumor, showing near-tetraploid chromosome number in a cell, non-reciprocal translocations (t) and dicentric chromosomes (dic) indicated by arrowheads; scale bar 10 μm.

Later study further confirmed the role of tetraploidy in tumorigenesis in mice. Upon prolonged passaging *in vitro*, diploid mouse ovarian surface epithelial cells (MOSEC) undergo cytokinesis failure at a high frequency, form tetraploid and subsequently, aneuploid cells (Lv et al., 2012). The intraperitoneal injection of aneuploids (late passages) into C57BL/6 mice induced tumor formation on the intestinal surface, whereas injection of diploids (early passages) did not. Of note, the p53 status in the cells from resulting tumors was not investigated. Thus, possible p53 pathway deregulation could allow the proliferation in aneuploid state and tumor growth.

Another study describes the association of Notch pathway deregulation, tetraploidy and CIN in meningiomas (Baia et al., 2008). In this study, tetaploidy was induced by overexpression of HES1, the *downstream* effector of Notch signaling. The authors show that in contrast to diploid cells, tetraploids display numerical and structural abnormalities, as well as prominent features of CIN – multipolar mitoses, nuclear blebbing and nuclear bridges, and only a slight increase in spontaneous apoptosis.

Similarly to previously discussed study from Lv and colleagues, the authors did not investigate the p53 status of the meningiomas, however, they suggest defective tetraploidy checkpoint as a cause of observed CIN and proliferation after tetraploidization.

Expression of transcription factor cut homeobox 1 (CUX1) was shown to activate a program causing aneuploidy after tetraploidization (Sansregret et al., 2011). Upon induction of tetraploidy with transient cytokinesis failure by blebbistatin treatment cells, mock-expressing cells underwent predominantly multipolar mitosis and died, whereas cells overexpressing CUX1 were shown to undergo predominantly bipolar mitosis. In this scenario, the proposed mechanism of action is prolongation of mitosis, which allows more time for pair-wise clustering of centrosomes. Observed progeny displayed subtetraploid aneuploidy associated with tumorigenesis upon injection into mice. Similarly to the studies of Lv and colleagues and Baia and colleagues, p53 status of the resulting aneuploid cells was not addressed. Moreover, the observed aneuploidy could be attributed to CUX1 overexpression but not tetraploidization itself.

In summary, evidence suggests the oncogenic potential of transient tetraploidy and association with complex aneuploidy and CIN. However, little is known about the molecular mechanisms underlying the transitions from tetraploidy to CIN.

3. Molecular mechanisms triggering CIN.

The mechanisms driving chromosomal instability likely affect both the chromosome segregation fidelity as well as the ability to arrest after chromosome missegregation. Up to date, different proteins were shown to be associated with whole chromosome numerical instability. They function in spindle assembly checkpoint (SAC), formation of kinetochore-microtubule interactions, mitotic spindle organization, cytokinesis, centrosome number control, sister chromatid cohesion and cell cycle regulation.

3.1. Aneuploid state *per se* as a trigger of CIN.

Up to date, the causal relationship between aneuploidy and CIN remains poorly defined. On one hand, gene mutations can trigger CIN, subsequently resulting in gross aneuploidy as a “secondary effect”. On the other hand, aneuploidy leads to a gene and protein dosage imbalance, which can result for example in imbalance and

insufficient functions of the protein machineries involved in chromosome segregation and maintenance, thus destabilizing the genome. According to this hypothesis, aneuploidy itself can be a catalyst of persistent changes in the karyotype without a gene mutation prerequisite (Duesberg and Li, 2003). Moreover, even a slight increase in the instability of a newly formed aneuploid might be sufficient to promote stronger CIN, if the initial chromosome changes favor chromosome missegregation (Anderson et al., 2001; Matzke et al., 2003).

The possibility that aneuploidy can drive genetic instability was directly tested in single chromosome-disomic yeast *Saccharomyces cerevisiae* strains: approximately 70% (9 out of 13) disomic strains displayed increased levels of chromosome missegregation in comparison to euploid controls (Sheltzer et al., 2011). Another study showed that the extent of CIN correlates with a deviation from euploid DNA content: haploid (1N) yeast strains were more stable than strains with 1.5 to 2N ploidy (Zhu et al., 2012).

In summary, results suggest that aneuploidy itself at least in budding yeast can further promote CIN. Whether similar scenario is taking place in higher eukaryotes remains poorly investigated.

3.2. Loss of sister chromatid cohesion as a cause of CIN.

A linkage between sister chromatid pairs from the replication until the onset of anaphase is maintained by a ring-like cohesin complex, consisting of three main subunits Smc1, Smc3, Ssc1/Mcd1 and Scc3 (Michaelis et al., 1997; Tanaka et al., 2000, for review see Peters and Nishiyama, 2012). Establishment of sister chromatid cohesion is essential for tension generation on sister kinetochores and, hence, for proper chromosome biorientation in metaphase. Thus, sister chromatid cohesion is indispensable for accurate chromosome segregation. Centromere and kinetochore dysfunction, and weakened sister chromatid cohesion are common causes underlying the chromosome missegregation (Manning et al., 2010; Sonoda et al., 2001). Mutations in the components of the cohesin complex as well as other regulators of sister chromatid cohesion were proposed to be a potential cause of CIN in colorectal cancers (Barber et al., 2008). Yet, in overall, these mutations are not very frequent in cancers.

Deficiency in key components of cohesion complex Ssc1/Mcd1 causes chromosome misalignment in metaphase and subsequent chromosome missegregation (Morrison et al., 2003). Similarly, Smc1 downregulation leads to higher frequency of micronucleation and aneuploidy (Musio et al., 2003). Mutational inactivation of another member of cohesin complex STAG2/Scc3 also promotes CIN (Solomon et al., 2011). RNAi-mediated depletion, as well as haploinsufficiency of Sgo1 (one of the key regulators of cohesion establishment), causes CIN in colorectal cancers (Iwaizumi et al., 2009; Yamada et al., 2012). Moreover, mutations, downregulation and overexpression of separase, which cleaves cohesins at the onset of anaphase, was reported to trigger CIN (Shepard et al., 2007; Wirth et al., 2006; Xu et al., 2011; Zhang et al., 2008a). Interestingly, high levels of separase were identified in human breast cancer. Cells derived from these tumors displayed premature chromosome disjunction and lagging chromosomes (Zhang, Ge et al. 2008). Similarly, depletion of securin, a separase inhibitor, also instigates CIN (Jallepalli et al., 2001). Finally, a moderate but recurrent cohesion defect associated with CIN was observed in tetraploid yeast (Storchova et al., 2006).

Taken together, the levels of cohesin complex proteins and their cofactors should be tightly regulated to ensure chromosome segregation fidelity. However, since cohesin complex has been also implicated in several other cellular functions (Dorsett, 2011), the mechanistic link between cohesion defects and CIN development remains to be investigated.

3.3. Alterations in the spindle assembly checkpoint (SAC).

Another mechanism that can contribute to CIN is the defective spindle assembly checkpoint (SAC), complex protein machinery that controls proper execution of mitotic events and ensures faithful chromosome segregation. SAC arrests or delays cell division until all chromosome kinetochores are stably and properly attached to the microtubules emanating from the opposite poles of the mitotic spindle. In recent years the key components of the SAC have been characterized in great detail (for review see Musacchio and Salmon, 2007). One major SAC gene group comprises *MAD* (Mitotic Arrest-Deficient) genes, such as *MAD1*, *MAD2* and *MAD3* (*BUBR1* in humans); another one is *BUB* (Budding Uninhibited by Benzimidazole) genes, such as *BUB1* and *BUB3*. The protein products of SAC genes negatively regulate Cdc20, a cofactor of ubiquitin ligase protein complex APC/C (anaphase-promoting

complex/cyclosome). The latter mediates the polyubiquitination of its substrates, such as cyclin B and securin, subsequently destructed by the 26S proteasome. Upon protease-mediated degradation of cyclin B, major mitotic kinase CDK1 is inactivated, leading to a rapid onset of anaphase.

Therefore, by controlling Cdc20 activity, SAC monitors microtubule-kinetochore attachments and halts the onset of anaphase until all chromosome pairs are attached to respective spindle poles and are under sufficient tension (Figure 4). Microtubules emanating from spindle poles grow and stochastically capture the kinetochores, hereby, establishing kinetochore-microtubule (KT-MT) attachment. The common concept is that even a single chromosome mal-attachment (Figure 4) is sufficient to keep SAC active and to prevent anaphase onset (Rieder et al., 1995). This delay in mitosis allows chromosome passenger complex (CPC), comprising Survivin, Borealin and INCENP (INner CENtromere Protein), and Aurora B kinase to facilitate formation of a *de novo* unattached kinetochore (Vader et al., 2006). An unattached kinetochore can be then captured by microtubules from the correct spindle pole. However, merotelic attachment (i.e. when at least one of the sister chromatids is attached to microtubules from both spindle poles) cannot be detected by SAC, because microtubule occupancy of merotelic kinetochores is similar to the occupancy in correct amphitelic attachments (Cimini et al., 2001; Cimini et al., 2003). Thus, merotelically attached kinetochores are oriented back-to-back and are under sufficient tension to prevent SAC activity, leading to chromosome missegregation (Thompson and Compton, 2008).

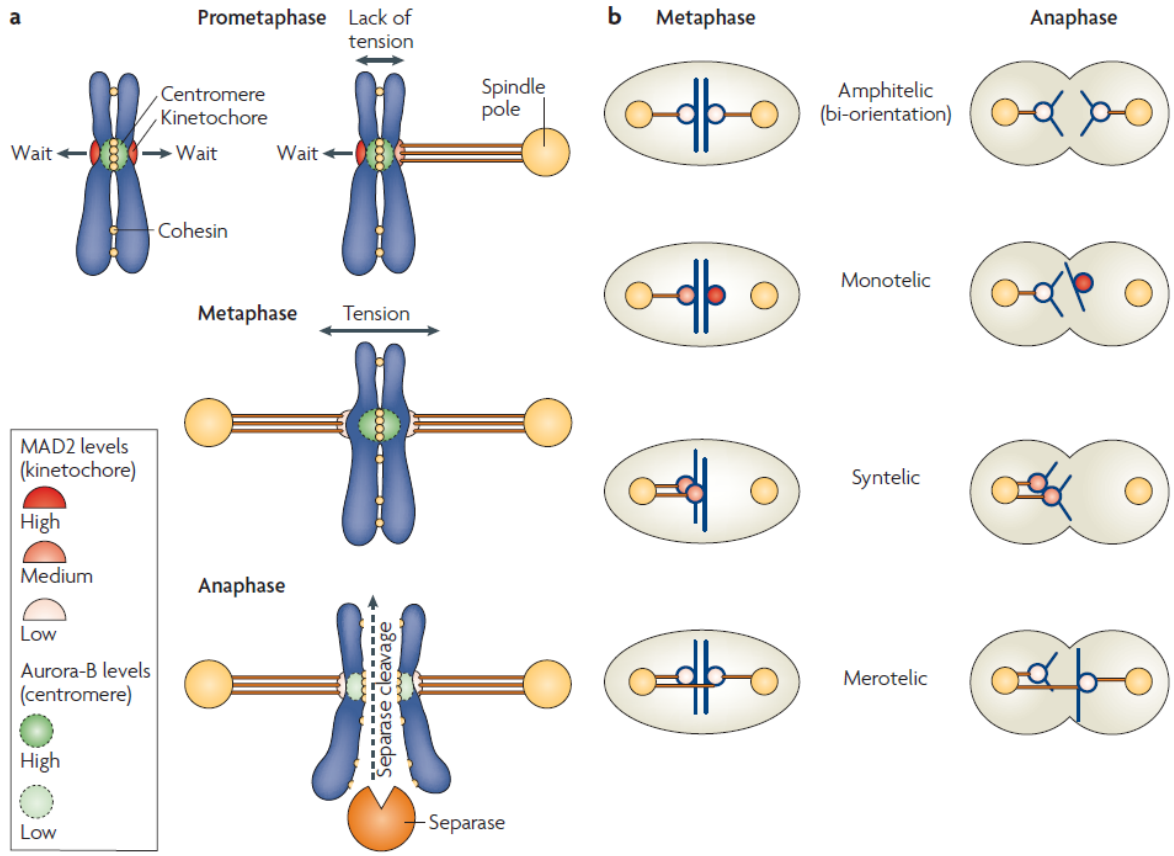

Figure 4. Chromosome attachment in mitosis and SAC activation (from Musacchio and Salmon, 2007).

(a) Mad2 levels are high at the unattached kinetochores, moderately high at a kinetochore attached in a monotelic chromatid pair, and very low upon establishment of a proper amphitelic attachment. Aurora B is activated by a lack of tension on sister kinetochores, upon tension establishment Aurora B activity at the sister kinetochores is low. When all KT-MT attachments are amphitelic, the SAC signal ceases, separase cleaves cohesins, thus promoting sister chromatid separation in anaphase. (b) Examples of proper (amphitelic) and improper (synthelic, merotelic) KT-MT attachments. Monotelic is a normal condition during prometaphase before biorientation establishment.

The defects of SAC machinery due to the mutations or gene deregulations manifest itself in mitotic errors and frequently leads to CIN and tumor formation in mice. For example, Mad2 haploinsufficiency causes a SAC defect manifested by chromosome missegregation and tumorigenesis in mice (Michel et al., 2001). Interestingly, aneuploidy is also observed upon Mad2 overexpression (Sotillo et al., 2007), as well as Mad1 overexpression (Ryan et al., 2012). Overexpression, downregulation or mutation in another SAC protein Bub1 is also associated with CIN (Cahill et al., 1998; Musio et al., 2003; Ricke et al., 2011). A biallelic mutation in BUB1B gene, encoding BubR1 protein causes mosaic variegated aneuploidy (Hanks et al., 2004).

This aneuploidy was shown to be associated with CIN and tumorigenesis (Matsuura et al., 2000). Taken together, the deregulation or partial inactivation of SAC components attenuates SAC and triggers CIN. Notably, complete inactivation of the SAC is lethal in different cell lines and homozygous deletion of key checkpoint components is embryonic lethal in mice (Thompson et al., 2010).

Despite the accumulating experimental evidence, the role of the attenuated SAC response in the common occurrence of CIN and cancer is largely debated in the field. CIN cancer cell lines show rather a robust SAC response to spindle poisons (Tighe et al., 2001); moreover, CIN cell lines halt anaphase onset in the presence of misaligned chromosomes (Gascoigne and Taylor, 2008). Furthermore, CIN cells frequently die during prolonged mitotic block (Brito and Rieder, 2009) and cannot survive without functional SAC (Kops et al., 2004). Lastly, analysis of 132 colorectal cancer cell lines showed no mutations in SAC genes (Barber et al., 2008). These findings support the view that SAC functions normally in the majority of cancer CIN cell lines.

3.4. Multiple centrosomes and multipolar division.

Aberrant chromosome and centrosome numbers frequently coincide in cancer cells (Hardy and Zacharias, 2005). For a long time multiple centrosomes were considered to be the major source of CIN in a wide range of human cancers from solid tumors to hematological malignancies (Boveri, 2008; Chan, 2011; Lingle et al., 2002; Nigg, 2002; Salisbury et al., 1999). Several different mechanisms were described to cause centrosome amplification (Doxsey, 2001; Ko et al., 2005; Mussman et al., 2000). Four main models of centrosome amplification were proposed: centrosome overduplication, abortive cell division, cell fusion and *de novo* centriole formation (Nigg, 2002).

Independently of the origin, centrosome amplification very frequently manifests in chromosome missegregation. Multiple centrosomes cause multipolar spindle formation in prometaphase. This state is often followed by direct progression to anaphase and chromosome division in a multipolar manner causing highly imbalanced aneuploidy. The work of David Gisselsson and colleagues provided direct evidence for genetic variability and near-random chromosome segregation in cells undergoing multipolar division (Gisselsson et al., 2008). Daughter nuclei formed

during multipolar division frequently displayed sister chromatid nondisjunction and nullisomies. A follow-up study on the Wilms tumor explained the reason for high frequency of trisomies in cancer cells (Gisselsson et al., 2010). Cells can progress through anaphase in a tripolar manner (the most frequent type of multipolar anaphase), when each of the daughter nuclei gets nearly a third of parental DNA material. This step is often followed by an asymmetric cytokinesis, resulting in two daughter cells, thus generating a trisomy and monosomy in diploid cells. However, in tetraploid cells the chromosome distribution in tripolar mitosis increases the probability of random segregation. Importantly, multipolar divisions are poorly tolerated and the viability of the progeny after multipolar mitoses is low (Ganem et al., 2009). This suggests that multipolar divisions might not be the sole source of CIN in cells with multiple centrosomes.

Interestingly, many cancer cells develop an adaptation to suppress multipolar cell divisions – clustering of centrosomes. Clustering leads to the reduction of spindle pole numbers, in particular, it leads to bipolar spindle formation (Brinkley, 2001; Kwon et al., 2008; Murphy, 2003; Quintyne et al., 2005). A stable propagation and maintenance of the karyotypes in the presence of multiple clustered centrosomes was reported for *Drosophila melanogaster* S2 cells (Basto et al., 2008); however, other reports suggest that centrosome clustering is often associated with chromosome missegregation. Cells that form a multipolar intermediate in metaphase often display lagging chromosomes in a bipolar anaphase (Ganem et al., 2009; Silkworth et al., 2009). The proposed mechanism for formation of lagging chromosomes in anaphase is an accumulation of unresolved merotelic kinetochore-microtubule attachments due to the extra centrosome coalescence at the anaphase onset (Figure 5). This mechanism is consistent with the presence of multiple centrosomes and proliferation in CIN state, and has been proposed as a possible cause of CIN in cells with multiple centrosomes.

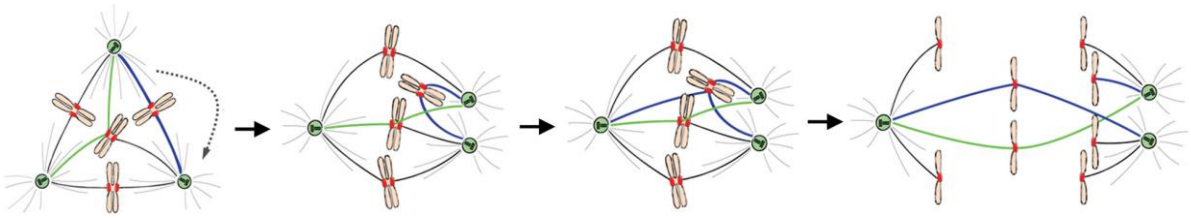

Figure 5. Multipolar intermediate formation leads to merotely (from Ganem et al., 2009).

Merotelic attachments are formed in a multipolar (here, tripolar) intermediate. They can remain unresolved before extra centrosome clustering. Clustering of extra centrosomes promotes additional merotelic attachment. If remaining incorrected, merotelically attached chromosomes lag in anaphase and cause chromosome missegregation.

Bipolar division strongly reduces the chances of both lethal nullisomies and newly arising complex aneuploidies, thus supporting the proliferation in contrast to multipolar division. Clearly, a bipolar spindle is more robust and less missegregation-prone in the cells with normal centrosome numbers than in the cells with multiple clustered centrosomes. This view is supported by a recent work from our laboratory, where we show that similar frequency of cell cycle arrest was observed after chromosome missegregation in tetraploids in bipolar anaphase, as well as in multipolar metaphase followed by bipolar anaphase and by multipolar anaphase alone. Our data suggest that the formation of a multipolar intermediate followed by bipolar division can trigger cell cycle arrest to similar levels as multipolar division (Kuffer et al., 2013).

Therefore, it is reasonable to speculate that cells that reduced their centrosome numbers early after centrosome amplification get a selective growth advantage. This view is further supported by the fact that rounds of repeated cytokinesis failure did not lead to centrosome amplification in various cell lines (Krzywicka-Racka and Sluder, 2011). Likely, centrosome amplification is just a transient condition leading to aneuploidy, but cannot be a sole source of CIN due to deleterious consequences of multipolar mitosis on the chromosome copy number and associated protein imbalance.

In summary, centrosome amplification causing an increase in merotelic attachment formation represents one of the common mechanisms of CIN. However, the fact that increased centrosome numbers are not maintained for a long period after formation argues against the role of extra centrosomes as the exclusive triggers of CIN.

3.5. Alteration in mitotic spindle function.

3.5.1. Defects in kinetochore organization and function.

Kinetochore-microtubule (KT-MT) attachments are highly dynamic in metaphase, and form stochastically by a “search-and-capture” mechanism (Mimori-Kiyosue and Tsukita, 2003). That means that the plus-ends of microtubules (hereafter MTs)

undergo persistent association and dissociation with the kinetochores, therefore constantly attempting to establish proper attachments and allowing possible mitotic error correction (Nicklas and Ward, 1994).

Kinetochore consists from inner kinetochore, associated with centromeric DNA, and more dynamic outer kinetochore, which is formed around the time of the nuclear envelope breakdown (reviewed in Maiato et al., 2004). The innermost part of the kinetochore is composed of histone variant CENPA and other CENP proteins (reviewed in Musacchio and Salmon, 2007). The outermost part of kinetochore is responsible for interaction with the MTs of the spindle; this layer consists of outer kinetochore or KNL1 complex/Mis12 complex/Ndc80 complex (KMN) and fibrous corona. The corona proteins are generally more labile than other kinetochore proteins and the protein content is dependent whether the MTs are anchored to the KT or not. Upon establishment of the KT-MT interactions, the amount of SAC proteins diminishes and the amount of such as proteins of Ran pathway, APC and other proteins involved in proper MT anchoring increases (Joseph et al., 2004; Kaplan et al., 2001; Salina et al., 2003; Shah et al., 2004; Tirnauer et al., 2002).

Alterations in the kinetochore structure cause defects in chromosome attachments, and, subsequently, mitotic abnormalities. For example, the dysfunction in Ndc80 complex manifests itself in the absence of KT-MT attachments, suggesting its essential role in establishment of stable attachments (DeLuca et al., 2002; Martin-Lluesma et al., 2002). Similarly, depletion of Mis12 complex subunits prolongs mitosis and leads to defects in chromosome alignment and biorientation (Kline et al., 2006). Inhibition of an Hsp90 using RNAi triggered delocalization of several key kinetochore proteins such as CENP-H, CENP-I, and BUB1 and caused chromosome misalignment and aneuploidy (Niikura et al., 2006). Interestingly, RNAi silencing of kinetochore-bound MT-associated proteins APC and EB1 was shown to cause misalignment of sister kinetochores, anaphase lagging and aneuploidy, without affecting the KT-MT binding *per se* (Draviam et al., 2006).

In summary, impairment of the kinetochore structure might cause defects in mitotic progression and subsequently lead to aneuploidy.

3.5.2. Alterations in the mitotic spindle machinery.

In recent years, a growing attention has been drawn to the role of mitotic spindle

dynamics in faithful chromosome segregation maintenance. This emerging interest can be readily explained by the fact, that mitotic spindle orchestrates virtually all chromosome movements in mitosis (Compton, 2000). Thus, high liability and dynamicity are prerequisites for the mitotic spindle organization. It is ensured by two important mechanisms. First, mitotic MTs display a higher turnover rate than interphase MTs and undergo continuous GTP hydrolysis-dependent lengthening and shortening, necessary for spindle formation and force generation within the spindle (Mitchison and Kirschner, 1984; Saxton et al., 1984). The dynamic instability is intrinsic to tubulin itself as was shown by *in vitro* experiments (Hyman and Karsenti, 1996). Second, mitotic MTs cross-bridge and slide relatively to adjacent MTs (Figure 6). Spatial and temporal control of MT dynamics is modulated by many microtubule-associated proteins (MAPs) and microtubule motor proteins, kinesins and dyneins, directly interacting with tubulin subunits. Growing evidence suggests that microtubule dynamics in mitosis is not driven by one single protein: instead, a balance of synergic and antagonistic forces generated by multiple motors is necessary to drive spindle movements.

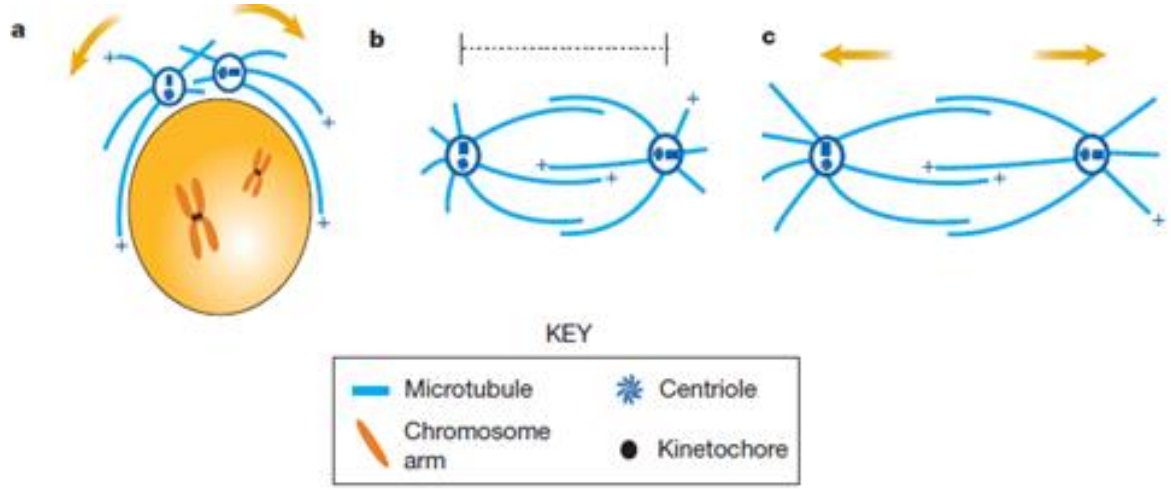

Figure 6. Spindle pole and chromosome movements during mitosis (adapted from Sharp et al., 2000).

MTs and MT motors orchestrate spindle assembly, maintenance and elongation. (a) Bipolar spindle assembly. (b) Metaphase spindle establishment. (c) Spindle elongation in anaphase B. "+" sign marks plus-ends of the MTs.

Mitotic spindle organization begins early in the prophase, when long and relatively stable interphase MTs disappear and more numerous short astral MTs begin to

nucleate from the duplicated centrosomes, extending their plus-ends outwards. The separation of centrosomes is ensured by a two-step mechanism. First, centrosomes are aligned by minus-end-directed motors, which pull on MTs and thus align them. Second, plus-end-directed MT kinesins (such as kinesin-5) push the spindle poles apart as the polar MTs elongate; minus-end-directed dynein, localized to cellular cortex, pulls on the asters towards the cortex and thus assists in centering of the MT asters (Laan et al., 2012). Subsequently, rapid fluctuation in MT length allows the MTs to capture chromosomes as the nuclear envelope (NE) breaks down. Establishment of the KT-MT interaction can occur through two possible scenarios. Either a kinetochore is captured directly by a plus-end of the MT, or more commonly, a kinetochore binds the MT's lateral side and slides along it towards the plus-end assisted by kinesin-14 proteins (Tanaka et al., 2005). Finally, lateral attachment is converted to a plus-end attachment and the bound kinetochores are pulled towards spindle poles by end-on pulling (depolymerization of the same microtubules). That helps to properly orient the chromatid pair, thus enabling capture of the sister kinetochore by MTs emanating from the opposite pole. Further, each kinetochore becomes attached to more microtubules nucleated from the nearest spindle pole. Kinetochore-bound MTs, now termed K-fibers, guide sister chromatid congression to the spindle equator. Along congression, chromosomes are oscillating towards and away from the spindle poles. This oscillatory behavior is supported by a combined pushing action of plus-end directed kinesins (for example, kinesin-8 proteins) and tubulin *de novo* polymerization at the kinetochores, as well as pulling action of kinetochore-associated minus-directed dynein and kinesin Kif10/CENP-E (Brown et al., 1996). Thus, kinetochores also actively participate in the spindle force generation in prometaphase. The opposing forces are balanced upon the alignment of the chromosomes at the spindle equator, therefore enabling metaphase plate formation.

Upon anaphase onset K-fibers shorten and the sister chromatids are pulled to the respective poles: this period is termed anaphase A. Depolymerization of the plus-ends enables pulling of the chromosomes apart and does not require ATP-dependent motor action at this stage. Additionally, kinetochores induce depolymerization of K-fibers at their plus ends, 'chewing up' microtubule tracks thus following the depolymerizing microtubule end (Pac-Man model) (Liu and Onuchic, 2006). In anaphase B, polar non-kinetochore MTs elongate and slide along each

other with the help of plus-end-directed kinesins (kinesin-5 proteins), thus pushing the spindle poles further apart. This movement is strengthened by dynein-mediated pulling forces on astral microtubules bound to cell cortex (poleward flux). Chromosome separation is followed by telophase and reconstitution of nuclear envelope. Cytokinesis, executed by combined action of actin and myosin, finalizes cell division. Astral MTs in the spindle midzone play an essential role in guiding a cleavage furrow to the former spindle equator by stimulating the cell cortex. However, the exact mechanism of cortex stimulation by MTs in cytokinesis remains unclear.

The orchestration of mitosis and cytokinesis requires finely balanced activity of motor and non-motor MT-associated proteins, however, it remains enigmatic. An in-depth understanding of this machinery can be beneficial for investigation of the chromosome segregation and CIN.

3.5.2.1. MAPs and their role in MT dynamics

Microtubule associated proteins (MAPs) are non-motor proteins that can directly bind to the MTs and regulate their assembly and stability. Destabilization of the MTs can occur not only by depolymerization from a MT end, but also through severing mechanism that generates an internal break in the MT. This reaction requires an activity of the MT severing MAP enzymes, namely fidgetin, katanin, spastin and Op18/stathmin (Cassimeris, 2002; Roll-Mecak and McNally, 2010; Roll-Mecak and Vale, 2008). In *Drosophila melanogaster*, severing proteins were described to act in a Pac-Man flux. Fidgetin and spastin contribute to MT minus-end depolymerization and flux at centrosomes, whereas katanin localizes at the centromeric region and stimulates chromosome motility by Pac-Man mechanism (Zhang et al., 2007). Inhibition of these factors causes elongation of the MTs. For example, inhibitory phosphorylation of katanin, that occurs in allotetraploid *Xenopus laevis* leads to longer spindles in comparison to the related diploid species *Xenopus tropicalis* (Loughlin et al., 2011). Additionally, the absence of spastin was described to cause non-disruption of midzone MTs that subsequently manifests in a cytokinesis failure (Connell et al., 2009). Overall, the consequences of severing enzymes deregulation and/or mutations are currently poorly described. However, given their important role in MT destabilization, it is reasonable to speculate, that loss of function of these

enzymes can result in increased stability of MTs and thus impair proper KT-MT dynamics.

Many types of up-to-date characterized stabilizing MAPs specifically function at the microtubule plus-ends and regulate their stability. In addition, many MAPs can have other functions in spindle organization. For example, MAP TPX2 plays an important role in MT nucleation and stabilization. Additionally, TPX2 recruits Aurora A, and this recruitment is important for proper chromosome alignment to the spindle (Kufer et al., 2002). TPX2 conditional knockout and haploinsufficiency have detrimental effects on MT nucleation that leads to aberrant mitotic spindle formation and chromosome segregation errors. Moreover, TPX2-haploinsufficient mice are prone to developing aneuploid adenocarcinomas and lymphomas (Aguirre-Portoles et al., 2012). Remarkably, overexpression of TPX2 was described for many tumors and strongly correlates with CIN in several human cancers (Asteriti et al., 2010; Carter et al., 2006). This suggests that tight regulation of TPX2 is essential for maintenance of the genome stability. Overexpression of another MAP XMAP215/ch-Tog is observed in liver and colon tumors (chTOG, Colonic Hepatic Tumor Overexpressed Gene) (Charrasse et al., 1995). It plays an important role in spindle pole organization and spindle MT stabilization by crosslinking K-fibers and dampening MT disassembly (Barr and Gergely, 2008; Booth et al., 2011; Gergely et al., 2003). Overall, abundant presence of MT-stabilizing proteins in tumors might cause MT over-stabilization effect. This defect in MT dynamics might potentially lead to slower disassembly of the incorrectly attached MTs at the kinetochore, thus increased rates of chromosome missegregation.

3.5.2.2. Kinesins and their role in MT dynamics

As described above, many mitotic spindle movements are energy-dependent, thus requiring motor proteins that couple ATP hydrolysis and mechanical force, such as kinesins. In mammalian cells, the kinesin superfamily comprises around 40 proteins that form 14 families (Hirokawa et al., 2009; Lawrence et al., 2004). Typically, kinesins are heterotetramers whose motor subunits (heavy chains, KHCs) dimerize and bind to two light chains (KLCs), although some variations in structure can be present across the superfamily. KHC domains share a high sequence and fold homology, consisting of globular domain with an ATP-binding core and MT-

interacting outer surface (Su et al., 2012), and a short neck domain, binding to KLCs. Processive movement of kinesins along the MT utilizes one ATP molecule per step. Most kinesins have uni-directional motility and are plus-end-directed, with the exception of minus-end-directed members of kinesin-14 family (Ambrose et al., 2005).

Kinesins have been implicated in various activities in the cell. For example, in interphase, kinesins transport cargo along the MTs, such as organelles and other structures. Mitotic kinesins (12 out of around 40 kinesins in total) function in polar ejection force generation on chromosome arms, chromosome congression, spindle pole separation and cleavage furrow positioning.

An active MT depolymerization is essential to carry out some of these functions. The best characterized to date is the kinesin-13 family of nonmotile depolymerases, consisting of three members in mammalian cells: Kif2A, Kif2B and Kif2C/MCAK (mitotic centromere-associated kinesin) (Moore and Wordeman, 2004; Wordeman, 2005). In contrast to other kinesins, kinesin-13 proteins show a different microtubule-binding pattern: only one molecule out of two binds to adjacent filaments (Mulder et al., 2009). This binding, and subsequently the depolymerization function, can be inhibited upon the detyrosination of α-tubulin, leading to MT stabilization (Peris et al., 2009). Members of kinesin-13 family have distinct and non-overlapping functions in mitosis. Kif2A localizes to the minus-ends of the centrosome MTs and is involved in the formation of a bipolar spindle (Ganem and Compton, 2004). Kif2B also localizes to centrosomes and the spindle midzone, where it plays role in establishment of bipolarity, chromosome movement, and cytokinesis (Manning et al., 2007). Furthermore, Kif2B localizes to the kinetochore, where it promotes the correction of KT-MT attachment errors specifically in prometaphase acting *downstream* of Aurora B-mediated phosphorylation of the KMN network (Bakhoum et al., 2009b).

Similarly, another kinesin-13 protein Kif2C/MCAK plays a role in the correction of incorrect attachments, but in the later stages of metaphase. Kif2C/MCAK kinetochore localization and activity is dependent on the Aurora B phosphorylation (Andrews et al., 2004). Depletion of Kif2C/MCAK manifests in slow MT turnover at the kinetochores (Wordeman et al., 2007). Moreover, RNAi depletion of either Kif2B or Kif2C/MCAK blocks the release of faulty attachments, thus preventing error

correction and promoting chromosome missegregation (Bakhoum et al., 2009b). Remarkably, overexpression of Kif2B or Kif2C/MCAK suppresses the incidence of lagging chromosomes in CIN cell lines, providing compelling evidence that stimulation of MT disassembly, at least partially, rescues CIN phenotype (Bakhoum et al., 2009b). Further support of this evidence was provided by the finding that KT-MT attachments in CIN cancer cells are inherently more stable than in normal cells (Bakhoum et al., 2009a). Additionally, Kif2C/MCAK helps focusing microtubules at aster centers and facilitates asters to bipolar spindles transition in an Aurora A kinase-dependent manner (Zhang et al., 2008b). Taken together, kinesin-13 proteins represent a family of potent MT depolymerases whose activity is essential for efficient KT-MT attachment error correction.

Another well-characterized family of plus-end directed kinesins essential for mitotic progression, is kinesin-8 family: Kif18A, Kif18B and Kif19 in mammals, as well as *S. cerevisiae* homolog Kip3 and *S. pombe* Klp5 and Klp6 (Lawrence et al., 2004). In contrast to kinesins-13, kinesin-8 proteins, such as Kif18A and yeast Kip3, are highly processive motors involved in the regulation of the MT length. Importantly, they act both as stabilizers and destabilizers of the MTs, depending on the context. For example, it was shown that Kif18A could directly depolymerize MTs (Mayr et al., 2007). Other works report that Kif18A dampens the growth of MT plus-ends by slowing down both polymerization and depolymerization of the MT plus-ends (Du et al., 2010; Stumpff et al., 2011). Similarly, yeast Kip3 is described to act as a plus-end-depolymerase for growing astral MTs during spindle positioning, and a stabilizer for shrinking MTs (Gupta et al., 2006; Varga et al., 2009). The integrated effect from opposing functions of kinesins-8 is explained by a concentration-threshold model, where high velocity and processivity of kinesins-8 leads to accumulation at the plus-ends and rapid depolymerization of MTs; furthermore, lower concentration of kinesins-8 reaches shrinking MTs, thus favoring MT stabilization (Stumpff et al., 2008; Su et al., 2011). Hence, kinesin-8 members serve as essential regulators of MT length in mitosis and the effects of kinesins-8 seem to be concentration-dependent.

Reported data demonstrate the presence of excessively long MTs in the cells upon kinesin-8 depletion and mitotic spindle elongation (Du et al., 2010; Gandhi et al., 2004; Goshima et al., 2005; Mayr et al., 2007; Rischitor et al., 2004; Straight et al.,

1998; West et al., 2001). In parallel to increased spindle length, Kif18A depletion impairs chromosome congression to metaphase plate, causes loss of tension on sister kinetochores and activates Mad2-dependent SAC response (Mayr et al., 2007). Further studies revealed an unexpected role for Kif18A in chromosome oscillations in mitosis. Kif18A reduces the amplitude of kinetochore oscillations by pausing MT growth, thus slowing down poleward movement in anaphase (Stumpff et al., 2008). Hence, Kif18A, together with polar ejection forces, promotes chromosome alignment in metaphase (Stumpff et al., 2011; Stumpff et al., 2012). Observed defects in chromosome alignment upon Kif18A depletion were proposed to be mediated by kinesin Kif10/CENP-E (kinesin-7 family). Kif10/CENP-E levels are reduced upon Kif18A depletion and re-expression of Kif10/CENP-E rescues the chromosome misalignment (Huang et al., 2009a).

In contrast to mitotic spindle-associated and kinetochore-associated kinesins, a subgroup of mitotic kinesins, called chromokinesins, can bind to chromosome arms. Some chromokinesins localize to the mitotic spindle as well as to the midzone. A well-characterized kinesin-4 family consists of Kif4A and Kif4B in humans; members of this family were also identified in other organisms (Lawrence et al., 2004; Mazumdar and Misteli, 2005). A representative kinesin Kif4A was shown to be essential for the chromosome condensation and faithful chromosome segregation: RNAi silencing of Kif4A causes early hypercondensation of chromosomes, misalignment of chromosomes, abnormal spindle geometry such as multipolarity and unfocused spindles during prometaphase and metaphase. Furthermore, Kif4A together with Kif22/Kid (kinesin-10) that agonize and antagonize polar ejection force, respectively, and abovementioned Kif18A cooperate in promoting congression of bioriented chromosomes. In anaphase, Kif4A depletion leads to MT elongation and lagging chromosomes, causing aneuploidy (Mazumdar et al., 2004; Shrestha et al., 2012; Zhu et al., 2005). A complete loss of Kif4A was also reported to induce aneuploidy and tumorigenesis in mice (Mazumdar et al., 2006). At the final stages of cell division, Kif4 deficiency manifests in mislocalization of key cytokinesis kinesins and CPC proteins and, ultimately, in cytokinesis failure (Kurasawa et al., 2004).

A plethora of other kinesins was described to be associated with regulation of mitotic progression. One of the key kinesins acting in establishment of the spindle pole separation is plus-end-directed Kif11/Eg5 kinesin (Sawin et al., 1992). Chemical

inhibition of Kif11/Eg5 by monastrol leads to monopolar spindles and thus tensionless chromosome attachments (Cochran et al., 2005; Kapoor et al., 2000). Moreover, further study on Kif11/Eg5 revealed a role of spindle elongation forces in merotelic attachment correction. Partial inhibition of Kif11/Eg5 that reduces spindle length decreased anaphase lagging in primary and unstable cancer cell lines, thus suggesting that longer spindles might be more merotelic attachment-prone (Choi and McCollum, 2012). An important, although non-essential role in establishing spindle bipolarity is carried out by Kif15/Hklp2 kinesin that is complementary to Kif11/Eg5. An important, although non-essential role in establishing spindle bipolarity is carried out by Kif15/Hklp2 kinesin that is complementary to Kif11/Eg5. Presence of Kif15/Hklp2 is sufficient to prevent metaphase spindle collapse when Kif11/Eg5 is inhibited and to promote spindle elongation (Tanenbaum et al., 2009; Vanneste et al., 2009). A minus-end-directed KifC1/HSET opposes Kif11/Eg5 activity and cross-links MTs (Cai et al., 2009); moreover, KifC1/HSET is essential for centrosome clustering function in cells with multiple centrosomes. Silencing the KifC1/HSET leads to centrosome de-clustering and multipolar anaphase (Kwon et al., 2008). It also manifests in an increase in lagging chromosomes and abnormal karyotypes, suggesting its important role in the genome stability maintenance (Kim and Song, 2013). Kif22/Kid is involved in the polar ejection force generation on chromosome arms; upon inhibition of Kif22/Kid the chromosomes fail to oscillate in metaphase (Antonio et al., 2000; Levesque and Compton, 2001). Kif10/CENP-E is important for monooriented chromosome gliding along the K-fibers of already bioriented chromosomes upon alignment in metaphase (Kapoor et al., 2006). Kif23/CHO1/MKLP1 and KLP3A kinesins function in a midzone formation together with GTPases and members of CPC (Straight and Field, 2000).

In conclusion, since MTs play a critical role in cell division, they have been regarded as very attractive therapeutic target for cancer treatment for many years. MT poisons, such as taxanes (taxol and derivatives) and vinca alkaloids (vinblastine, vincristine), demonstrated high clinical efficiency in killing tumor cells. Poisons disrupt MTs (vinca alkaloids and nocodazole) or stabilize GDP-bound tubulin (taxanes). However, a large body of evidence suggests that the effects of MT poisons are strictly concentration-dependent. For example, in high concentrations, nocodazole causes mitotic arrest, followed by cyclin B degragation-dependent

mitotic slippage or death in mitosis. In contrast to that, at lower concentrations of nocodazole mitosis is prolonged, but cells eventually divide with mitotic errors and either die in a subsequent cell cycle or further proliferate and accumulate aneuploidy (Jordan et al., 1992). Similarly, whereas higher concentration of taxol is efficiently killing tumor cells, lower concentrations cause delay in mitosis that subsequently leads to formation of aneuploid cells (Ikui et al., 2005). Therefore, a better understanding of changes in MT dynamics in tumorigenesis might help to develop new strategies for cancer treatment. In this context, kinesins that cooperate with each other, dyneins and MAPs in the spindle positioning and chromosome movement represent a good target for cancer treatment. This suggestion is further supported by the fact that deregulation of many kinesins was identified in different cancers. The kinesin expression analysis may play an important role in tumor detection, cancer prognosis, and may help to establish novel strategies for cancer treatment (Huszar et al., 2009; Yu and Feng, 2010).

3.5.3. Defects in mitotic error correction.

Correction of faulty KT-MT attachments is rate-dependent on the release of the kinetochore from MTs. Once released, the unattached kinetochore triggers the SAC response that in turn provides time for the error correction. The key orchestrator of mitotic error correction is a serine-threonine kinase Aurora B. Together with Survivin, Borealin and INCENP, Aurora B localizes at the centromeric region and forms a Chromosome Passenger Complex (CPC) (Ruchaud et al., 2007). Common concept of Aurora B activity is that it phosphorylates targets localized in the outer kinetochore KMN network. The phosphorylation destabilizes faulty attachments and facilitates the incorrect attachment release (Cheeseman et al., 2002; Welburn et al., 2010). The released kinetochore can be eventually re-captured by the MTs emanating from the correct pole. Aurora B phosphorylation of the KMN network creates a gradient of MT binding activity. Once a correct KT-MT attachment is established and sister chromatids are properly bioriented, kinetochores are pulled out outside of the Aurora B activity zone. Hence, the correct KT-MT attachments escape from the zone with high Aurora B activity and get stabilized (Liu et al., 2009; Vader et al., 2006).

Overexpression of Aurora B has been identified in many tumors exhibiting CIN (Carter et al., 2006; Lin et al., 2010; Smith et al., 2005; Vischioni et al., 2006). In fact, Aurora B overexpression was shown to trigger tetraploid cell formation; the

latter in turn promoted tumorigenesis upon injection into nude mice (Nguyen et al., 2009). Another study showed that overexpression of Aurora B increases the frequency of lagging chromosomes, thus causing near-diploid aneuploidy and CIN (Ota et al., 2002). Interestingly, RNAi depletion of Aurora B and INCENP in *Drosophila melanogaster* S2 cells inhibited chromosome alignment at the metaphase plate and caused high frequency of lagging in anaphase (Adams et al., 2001). Similar chromosome alignment and segregation errors, followed by subsequent cytokinesis failures upon Aurora B depletion were also observed in chicken DT40 cells (Hegarat et al., 2011). Interestingly, a recent study showed that a SAC protein Mad2 has a SAC-independent function. CIN cells frequently overexpress Mad2 and display lagging in anaphase. Higher levels of Mad2 are responsible for Aurora B mislocalization at the centromere in a Cdc20-dependent manner, thus possibly leading to defects in mitotic error correction (Kabeche and Compton, 2012). Finally, inhibition of Aurora B in human tetraploid cells leads to massive cell death (Marxer et al., 2012). Since tetraploids have substantially higher frequency of incorrect KT-MT attachments because of increased merotely, it is likely that they have a stronger requirement of functional error correction machinery and hence for CPC.

Depletion of borealin in human cells leads to formation of bipolar spindles associated with ectopic microtubule asters and followed by chromosome missegregation (Gassmann et al., 2004). However, the role and targets of CPC in chromosome segregation as well as the exact mechanisms of CPC-mediated error correction still remain to be studied in more detail.

In summary, alterations in KT-MT error correction machinery and kinetochore defects, in particular in Aurora B kinase deregulation is frequently linked to CIN (Giet et al., 2005; Katayama et al., 1999). However, the role of Aurora B and CPC proteins in carcinogenesis remains elusive, as mutations in this machinery are rather rare in cancer.

3.6. Deregulation of the cell cycle arrest pathways.

A malfunction of cell cycle regulators (e.g. transcription factors or cyclins) can also contribute to CIN and tumorigenesis. One of the central players in the maintenance of the genome stability and tumor suppression is p53. Inactivation of p53 due to mutations is the most commonly observed alteration in human cancer (Rivlin et al.,

2011). p53 haploinsufficiency results in Li-Fraumeni syndrome associated with a very high predisposition to tumorigenesis (Varley, 2003). Moreover, p53 mutants frequently not only lose tumor suppression function but even obtain an oncogenic potential (Brosh and Rotter, 2009). However, targeted inactivation of p53 alone is not sufficient to promote CIN (Bunz et al., 2002). Instead, CIN was shown to develop upon inactivation of both the Mad2- and p53-dependent checkpoints (Burds et al., 2005). Therefore, p53 loss is not sufficient to promote CIN and requires additional changes (for example, on mitotic level) in human cells.

In turn, p53 proficiency is important for abrogating the proliferation of cells with abnormal karyotypes (Andreassen et al., 2001; Donehower et al., 1995; Ganem and Pellman, 2007; Livingstone et al., 1992), when missegregation even of a few chromosomes triggers p53 accumulation in the nucleus (Thompson and Compton, 2010). This p53 activation prevents highly missegregating tetraploid cells from further proliferation already after the first tetraploid mitosis (Kuffer et al., 2013). Thus, it becomes clear why tetraploid progeny has been analyzed mostly in p53-negative cells so far (Fujiwara et al., 2005; Lv et al., 2012; Vitale et al., 2010). Interestingly, p53-proficient tetraploid cells that escape the arrest fate maintained chromosomal stability, suggesting absence of other defects that can contribute to CIN (Ho et al., 2010).

The activity of p53 can be attenuated or completely abolished upon overexpression of its inhibitors Mdm2 and MdmX that mediate p53 export from the nucleus and monoubiquitination for proteasome degradation (Badciong and Haas, 2002; Moll and Petrenko, 2003). Overexpression of Mdm2 was reported to facilitate tumorigenesis (Wade and Wahl, 2009). Moreover, Mdm2 overexpression in mouse leads to multiple centrosomes and multipolarity in mitosis, and, subsequently, CIN exactly as p53 absence (Carroll et al., 1999). Similarly, Mdm2-overexpressing mice have a higher incidence of aberrant karyotypes and develop cancers (Wang et al., 2008b). Accordingly, Mdm2 heterozygous murine cells are chromosomally stable (Wang et al., 2006). However, lack of MdmX complemented with loss of p53, instead, manifests in CIN and even faster tumor development than due to loss of p53 alone (Matijasevic et al., 2008). Although it remains enigmatic which effects of Mdm2 and MdmX are exerted in a p53-dependent and p53-independent manner, clearly Mdm2 and MdmX level changes affect chromosome stability.

A *downstream* target of p53, p21, serves as a direct inhibitor of Cdk1 and an executor of p53-mediated arrest: activation of p21 even in absence of p53 is sufficient to suppress aneuploidy (Barboza et al., 2006). Decrease in p21 levels strongly correlates with CIN in high and low grade premalignant liver lesions as well as hepatocarcinomas (Lee et al., 2009b), suggesting potential role of p21 deregulation in the development of liver cancers.

Other tumor suppressor Rb protein, which is mutated in retinal cancer (retinoblastoma) and some other cancers, act as a regulator of E2F family of transcription factors. Deregulation of Rb pathway and abnormal activation of E2F transcription factors lead to E2F-dependent Mad2 overexpression, causing CIN in p53-deficient cells (Hernando et al., 2004; Schvartzman et al., 2011). In addition, proper function of Rb is important to limit the proliferation of tetraploid cells (Andreassen et al., 2001; Borel et al., 2002).

Deregulation of cyclins was also reported to promote CIN: for example, steady expression of cyclin E, a regulator of Cdk2 (cyclin-dependent kinase 2) leads to abnormalities in S-phase, CIN and tumorigenesis (Spruck et al., 1999; Willmarth et al., 2004). Notably, in this case the S-phase defect does not manifest in abnormally high centrosome numbers that could explain CIN. However, another study reports centrosome overamplification upon cyclin E overexpression (Nakayama et al., 2000). Continuous expression of another regulator of G1 to S transition cyclin D1 was linked to enrichment of the genes of the CIN signature (Casimiro et al., 2012; Casimiro and Pestell, 2012).

Apart from the defects triggered by defects of the above-mentioned cell cycle regulators, some other mutations and deregulations associated with aneuploidy and CIN were described. The examples include: Notch pathway in meningiomas (Baia et al., 2008), tumor suppressors BRCA1 and BRCA2 in breast cancer (Joukov et al., 2006; Miyoshi et al., 2002; Popova et al., 2012), transcription factor c-Myc (Menssen et al., 2007), GTPase Ran-binding protein RanBP1 (Tedeschi et al., 2007), FoxM1 (Laoukili et al., 2005; Teh et al., 2010), DNA damage response kinase ATM (Shen et al., 2005) and many others. For many of them the direct mechanistic link between genetic and expression changes and CIN remains unclear.

In conclusion, much insight has been gained into the mechanisms driving faithful chromosome segregation and the maintenance of the numerical chromosomal stability. First, the CIN-associated defects can arise on the mitotic level through malfunctions of the mitotic spindle, sister chromatid cohesion, KT-MT attachment error correction or the SAC, manifesting as chromosome missegregation. Second, attenuated response to chromosome missegregation can allow proliferation of abnormal karyotypes. Currently, a large body of clinical evidence suggests that CIN is the dominant cause of tumor unresponsiveness to therapy. Thus, targeted manipulation of the chromosome segregation machinery and other CIN signature genes and pathways can be used for the therapeutic purposes in cancer treatment.

Aim of This Study

Whole chromosome instability (CIN) is a common hallmark of many cancers that is associated with a poor clinical prognosis. In recent years, significant advance has been made in deciphering the mechanisms leading to persistent chromosome missegregation. A route to CIN through a tetraploid intermediate formation has been proposed previously. Mounting evidence supports the view that tetraploidy is a transient state that results in aneuploidy, CIN, and, eventually, in tumorigenesis, at least in p53-deficient cells (Fujiwara et al., 2005; Lv et al., 2012). However, the route from tetraploidy to aneuploidy and CIN remains largely elusive. Initially, multiple centrosomes were suspected to be the major cause of CIN in tetraploid cells. Yet, the fact that multiple rounds of cytokinesis failures do not establish centrosome amplification (Krzywicka-Racka and Sluder, 2011) argues against the role of multiple centrosomes as the sole source of CIN in tetraploid progeny.

The aim of my study was to determine which adaptations allow the cell proliferation after tetraploidization and what mechanisms contribute to chromosomal instability in posttetraploid progeny. Furthermore, I aimed to investigate whether single tetraploidization alone is sufficient to trigger CIN and whether it depends on p53 presence and function in posttetraploid cells. In more detail, my objective was to:

1. Generate posttetraploid progenies (PTs) after induced cytokinesis failure in stable diploid cell lines.
2. Investigate the chromosome segregation fidelity in the PTs in comparison to progenitor diploid and tetraploid (immediately after cytokinesis failure) cell lines.
3. Assess the contribution of extra centrosomes to CIN in PTs.
4. Explore further alterations that can be involved in CIN development such as:
   4.1. Changes in the microtubule dynamics and spindle geometry.
   4.2. Alterations in the spindle assembly checkpoint.
   4.3. Defects in the cell cycle arrest after chromosome missegregation.

Results

1. Isolation and characterization of posttetraploid cells.

1.1. *In vitro* evolution of cells after tetraploidization.

In order to investigate the consequences of tetraploidization, two p53-proficient near-diploid and chromosomally stable cell lines were used: HCT116 and hTERT RPE1. HCT116 is a human colorectal carcinoma cell line characterized by microsatellite instability (MIN). hTERT RPE1 (hereafter, RPE1) is a retinal pigment epithelium cell line immortalized by the expression of human telomerase. To allow chromatin visualization, both cell lines stably express histone 2B conjugated to GFP (H2B-GFP).

Cytokinesis failure induced by actin inhibitor dihydrocytochalasin (DCD) treatment, results in the formation of tetraploid binucleated cells with the frequency of binucleation reaching 70-80%. Estimated 600 cells for each cell line were plated by limiting dilution on 96-well plates (approximately 0.5 cell/well) and allowed to propagate for six weeks (Figure 7).

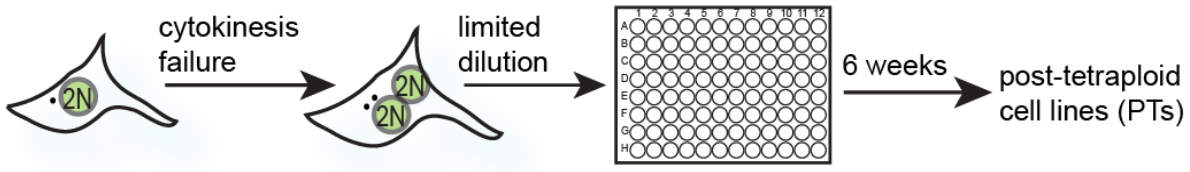

Figure 7. Generation of the PTs: a schematic depiction of the experimental strategy.

After six weeks, 72 cell populations that originated from HCT116 and 64 from RPE1 were recovered. Flow cytometric analysis confirmed a near-tetraploid DNA content in eight of the HCT116-derived cell lines and in seven of the RPE1-derived cell lines (Figure 8), further referred to as Posttetraploids (HPT – derived from HCT116, RPT – derived from RPE1). Low recovery efficiency (approximately, 1%) of the posttetraploid progeny is readily explained by the fact that the majority of tetraploid cells fail to propagate further because of p53-dependent cell cycle arrest and subsequent death (Andreassen et al., 2001; Fujiwara et al., 2005; Kuffer et al., 2013; Vitale et al., 2008; Vitale et al., 2010).

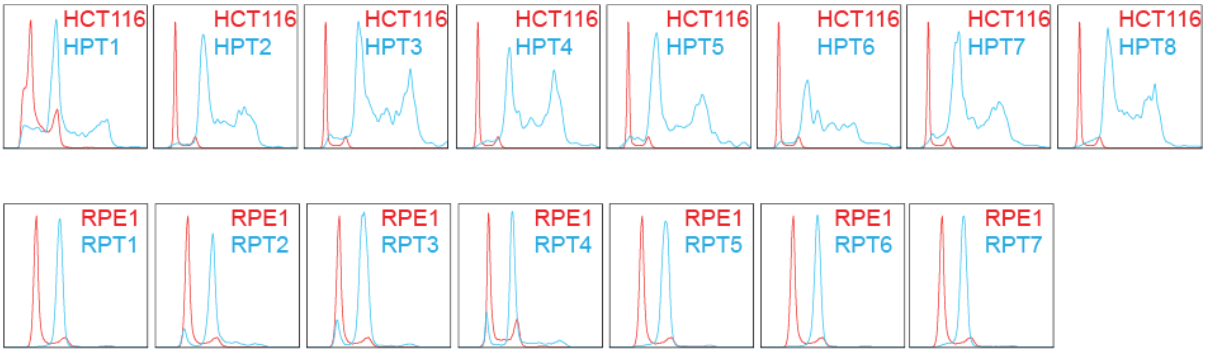

Figure 8. DNA content profile of HPTs and RPTs

DNA content profile of HPTs (top row) or RPTs (bottom row) assessed by flow cytometry after propidium-iodide staining of DNA.

This approach allowed me to obtain proliferating near-tetraploid cell populations from cells that underwent transient tetraploidization.

1.2. Cell cycle and growth characteristics of the posttetraploid cells.

To characterize the obtained posttetraploid cells the proliferation and growth analyses of the obtained posttetraploid cell lines were carried out. First, I characterized the duration of the interphase in posttetraploids. No prominent growth defects were observed, as the median interphase duration determined by live cell imaging was 18.30 h for HPT1 and 20.95 h for HPT2, similar to the parental diploid cell line (19.30 h, Figure 9A). Previous reports on the duration of mitosis, measured as the time from nuclear envelope breakdown (NEBD) to onset of anaphase (OA), suggest that mitosis is prolonged in newly formed tetraploid cells due to the presence of extra centrosomes and extra chromosomes (Yang et al., 2008). As expected, mitosis takes longer in newly generated tetraploids (median 45 min, Figure 9B). Remarkably, the time in mitosis in PT cell lines was similar to the control diploids, with median 27 min for HPT1, 24 min for HPT2 and 24 min for HCT116 (Figure 9B).

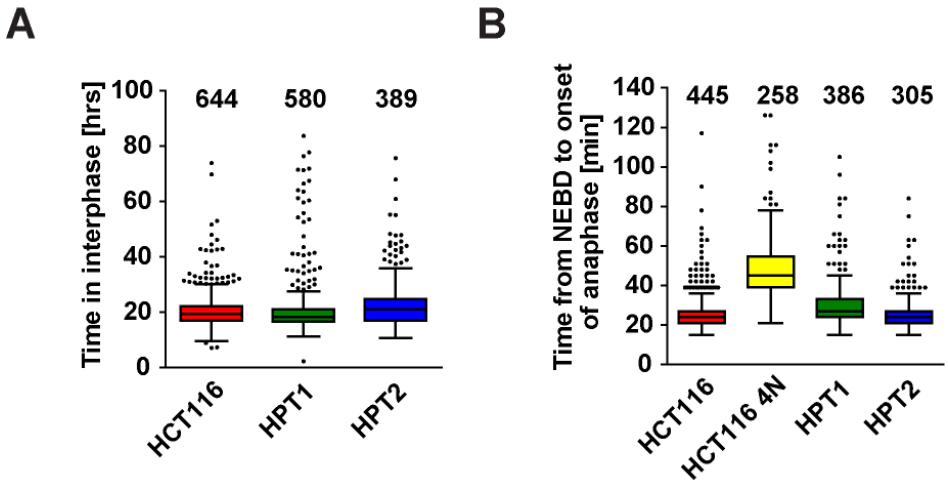

Figure 9. The length of interphase and time from NEBD to OA in HCT116 and its derivatives.
(A) Time in interphase in HCT116 and HPTs measured from the anaphase onset to the next NEBD, Tukey range and median are plotted, four experiments. (B) Time in mitosis in diploid and tetraploid HCT116 and HPTs measured from NEBD to the anaphase onset, Tukey range and median are plotted, four experiments. Numbers above the box and whiskers in both (A) and (B) plots indicate the number of cells analyzed.

Furthermore, the PTs do not accumulate non-proliferating cells, as observed by the number of the cells entering at least two mitoses during 96 h of live cell imaging (Figure 10A). Moreover, the PTs do not accumulate dead cells as indicated by no increase in the percentage of cells with permeabilized membranes (Figure 10B).

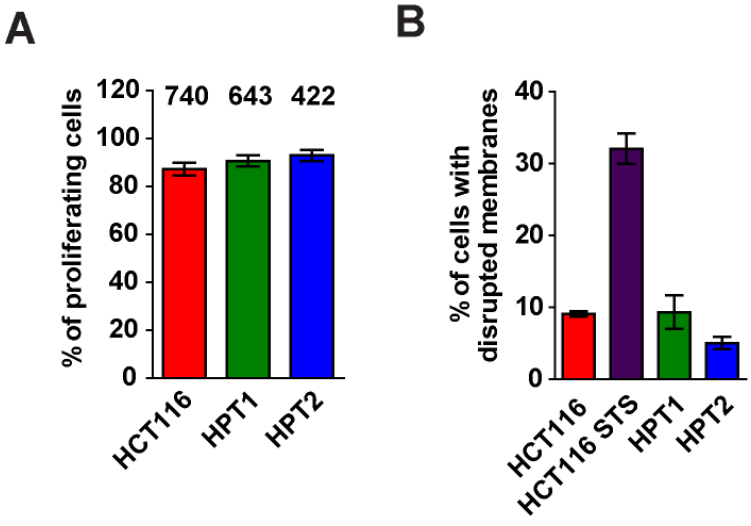

Figure 10. Numbers of non-proliferating and dead cells in culture.
(A) Percentage of proliferating cells evaluated as the number of cells undergoing at least two mitoses during timelapse image acquisition, mean and SD of four experiments. (B) Percentage of propidium iodide-positive cells in HCT116 and HPTs. Treatment with protein kinase inhibitor staurosporine (STS) was used as a positive control for cell death, mean and SEM of two experiments.

Taken together, posttetraploid cells do not display prominent changes in the interphase and mitosis duration (nuclear envelope to onset of anaphase); nor they arrest and die more frequently than progenitor diploid cells.

2. Aneuploidy and chromosomal instability of the posttetraploid cells.

2.1. Chromosome numbers in the posttetraploid cells.

Mounting evidence suggests that the progeny of tetraploid cells displays karyotypic variability (Fujiwara et al., 2005). To investigate the ploidy status of posttetraploids, I implemented standard karyotyping assay. As expected, comparing chromosome numbers between HCT116 (HCT116 H2B-GFP cell line used to generate HPTs) and a different independent subclone of HCT116 (HCT116 C4) did not reveal any substantial differences: median numbers were 44 and 45, respectively. Chromosome numbers strongly varied among both HCT116- and RPE1-derived posttetraploids, with a prevalence of chromosome loss (Figure 11A, B). Median numbers ranged between near-triploid and near-tetraploid (64.0 to 78.0) for HPTs and from diploid to near-tetraploid (46.0 to 80.0) for RPTs. HPT5 and HPT7 had median numbers reaching triploidy, and median chromosome numbers in RPT4 was diploid. Moreover, the RPT4 cells formed two karyotypic populations: near-triploid and near-diploid.

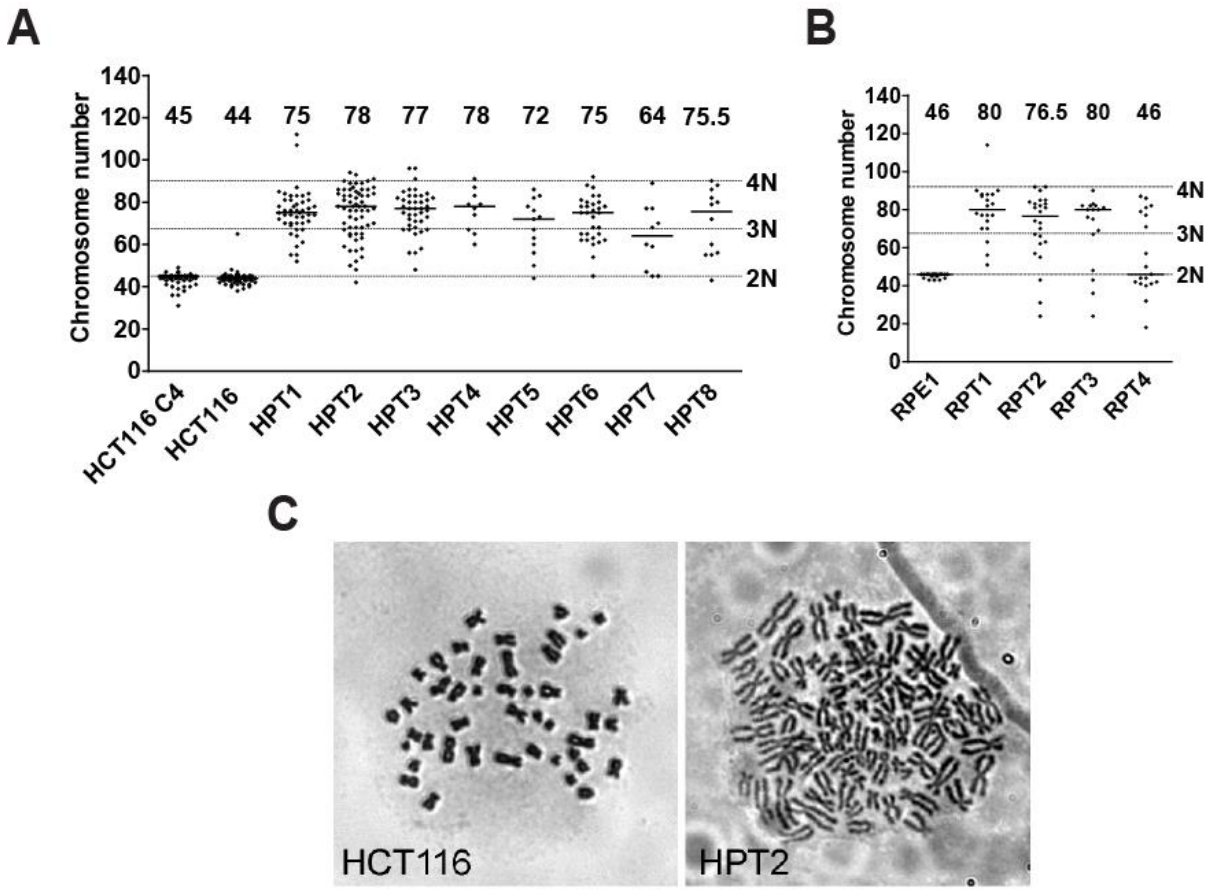

Figure 11. Chromosome numbers in HCT116, RPE1 and their posttetraploid derivatives.
Distribution of chromosome numbers and median values counted from metaphase spreads of (A) HCT116- and (B) RPE1-derived cell lines. Dashed lines mark diploid (2N), triploid (3N) and tetraploid (4N) values. The numbers above the scatter bars indicate the medians. (C) Representative metaphase chromosome spreads obtained from HCT116 and HPT2.

Thus, posttetraploid cells display a numerical aneuploidy with variable karyotype compositions that are compatible with survival.

2.2. Chromosomal instability in the posttetraploid cells.

Next, I aimed to understand whether observed aneuploidy is associated with ongoing CIN. The propagation of HPT1 and HPT2 cell lines for additional 12 passages showed that median numbers of chromosomes decreased from 75.0 to 67.5 for HPT1, and from 78.0 to 63.0 for HPT2; moreover, variability within the population remained high (Figure 12).

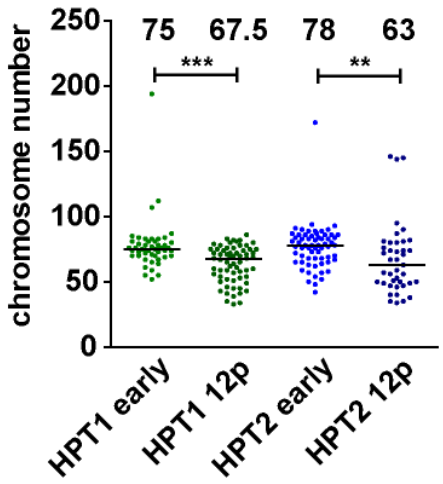

Figure 12. Chromosome number upon propagation for 12 additional passages in posttetraploid cells.

Distribution of chromosome numbers in early passages and 12 passages later (12p), median values of two independent experiments, differences are statistically significant (Mann-Whitney test, $p<0.05$). The numbers above the scatter bars indicate the medians.

This finding was further confirmed by fluorescence *in situ* hybridization (FISH) on four different chromosomes on interphase cells. FISH analysis proved that while the chromosome copy numbers remained nearly identical in early and late (after 36 passages) HCT116 cells, the chromosome copy numbers dramatically differed in HPT1 and HPT2 (Figure 13). Notably, I observed a very frequent loss of one copy of chromosome 7 in the majority of HPT1 by both FISH analysis and array-comparative genomic hybridization (aCGH) (Supplementary Figure 1).

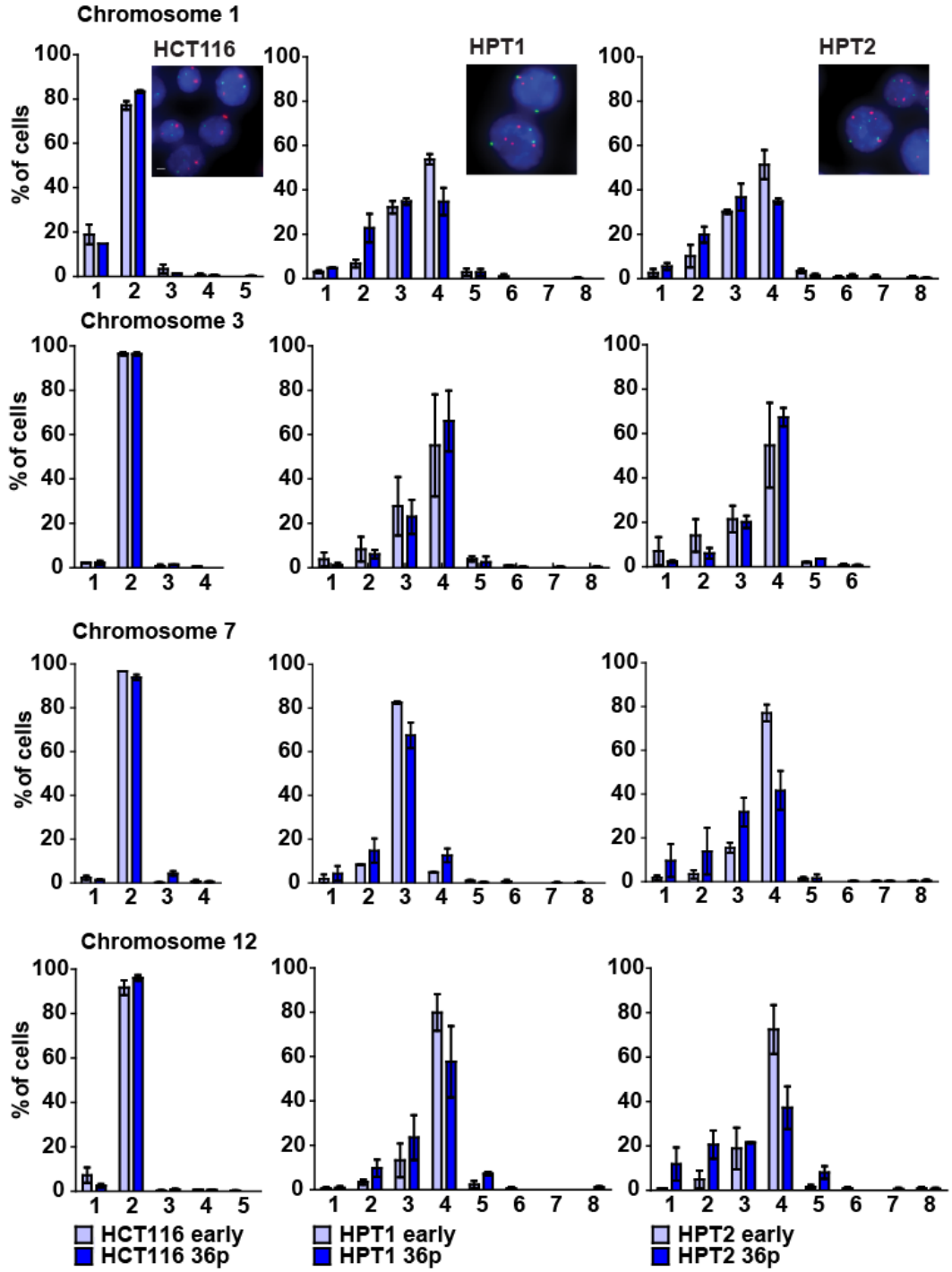

Figure 13. Chromosome numbers upon propagation in posttetraploid cells.

Comparison of chromosome number distribution of chromosomes 1, 3, 7, and 12 in early passages and 36 passages later. Mean and SEM of two independent FISH experiments. Numbers on x-axis indicate chromosome copy numbers. Insets: representative staining of chromosomes 1 (red) and 7 (green), DNA stained with DAPI, bar 10 μm.

Previously reported findings on unstable malignant tumors show that abnormal nuclear shapes may serve as markers of ongoing CIN (Gisselsson et al., 2001). This feature was also shared in posttetraploids: the cells displayed remarkable changes in the nuclear shape such as prominent nuclear blebbing and micronucleation (Figure 14, Figure 20).

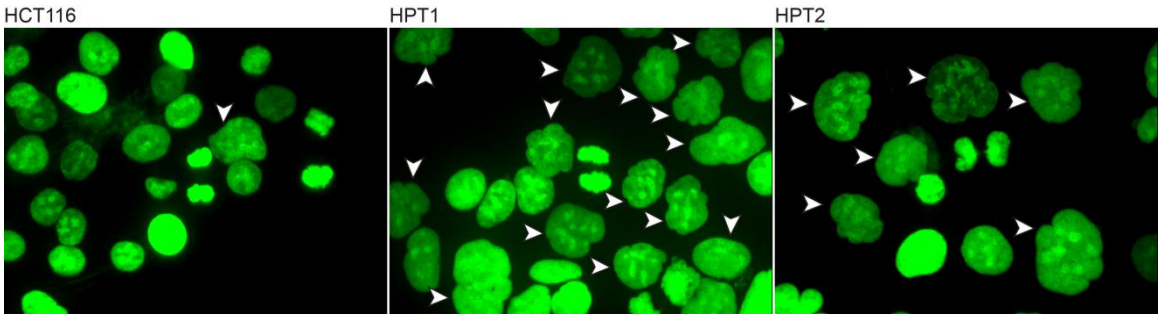

Figure 14. Nuclear blebbing in PTs.

DNA is stained with Sytox Green. Nuclei with blebbing are marked with white arrowheads.

Reported data also suggests an increase in structural chromosome aberrations in the cells with CIN cells with abnormal nuclear morphology (Gisselsson et al., 2001). Thus, I analyzed the frequency of structural chromosome alterations (specifically, chromosome translocations) in PT cells using multicolor FISH (Figure 15A). HPT1 and HPT2 display slight, but statistically insignificant increase in aberration ratio assessed as a frequency of all possible translocations per cell (Figure 15B). This ratio is calculated as number of chromosomes with translocations normalized to a total number of chromosomes identified in a given cell (chromosome spread). All identified aberrations were separated in two groups: constitutive and sporadic. Constitutive translocations comprised t(8;16), t(17;18) and t(10;16). First two translocations were previously identified in HCT116 using CGH and whole chromosome paint approaches (Masramon et al., 2000). Thus, HCT116 2N, analyzed in my work, obtained an additional constitutive chromosome translocation t(10;16). In addition to constitutive translocations, I observed also sporadic translocations. Sporadic translocations occur in some cells of HPT1 and HPT2 cell lines, with the frequency not exceeding one sporadic translocation per cell. The overall frequency of sporadic translocations is higher in HPTs in comparison with HCT116 2N cell lines (73% and 43% of all possible types of translocations in HPT1 and HPT2, respectively) in comparison to HCT116 2N (25%) (Table 1).

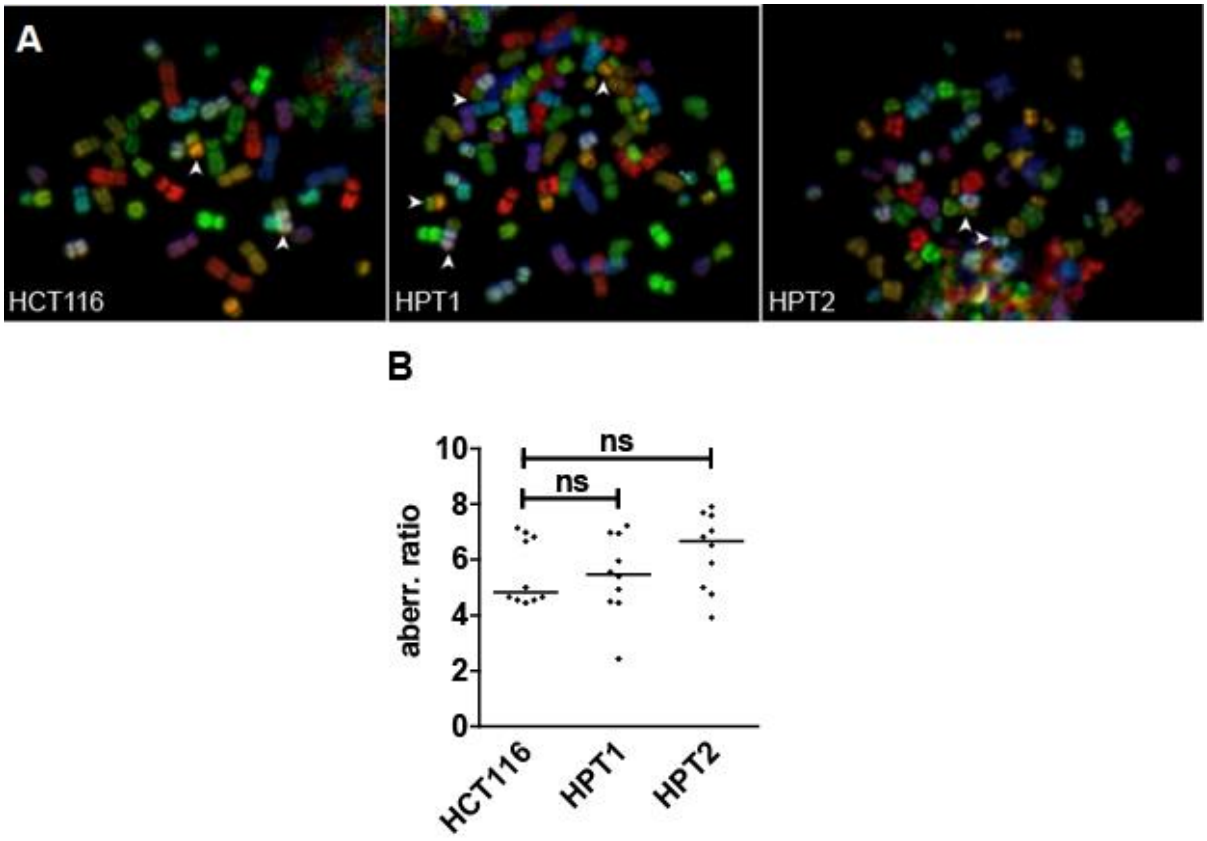

Figure 15. Total frequency of chromosomal translocations in HCT116 and its posttetraploid derivatives.

(A) Representative mFISH spreads images. Arrowheads indicate chromosome translocations. (B) Quantification of the chromosomal structural alteration frequency in HCT116 and its posttetraploid derivatives. Median is plotted; 10 cells were analyzed for each cell line; statistical significance was tested by Mood's median test.

cell line	translocation	cell ID										type of translocation
		1	2	3	4	5	6	7	8	9	10	
HCT116	t(17;18)	1	1	1		1	1	1	1		1	c
	t(6;17)	1										s
	t(10;16)		1	1	1	1		1	1	1	1	c
	t(8;16)		1	1	1	1	1	1	1	1		c
HPT1	t(1;13)	1										s
	t(17;18)	2	2	2	2	1	1	2	2	2	4	c
	t(6;16)										1	s
	t(19;22)	1										s
	t(5;15)		1									s
	t(2;13)			1								s
	t(10;18)							1				s
	t(13;18)			1								s
	t(10;16)				1		2	2			1	c
	t(8;16)	1	1		1	1	1	1	2	2		c
	t(14;21)				1							s
HPT2	t(8;16)	2	1	1		1	1	2	4	1	3	c
	t(10;16)	2		1	1	1	1	2	4	2	2	c
	t(17;18)	2	1	1	1		1	2	2	3	1	c
	t(14;17)				1							s
	t(3;16)					1						s
	t(5;8)							1				s
	t(10;19)								1			s

Table 1. Frequency of translocations for individual chromosomes in HCT116 and its posttetraploid derivatives.

Types of translocations: c – constitutive, s – sporadic. Constitutive translocation was defined when more than 50% of the cells contained at least one translocation of this type.

Finally, I assessed the numbers of all individual chromosomes, i.e. analyzed all chromosomes and all possible translocations, in HCT116 and its posttetraploid derivatives. As expected, in contrast to HCT116, maintaining nearly stable karyotype, HPTs displayed an increased rate of CIN and hypotetraploid aneuploidy (Figure 16A, B, C). Remarkably, smaller chromosomes are more frequently lost in the HPT1 than the large ones, consistent with previous observations in cancer cells (Duijf et al., 2012).

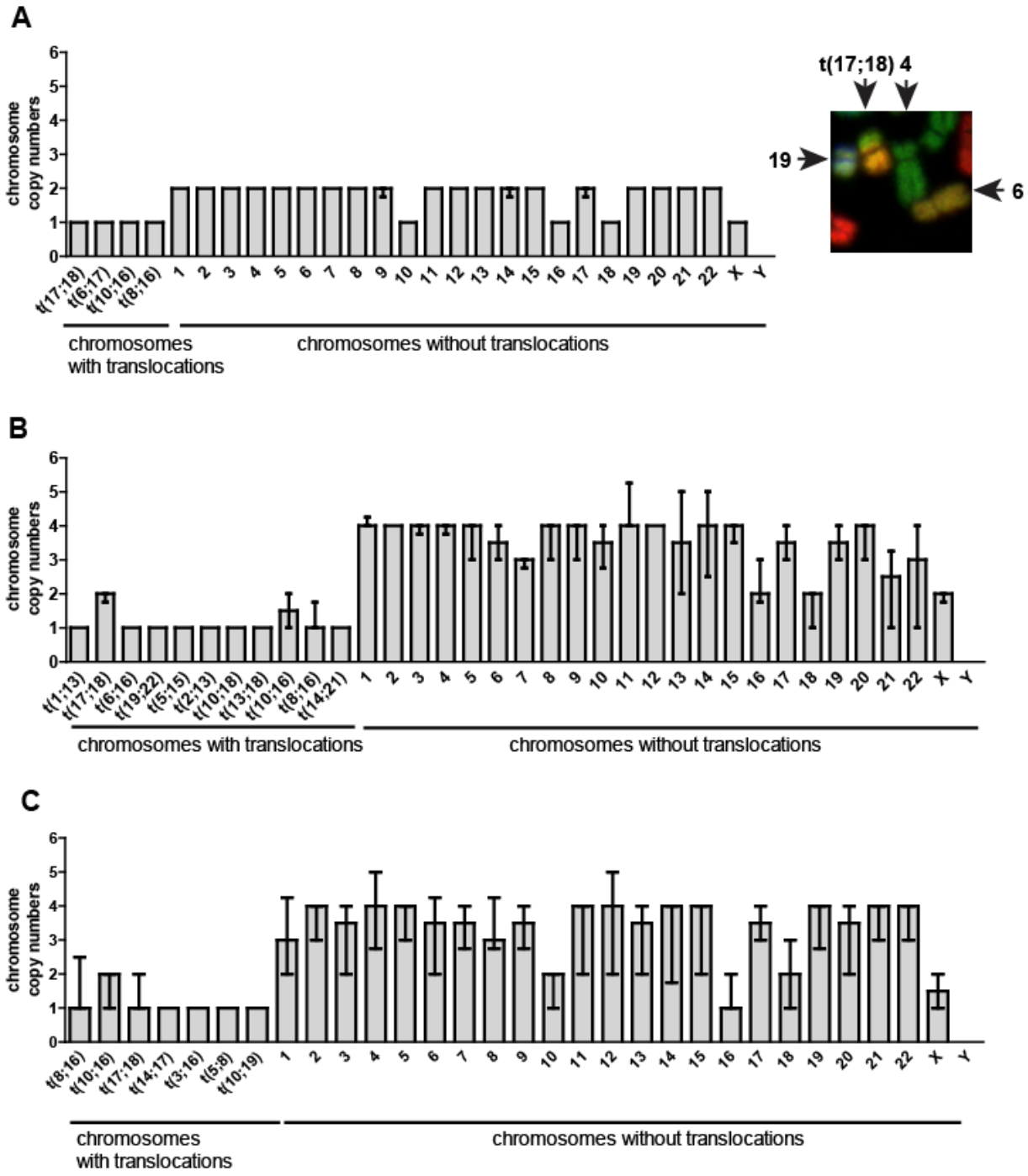

Figure 16. Chromosome content of HCT116 2N, HPT1 and HPT2

(A) Left: HCT116 2N, right: representative chromosomes 4, 6, 19 without translocations and chromosome translocation t(17;18), (B) HPT1 and (C) HPT2. Total of 10 cells was analyzed for each cell line. Median and interquartile range are plotted.

Taken together, proliferating posttetraploids, originating from survivors of transient tetraploidization consist of cells with variable chromosome numbers. This demonstrates that various karyotypic compositions are compatible with proliferation. The data show that transient tetraploidy triggers CIN in human cells.

2.3. Chromosome segregation errors in the posttetraploids.

To identify the source of chromosomal instability in posttetraploid clones, I analyzed occurrence of chromosome segregation errors in posttetraploid cells. First, I quantified the frequency of abnormal mitosis in anaphase and telophase in fixed cells. 4.7% of all mitoses in HCT116 cells are aberrant, whereas 15.8 % and 15.0 % of bipolar anaphases in HPT1 and HPT2, respectively, displayed aberrancies such as lagging chromosomes and anaphase bridges (Figure 17).

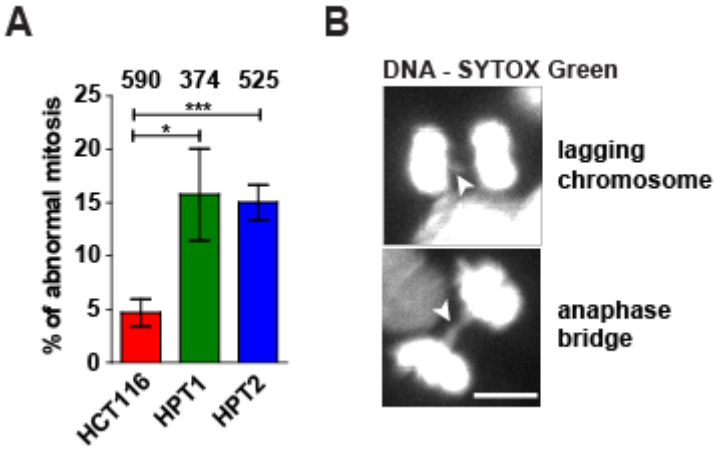

Figure 17. Lagging chromosomes and anaphase bridges in HCT116 and its posttetraploid derivatives.

(A) Percentage of abnormal mitoses evaluated in fixed images, mean and SD of three experiments. The numbers above the bars indicate the number of analyzed cells. (B) Examples of scored mitotic errors in fixed images, bar 10 μm.

Second, live cell imaging revealed that 27.1 % of the HCT116 showed abnormalities such as lagging chromosomes, micronucleation, anaphase bridges, absence of metaphase plate and rare multipolar divisions, while similar aberrations were detected in 37.9 % of mitoses in HPT1 and 43.3 % in HPT2 (Figure 18, Supplementary Figure 2). This is markedly lower than in newly generated tetraploids (the first mitosis after an induced cytokinesis failure), where 86.3 % mitoses display some defects (Figure 19).

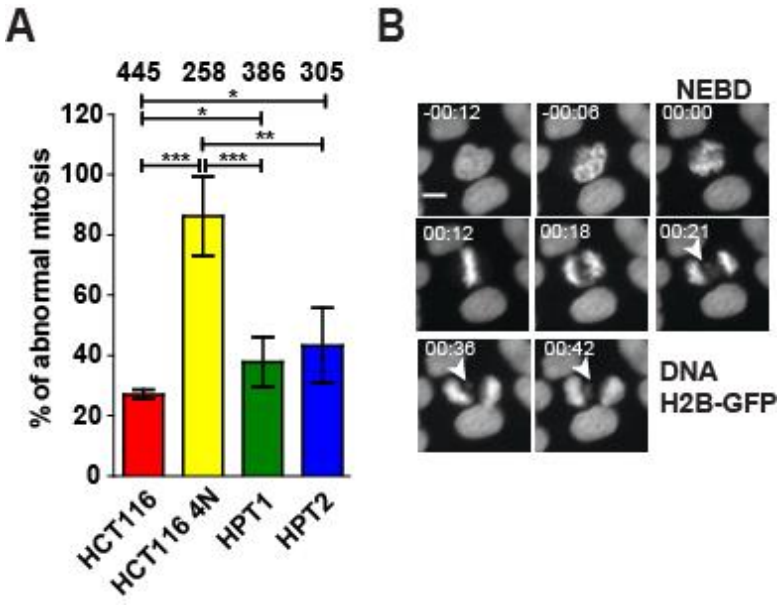

Figure 18. Abnormal mitosis in HCT116 and its posttetraploid derivatives.

(A) Percentage of erroneous cell divisions evaluated from time-lapse imaging in HCT116. Mean and SD of four experiments. The numbers above the bars indicate the number of analyzed cells. (B) Lagging chromosomes followed by micronucleus formation, bar 10 µm. Note that mitosis was classified as erroneous, if any defect was visible at least in one mitotic timelapse capture.

Thus, although the frequency of mitotic errors in PTs decreased in comparison to newly formed 4Ns, the frequency remains higher than in diploid HCT116, and is predominantly due to the lagging chromosomes and anaphase bridges. Frequent mitotic errors were also observed in RPT1 and RPT2, with a two-fold and four-fold increase, respectively, in comparison to RPE1 (Figure 19).

Lagging chromosomes are left behind during anaphase and often form so-called micronuclei (Figure 18B). As expected, the formation of micronuclei in the HPTs was increased as well (Figure 20).

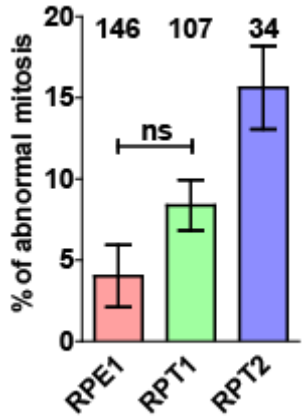

Figure 19. Abnormal mitosis in RPE1 and its posttetraploid derivatives.

Percentage of erroneous cell divisions evaluated by time-lapse imaging; mean and SEM are plotted; three experiments in RPE1 and RPT1 and two in RPT2, thus only RPT1 could be statistically evaluated. The numbers above the bars indicate the number of analyzed cells.

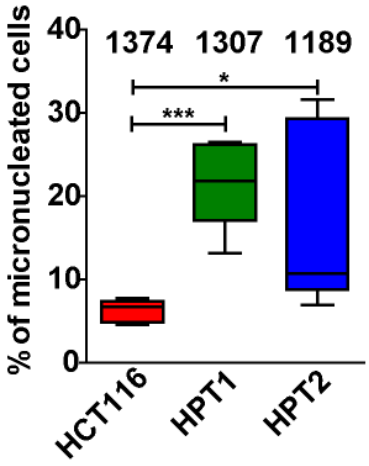

Figure 20. Micronucleation frequency in HCT116 and HPTs.

Percentage of interphase cells with micronuclei, median and Tukey range of seven independent experiments. The numbers above the bars indicate the number of analyzed cells.

Presence of mitotic errors in posttetraploid cells was further confirmed using high-resolution confocal microscopy. Lagging chromosomes and anaphase bridges were readily identified as both CREST-positive and CREST-negative (Figure 21). This suggests presence of mitotic errors in HPTs involving not only whole chromosome missegregation, but also missegregation of broken chromosomes (Supplementary Table 1, Supplementary Figure 3). The reason of this phenomenon is, however, unclear. It might be attributed, for example, to DNA damage repair defect causing chromosome breakage. Subsequently, a piece of chromosome without centromere cannot be attached to the MTs. Alternatively these fragments could be a result of

deletion within the centromeric region. As well, these fragments might occur after disruption of anaphase bridges. Together, presence of acentric fragments is in a concordance with slight increase in structural instability observed as sporadic translocations in mFISH analysis that can be attributed to fusion of broken chromosome parts (Figure 15, Figure 16, Table 2).

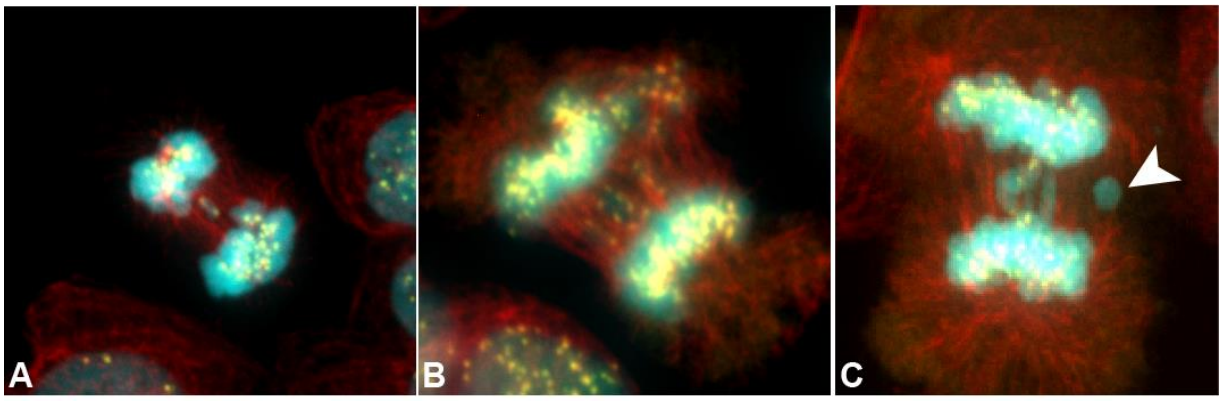

Figure 21. Lagging chromosomes in HCT116 and HPT1.

Lagging chromosomes in (A) HCT116 and (B), (C) HPT1. Arrowhead in (C) indicates acentric lagging chromosomal fragment. Note the presence of anaphase bridges, seen as stretches of DNA between the main DNA masses in (C). DNA is visualized with Sytox Green (cyan), MTs are visualized with a-tubulin antibody (red), centromeres are visualized with CREST antibody (yellow).

In summary, the progenies of tetraploids accumulate more mitotic errors than diploid cells. On the other hand, the frequency of mitotic errors is significantly lower than in newly formed tetraploids. These facts support our view that only moderate levels of CIN are compatible with extended survival. Moreover, an increase in lagging chromosomes and subsequent micronuclei formation suggests that merotelic attachments often arise in PT cells.

3. Causes of chromosomal instability in the posttetraploids.

A plethora of mechanisms can trigger chromosomal instability. Therefore, I assessed several possible mechanisms that can lead to persistent chromosome missegregation and accumulation of variable aneuploidy in cells.

3.1. Contribution of supernumerary centrosomes to chromosomal instability.

Cytokinesis failure that induces formation of binucleated tetraploid cells results in the gain of an extra centrosome. A duplication of centrosomes in the following cell cycle

leads to a formation of multipolar spindles causing severe chromosome missegregation. Thus, the levels of mitotic errors in PT cells might be elevated due to the extra centrosomes.

In order to assess the contribution of mitotic multipolarity to the CIN in the posttetraploids, I followed the posttetraploids and its progenitor diploids and newly formed tetraploids through mitosis using timelapse imaging. The timelapse imaging revealed that only 4.4 % of HPT1 and 3.3 % of HPT2 cells divided in a multipolar manner, in contrast to newly formed tetraploids that form multipolar spindles at a high frequency (Figure 22A, B). No multipolar mitosis was observed in the RPT cell lines (Figure 22C), oppositely to newly formed tetraploid RPE1 that undergo multipolar anaphase in 50.0 % of cases (Kuffer et al., 2013). This demonstrates that a bipolar anaphase formation is essential for propagation of cell lines evolved from tetraploid intermediates.

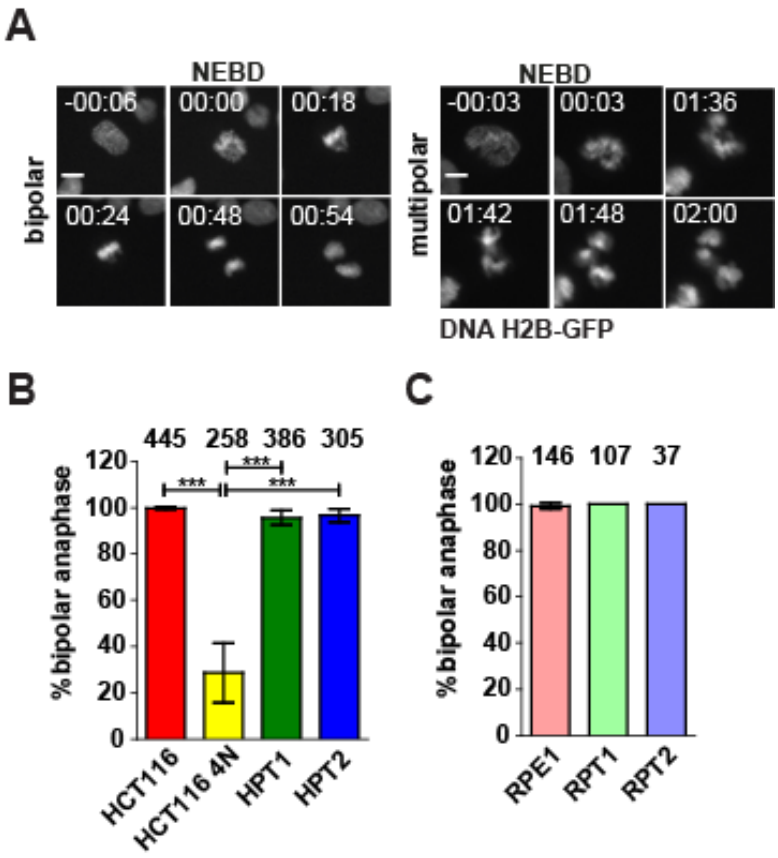

Figure 22. Bipolar mitosis in HCT116 and its derivatives.

(A) Representative images of cells undergoing normal bipolar and multipolar mitoses, bar 10 µm. (B) Percentage of bipolar mitoses in HCT116 and HCT116-derived cells as determined by live cell imaging. Mean and SD of four experiments, unpaired Student t-test. (C) Percentage of bipolar

mitoses in RPE1 and RPE1-derived cells as determined by live cell imaging. Mean and SD of three experiments. The numbers above the bars indicate the number of analyzed cells in all panels.

Observed bipolar anaphase can be attributed either to centrosome clustering (Brinkley, 2001; Kwon et al., 2008; Murphy, 2003; Quintyne et al., 2005) or to elimination of extra centrosomes (Krzywicka-Racka and Sluder, 2011). To distinguish between these two routes, the centrosome number was assessed by immunostaining of the centrosomal marker γ-tubulin in asynchronous culture (Figure 23A). The distribution of centrosome numbers in HPTs resembled the distribution in HCT116, with the median centrosome number of two (Figure 23B). The percentage of cells with more than two centrosomes was slightly increased in PT cells, as I quantified 1.9%, 7.7% and 6.3% for HCT116, HPT1 and HPT2, respectively. In contrast, I observed more than two centrosomes in 67.4% of newly generated tetraploids; with a median of three centrosomes per cell (Figure 23B). A statistical significance of the shift in median centrosome number distribution in all four cell lines was assessed by Mood's median test. Pairwise comparison of HCT116 and HCT116 4N using this test showed that the shift of the median is statistically significant (p-value = 0.04). The pairwise comparisons of HCT116 2N and HPT1, and HPT2 showed no statistically significant shift of median (p-value = 0.38 and p-value = 0.76, respectively), as well as comparisons of the HPTs between each other (p-value = 0.50). Interestingly, the reduction of centrosomes occurs relatively early after tetraploidization. As soon as after the first tetraploid mitosis the centrosome number distribution profile shifts towards the lower centrosome numbers. This effect is observed even more prominently after the second tetraploid mitosis (Supplementary Figure 4). Thus, the PT cell lines rapidly lost the extra centrosomes gained during tetraploidization.

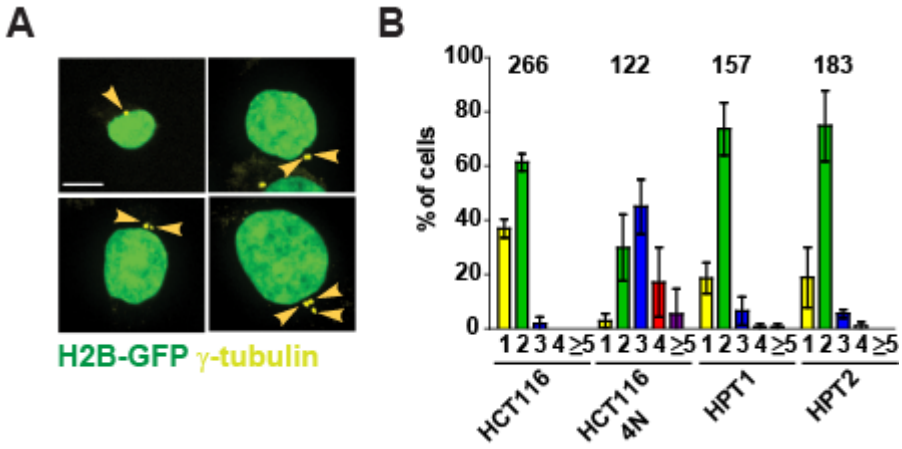

Figure 23. Centrosome numbers in HCT116 and its derivatives.

(A) Representative images of centrosome visualization by immunostaining, bar 10 μm. (B) Centrosome numbers in asynchronous cultures. X-axis: the number of centrosomes. Mean and SD of three experiments. The numbers above the bars indicate the number of analyzed cells in all panels.

To further confirm our finding on centrosome numbers and to exclude immunostaining scoring artifacts, I used RNAi was used to knock down KIFC1/HSET, a kinesin essential for centrosome clustering (Kwon, Godinho et al. 2008). Knockdown of KIFC1/HSET in HPTs and in control HCT116 did not increase the frequency of multipolar mitosis (Figure 24). In contrast, 92 % of the KIFC1/HSET RNAi-transfected newly generated tetraploids underwent multipolar mitosis in comparison to nearly 33.5 % of multipolar mitoses in mock-transfected tetraploids (Figure 24).

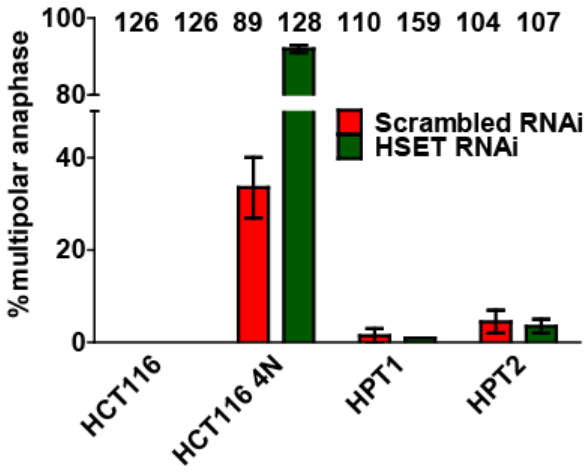

Figure 24. Frequency of multipolar mitosis upon RNAi inhibition of KIFC1/HSET.

Percentage of bipolar spindles upon inhibition of centrosome clustering by KIFC1/HSET knockdown, mean and SEM of two independent experiments. The numbers above the bars indicate the number of analyzed cells.

In conclusion, posttetraploids undergo almost exclusively bipolar mitosis and more importantly, centrosome numbers in posttetraploids are similar to those in diploids. The data suggest that robust bipolarity is crucial for survival after tetraploidization. Moreover, this observation rules out spindle multipolarity as the only source of chromosomal instability in PT cell lines.

3.2. Sister chromatid cohesion in posttetraploids.

Next, I investigated the possibility that sister chromatid cohesion might be attenuated in the posttetraploid cell lines, which in turn results in chromosome missegregation and merotelic attachments. Analysis of primary constrictions in mitotic spreads from diploid control cells and PT cells did not reveal an elevated frequency of cohesion defects. I observed a partial alteration in primary constrictions of at least one chromosome within a metaphase spread in 13.0 % cells in HCT116 and 13.9 % in both HPT1 and HPT2 (Figure 25A). Furthermore, measurements of interkinetochore distance revealed no significant differences between HCT116 and HPT2; the measured distance was 1.19±0.19 (mean±SD) for HCT116 and 1.19±0.22 for HPT2 in fixed cells (Figure 25B). The distance measured in HPT1 was slightly increased (1.25±0.19); however, this increase is much lower than the distance usually detected in cells with a defect in sister chromatid cohesion – 1.51 ± 0.07 (Manning, Longworth et al. 2010).

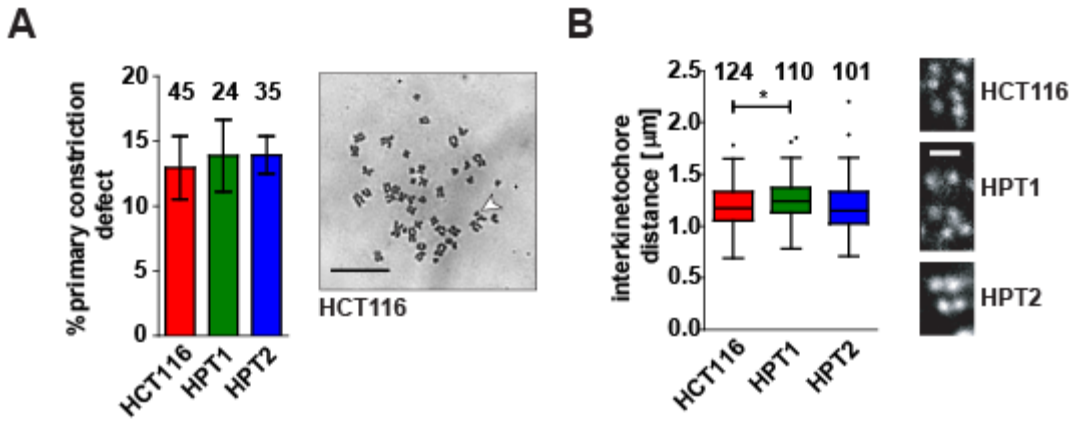

Figure 25. Sister chromatid cohesion in HCT116 and the posttetraploid cells.

(A) Left: cells with primary constriction gaps in at least one chromosome pair, mean and SEM of two independent experiments. Right: A representative cell displaying a cohesion defect in one chromosome pair. White arrowhead indicates primary constriction gap in separated chromosomes. Bar 10 µm. (B) Distance between sister kinetochores in HCT116 and HPTs, Tukey range and median are plotted, Mann-Whitney test. Bar 1 µm. The image analysis for panel (B) was carried out by Zuzana Storchova, Ph.D.

In conclusion, sister chromatid cohesion does not appear to play a role in CIN of posttetraploid cells.

3.3. Global gene expression changes in the posttetraploids.

3.3.1. Altered mitotic spindle dynamics.

In order to decipher the mechanisms triggering CIN in posttetraploids, I performed a global microarray-based gene expression analysis. The aim was to identify the recurrent changes on mRNA level that might be associated with CIN. I observed a prominent downregulation of several kinesins, many of which were associated with the progression through mitosis. Kinesin expression was often downregulated below the arbitrarily set cutoff -0.75 (log_2 ratio HPT/HCT116), which corresponds to 1.7 fold downregulation. The expression of 15 kinesins in HPT1 and 6 in HPT2 was altered (out of 38 kinesins); in particular, mitotic kinesins Kif18A and Kif18B, Kif15, Kif24, Kif4A and Kif2C were decreased in both analyzed PT cell lines (Figure 26A).

Furthermore, these mRNA changes are reflected at the protein level that can be observed using immunoblotting against Kif18A. mRNA changes were reflected for HPT2 but not HPT1 at the Kif15 protein level (Figure 26B). I detected a downregulation of Kif18A in seven and of Kif15 in six out of eight analyzed posttetraploids (Figure 26B, C). Importantly, cells obtained by prolonged passaging of HCT116 2N for 36 additional passages (HCT116 36p) show similar Kif18A and Kif15 protein levels as the progenitor HCT116 cells. Moreover, cells obtained by single-cell clone purification of HCT116 (HCT116 C4) also retained protein levels of Kif18A and Kif15 similar to HCT116. Thus, *in vitro* evolution of HCT116 by either prolonged passaging of HCT116 or evolution from a single HCT116 cell does not change analyzed kinesins' levels. This fact suggests that changes in the kinesin levels might be a consequence of prior tetraploidization.

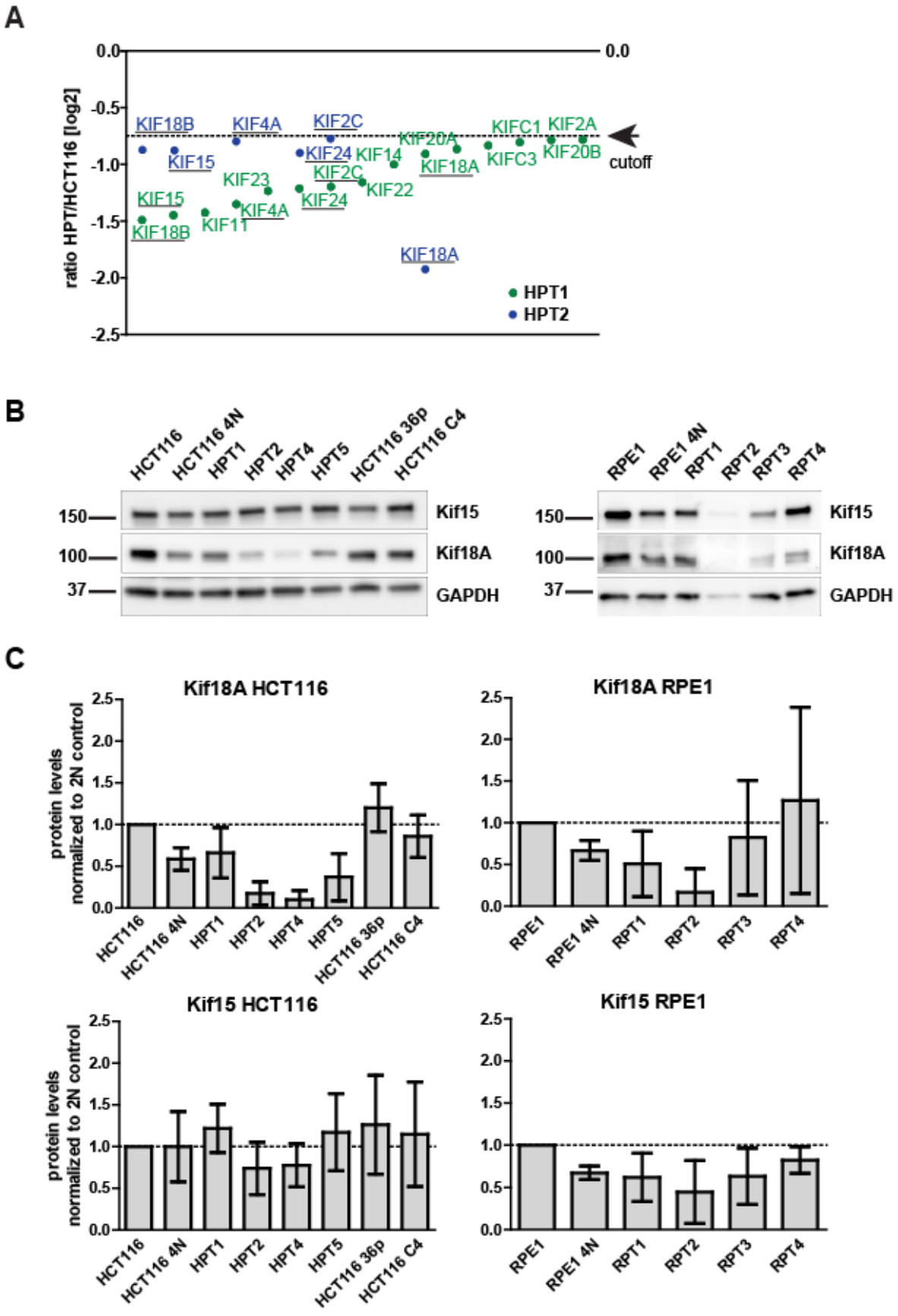

Figure 26. mRNA and protein level analysis of Kif15 and Kif18A in HCT116 and its derivatives.

(A) The log_2 values of ratio HPT/HCT116 of mRNA abundance changes. Only kinesins with log_2 values below -0.75 cutoff are plotted (fold-change - 1.7).The underscored kinesins are downregulated in both HPT1 and HPT2. Note that KIF18B in HPT1 does not pass the criteria for false discovery rate (FDR cutoff 0.01). (B) Representative immunoblotting of kinesins Kif15 and, Kif18A in both HCT116 and RPE1-derived cell lines. Loading control - GAPDH. (C) Immunoblotting quantification. Data was normalized first to a respective loading control (GAPDH) and further normalized to a respective diploid cell line levels (HCT116 or RPE1), mean and SD. All panels: three independent experiments.

Notably, observed abundance changes do not occur due to the gene copy alterations, as no underrepresentation of the corresponding coding regions was identified by aCGH (data not shown).

Kif18A represents a typical mitotic kinesin with well-described depolymerase activity (Mayr et al., 2007). To identify its interaction partners in mitosis I analyzed entries referred to as interacting partners of Kif18A in String database of known and predicted protein-protein interactions. Kif18A interacts with 16 proteins involved in mitotic progression according to STRING database. The interacting partners are: BIRC5, KIF2C/MCAK, BUB1B (BUBR1), CDCA8, NDC80, CDC20, CLASP1, CENPN, CENPA, CENPE (Figure 27). These factors are playing role in KT-MT binding, mitotic error correction and SAC.

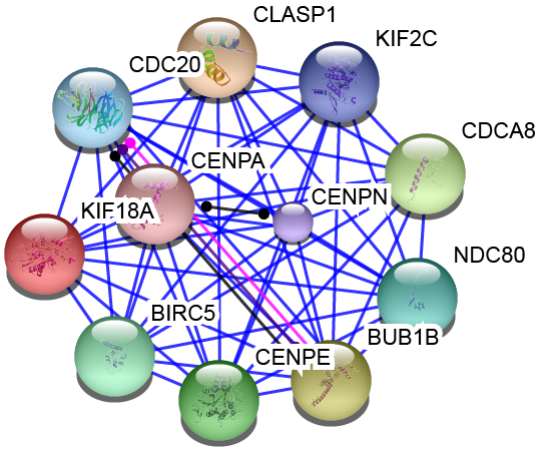

Figure 27. Interacting partners of Kif18A.

Connecting line color as annotated in the database: blue – binding, pink – posttranslational modification, black – reaction, purple – catalysis.

In summary, posttetraploid cells downregulate mitotic kinesins on mRNA level that could be confirmed on a protein level for Kif18A. These changes might be responsible for altered MT dynamics in mitosis.

3.3.2. Altered mitotic spindle geometry of posttetraploid cells.

Kinesins Kif18A and Kif4A and, to a lesser extent, Kif18B, regulate the dynamics of the MT plus-ends and limit the metaphase chromosome oscillations. Slower metaphase chromosome oscillations might suggest slower MT dynamics and presence of overly stable mitotic MTs. As a consequence, metaphase kinetochore distribution might be altered in the PTs. To address this possibility, we visualized the centromeres in cells arrested in metaphase. The distribution of the centromere signal intensity assessed by CREST antibody immunostaining along the spindle axis revealed no significant difference between diploid and PT cell lines (Figure 28A, B, Supplementary Figure 5).

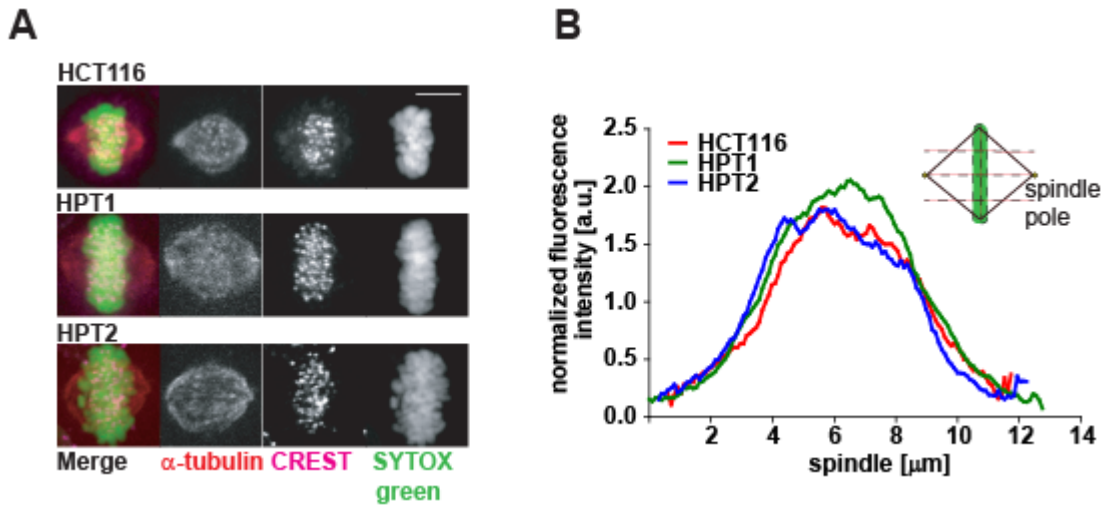

Figure 28. Centromere distribution in HCT116 and the posttetraploids.

(A) Mitotic spindles and centromere distribution in HCT116 and HPTs, bar 5 μm. (B) Normalized intensity of the CREST signal along the spindle in HCT116 and HPTs; 9 to 11 cells were measured for each cell line. The averaged signal intensity is plotted. Schematic inset depicts the line intensity measurement strategy. The image analysis was carried out by Zuzana Storchova, Ph.D.

A large body of evidence suggests that depletion of Kif18A and Kif4A results in excessively long MTs, thus causing mitotic spindle elongation. As expected, the spindle length in PTs (10.1 μm in HPT1 and 10.5 μm in HPT2) measured as pole-to-pole distance in metaphase-arrested cells immunostained with γ-tubulin antibody was longer than in HCT116 (median 8.6 μm) (Figure 29A, B - upper left). The median width of the spindle (the span of the α-tubulin signal at the site of the metaphase plate) increased as well, from 7.7 μm in HCT116 to 10.7 μm in both analyzed HPTs, likely in order to accommodate the increased chromosome numbers

(Figure 29B, upper right). Changes of both length and width of the spindle are indicative of longer astral MTs. Notably an increase in the spindle width is higher than in the spindle length, resulting in altered width-to-length ratio in cells. This altered length-to-width ratio is reflected by a significant change in the spindle angle (Figure 29B - bottom right).

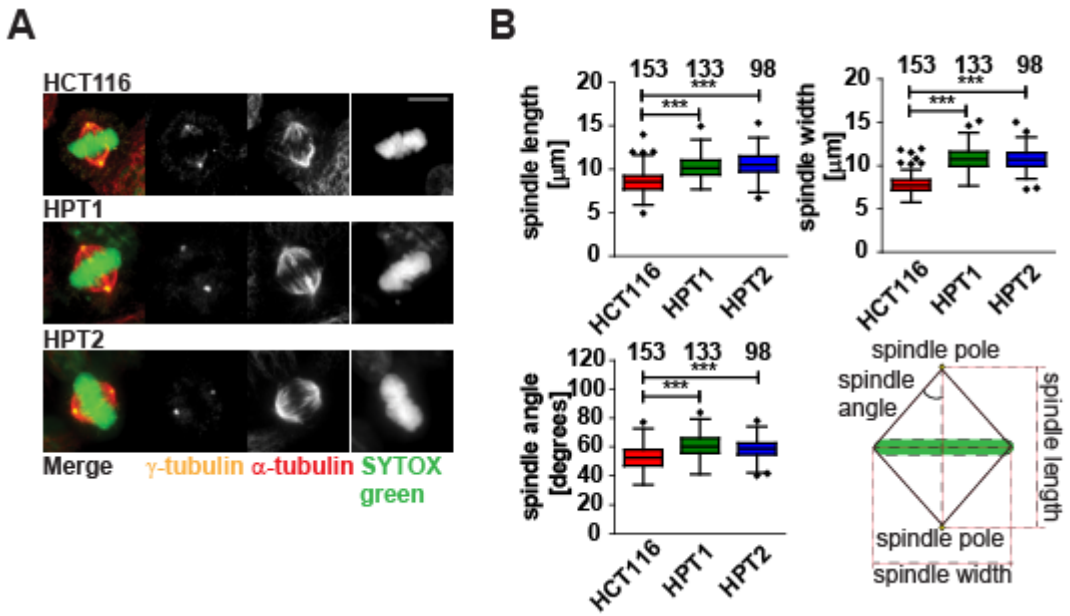

Figure 29. Spindle geometry in HCT116 and posttetraploid cells.

(A) Mitotic spindles and centrosomes in HCT116 and the HPTs, bar 10 μm. (B) Measurements of spindle length, width and spindle angle. Schematic depicts the parameter measurement strategy. Tukey range and median are plotted, Mann-Whitney test. The numbers above the bars indicate the number of analyzed cells.

In conclusion, cells that underwent transient tetraploidy adapted to increased numbers of chromosomes by modulating spindle geometry, and this is achieved by, among others, changes in expression levels of mitotic kinesins. There is a strong reason to speculate that in addition to spindle geometry changes upon deregulation of key mitotic kinesins, the MT dynamics are also altered. Downregulation of Kif18A, the kinesin with well-characterized MT depolymerase activity, together with elongation of mitotic spindle, support the hypothesis that K-fibers are more stable in PT cells. As a consequence, KT-MT attachment error correction can be slower in PTs than in progenitor diploid cells, leading to chromosome missegregation.

3.3.3. Other changes potentially causing chromosomal instability.

In addition, I explored the mRNA levels to identify other changes that can potentially contribute to the development of CIN in posttetraploid cell lines. I focused on factors, such as mitotic error correction, kinetochore association, microtubule severing, microtubule stabilizing, motor functions (kinesins), spindle assembly checkpoint, sister chromatid cohesion and cell cycle regulation. Transcription levels of many of these factors were altered, but most of the changes were not recurrent in both HPT1 and HPT2 (Supplementary Table 2). Recurrent changes in these genes are described in the Table 2.

ratio HPT1/HCT116 [log_2]	ratio HPT2/HCT116 [log_2]	recurrent up- or downregulation	gene name	function
-1.7191	-0.9624	down	KNTC1	**Spindle assembly checkpoint**
-1.9628	-2.4346	down	FIGNL1	**Severing MAPs**
-1.4473	-0.8892	down	KIF15	
-0.9071	-1.9064	down	KIF18A	
-1.4906	-0.8735	down	KIF18B	
-1.2126	-0.8985	down	KIF24	
-1.197	-0.7653	down	KIF2C	
-1.3506	-0.8004	down	KIF4A	**Kinesins**
-1.1085	-0.7614	down	SMC3	**Sister chromatid cohesion**
-1.7025	-1.4203	down	ESPL1	
1.26936	2.39047	up	CDKN1A	**Cell cycle regulation**

Table 2. Recurrent changes in the expression levels of factors, described to be associated with CIN.

Log_2 of the HPT/HCT116 for every individual gene entry are shown in the table. The median of three biological replicates for each gene entry was used. Up-/downregulation – log_2 of the ratio is more or equals 0.75 (up) or less or equals -0.75 (down). Values that do not satisfy FDR threshold are marked in red.

As seen in Table 2, apart from the mitotic kinesins, the expression of the gene KNTC1 (protein Rod) involved in spindle assembly checkpoint and kinetochore organization, severing MAP FIGNL1 (protein fidgetin), cohesin SMC3 and separase ESPL1 are downregulated as well. The contribution of changes in these factors to CIN in posttetraploids remains to be studied in a more detail.

3.4. Spindle assembly checkpoint alterations in the posttetraploids.

Knockdown of kinesin KIF18A was reported to induce a loss of tension on sister kinetochores and the SAC activation (Mayr et al., 2007). However, the duration of mitosis in PT cell lines is similar as in diploids, despite the increased frequency of mitotic errors (Figure 9B). Therefore, I hypothesized that the SAC response in PTs might be attenuated. In order to test the functionality of SAC, I used an MT depolymerizing drug nocodazole, which leads to partial or complete absence of microtubules and thus, in turn, to SAC activation. Treatment with a low concentration of nocodazole (0.5 ng/ml) resulted in prolonged mitosis measured as time from NEBD to the onset of anaphase similarly in all cell lines. The observed duration of this period was from 24 min to 159 min for HCT116, 27 min to 141 min for HPT1, from 24 min to 162 min for HPT2 (Figure 30A). Moreover, PTs maintained robust mitotic arrest in the presence of high concentration of nocodazole (200 ng/ml) that leads to a complete microtubule depolymerization and arrests the cells in metaphase. The median length of metaphase arrest before slipping out of mitosis was 17.3 h in HCT116, 16.0 in HPT1 and 15.9 h in HPT2 (Figure 30B). Thus, the SAC response to microtubule depolymerizing drug is not affected in cell lines derived from a tetraploid intermediate.

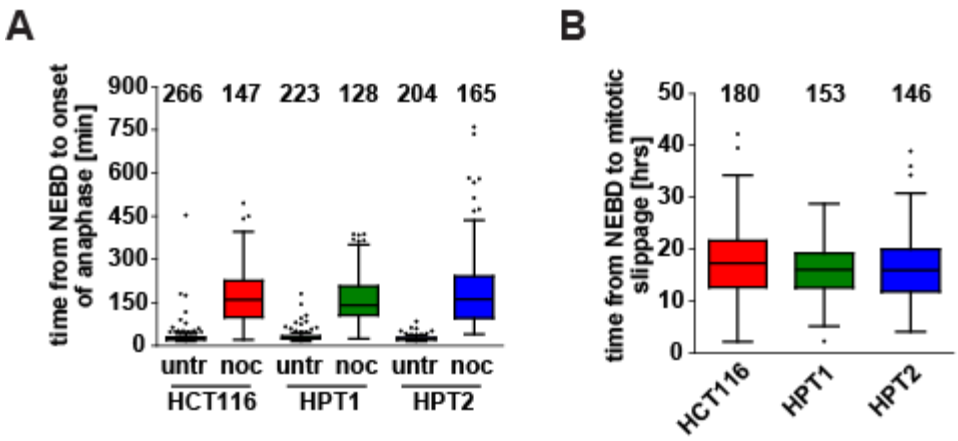

Figure 30. Spindle assembly checkpoint response to nocodazole treatment in HCT116 and posttetraploids.

(A) Time from NEBD to anaphase onset in presence of low concentration of nocodazole, Tukey range and median of three independent experiments. (B) Time from NEBD to mitotic slippage in presence of high concentration of nocodazole; Tukey range and median of three independent experiments. The numbers above the bars indicate the number of analyzed cells in both panels.

Second, I examined the SAC response to the lack of tension, mimicked by the treatment with VS-83, chemical inhibitor of kinesin Kif11/Eg5 (Muller et al., 2007). Inhibition of Kif11/Eg5 leads to the formation of monoaster spindles with intact microtubules, thus increasing the frequency of tensionless KT-MT attachments.

The majority of HCT116 cells (95 %) became arrested in the presence of VS-83 (20 µM) and exited mitosis without cell division after 14.7 hours, similarly as in response to a high nocodazole concentration (Figure 31A red bars, Supplementary Figure 7). Remarkably, only a half of HPTs could maintain an extended mitotic arrest that was followed by mitotic slippage. 52.6 % of HPT1 and 58 % of HPT2 divided into two daughter cells after 7.3 and 9.3 hours, respectively (Figure 31A red bars, 32C, Supplementary Figure 6). Similarly, comparison of RPE1 and RPT1 revealed that whereas only 18.5 % of RPE1 cells divided in the presence of VS-83 (10 µM), the frequency of cell divisions in this condition increased to 47.0 % in RPT1 (Figure 31D).

The dividing cells often underwent a highly aberrant mitosis with segregation errors. One explanation of the observed phenotype may be that the PT cells are more resistant to VS-83 and can form bipolar spindles even in its presence. To test this possibility, I fixed the VS-83-treated cells at the time point when the majority of observed cell divisions occurred and then stained DNA and α-tubulin (Figure 31B). 4.4 % of HCT116 cells formed bipolar spindles (Figure 31A, green bars), which corresponds well with the observed percentage of dividing cells (Figure 31A, red bars). The frequency of bipolar spindles was 20.8 % in HPT1 and 8.5 % in HPT2 (Figure 31A, green bars), which is much lower than the frequency of HPT cells dividing in the presence of VS-83 (Figure 31A, red bars).

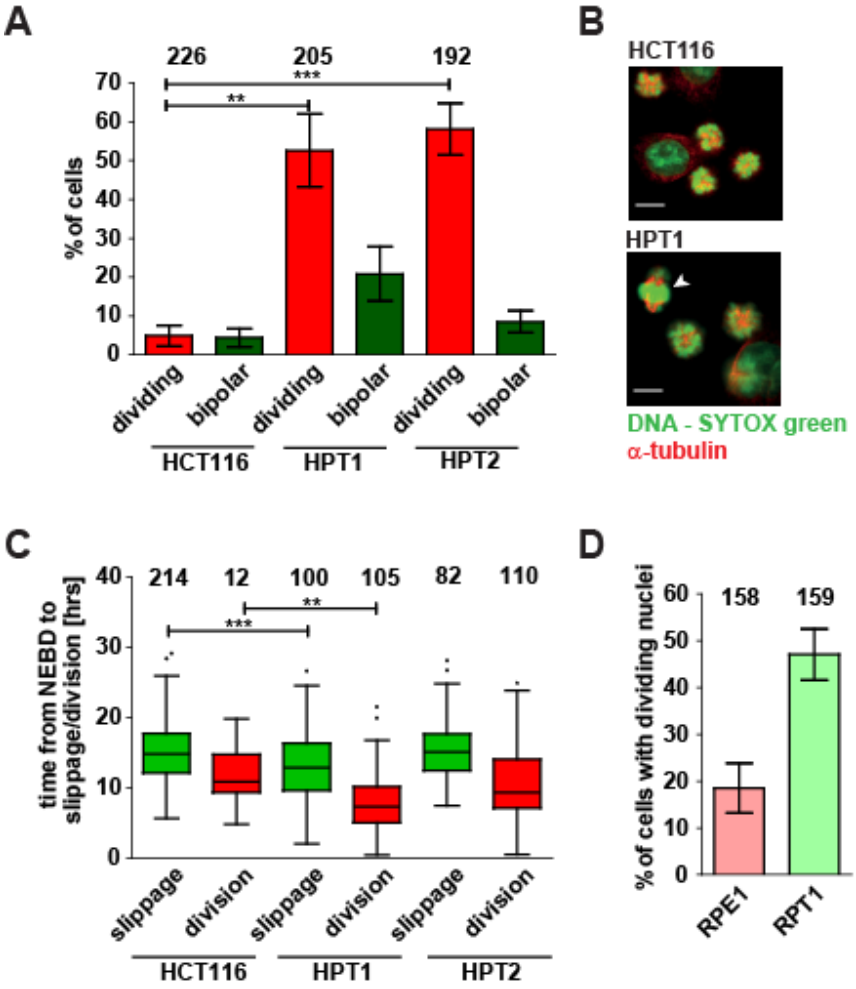

Figure 31. Proliferation of HCT116 and HPTs in the presence of VS-83.

(A) Percentage of cells dividing in the presence of VS-83 (live cell imaging, red bars) and maintaining a bipolar spindle in the presence of the inhibitor (immunostaining, green bars), each: mean and SD of three experiments, unpaired Student t-test. For representative progression through mitosis see Supplementary Figure 7. (B) Spindle geometry in the presence of VS-83 in HCT116 and PTs assessed by immunostaining, bar 10 μm. Arrowhead indicates a bipolar spindle. (C) The time from NEBD to mitotic slippage or cell division in presence of VS-83 (20 μM). Tukey range and median, Mann-Whitney test. (D) Percentage of RPE1 and its derivative RPT1 dividing in presence of Eg5 inhibitor VS-83 (10 μM). Mean and SEM of two experiments are shown. Numbers above the bars indicate the number of analyzed cells in all panels.

In conclusion, these observations demonstrate a specific SAC defect in the PT cells that allows an anaphase onset in presence of tensionless attachments. Potentially this SAC defect might add into a defective error correction, allowing division despite tensionless attachments.

3.5. Tolerance to chromosome missegregation in the posttetraploids.

Chromosomal instability post-tetraploidization was reported in most cases in p53-deficient cells to date (Fujiwara et al., 2005). p53-positive cells that survived tetraploidization were shown to be chromosomally stable (Vitale et al., 2010). The posttetraploids analyzed in the present work displayed CIN, yet their progenitor cell lines were p53-proficient. On one hand the PT cells display an increased frequency of abnormal mitoses, and on the other hand, this missegregation is not associated with an accumulation of non-proliferating cells (Figure 10A, B). p53 pathway can be activated in response to DNA double-strand breaks (DSB) induced by doxorubicin treatment (Figure 32). It suggests that this pathway cannot be completely inactive and a complete loss of p53 is not an essential prerequisite for the survival of cells with elevated levels of chromosome missegregation.

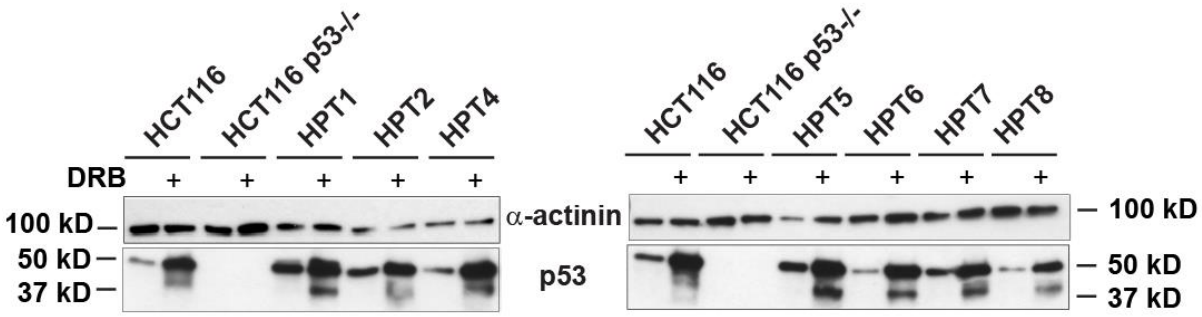

Figure 32. p53 immunoblotting in HCT116 and its posttetraploid derivatives.

Diploid p53 -/- HCT116 cells were used as a negative control, DNA-damaging drug doxorubicin (DRB) was used as a positive control, α-actinin was used as a loading control.

Despite this seemingly intact p53 pathway, live cell imaging revealed that only 11.0 % of HPT1 and 9.8 % of HPT2 cells became arrested after abnormal bipolar mitosis (Figure 33A, for fate analysis of single cells see Supplementary Figure 7). In contrast, 34.2 % of diploid and 54.1 % of newly formed tetraploid HCT116 cells that underwent abnormal bipolar mitosis became arrested or died in the subsequent interphase (Figure 33A). There is no statistically significant difference in the frequency of arrest after apparently normal mitosis (Figure 33A). Moreover, rare incidences of multipolar mitoses in HPT1 led to a cell cycle arrest or death at a similar frequency as in tetraploid cells, suggesting that human cells cannot adapt to such a severe chromosome misssegregation (Figure 33B). This suggests that only moderate chromosome missegregation is compatible with the proliferation, and

severe mitotic defects remain lethal.

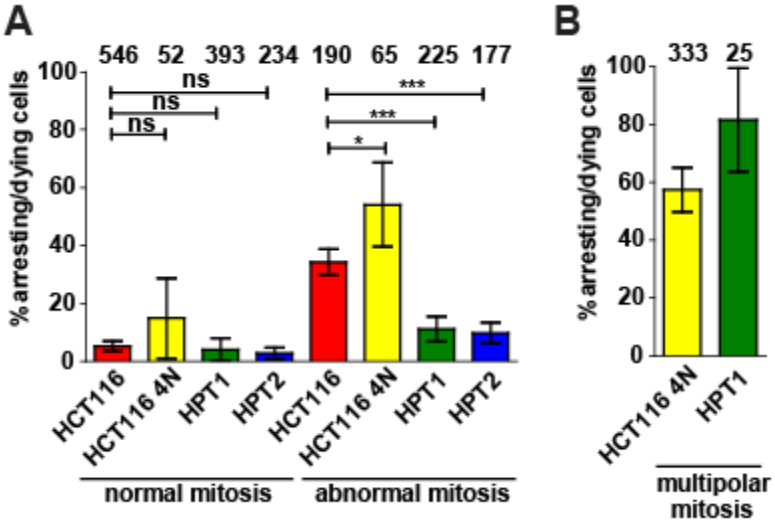

Figure 33. Cell cycle arrest and death after normal bipolar, abnormal bipolar and multipolar mitosis in HCT116 and its derivatives.

(A) Frequency of cell cycle arrest/cell death after bipolar mitosis with no apparent defects (normal mitosis) and with visible defects (abnormal mitosis). Mean and SD of four experiments, unpaired Student t-test. Numbers above represent the number of cells with the indicated phenotype. (B) Frequency of cell cycle arrest/cell death in response to multipolar mitosis. Mean and SD of four experiments. Numbers above indicate the number of cells with indicated phenotype.

To further support this hypothesis, I induced high levels of chromosome missegregation using non-toxic concentration of nocodazole (Figure 34A). In this case, proper MT-KT interaction is impaired, thus causing an increase in the frequency of lagging chromosomes, micronucleation and anaphase bridges. This severe chromosome missegregation subsequently leads to arrest and/or death in the following interphase with a high frequency (Figure 34B). This funding further supports the idea that posttetrapoids do not adapt to high rates of CIN.

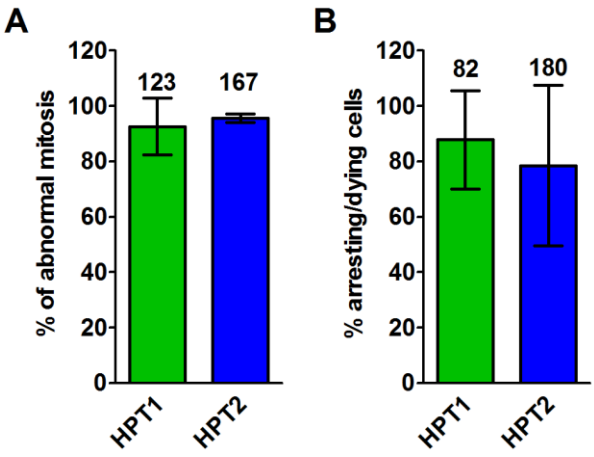

Figure 34. Frequency of abnormal mitosis and subsequent cell cycle arrest and/or death in interphase in posttetraploids.

(A) Frequency of abnormal mitotic figures and (B) frequency of cell cycle arrest/death after mitotic abnormalities induced by low concentration of nocodazole (0.5 ng/ml). Both: mean and SD of three experiments. Numbers above represent the number of cells with the indicated phenotype.

Taken together, the PT cell lines appear to be more tolerant to errors in bipolar chromosome segregation and continue proliferation despite moderate missegregation of chromosomes. Importantly, severe chromosome missegregation substantially affects cell viability in posttetraploids, implying that only moderate chromosome missegregation is compatible with further proliferation.

The decrease in the frequency of arrest and death after chromosome missegregation suggests that alterations in the p53 pathway might be essential to ensure proliferation of CIN cells. Previous reports indicate that missegregation of one or few chromosomes leads to accumulation of p53 in the nucleus and cell cycle arrest (Thompson and Compton, 2010). I investigated the possibility that nuclear p53 accumulation after abnormal mitosis is impaired in PT clones. To this end, I performed a micronucleation test followed by immunostaining with a p53 antibody. While nearly 50 % of HCT116 with micronuclei accumulated p53 in the nucleus or in the micronucleus, only 25 % of HPT1 and HPT2 cells displayed similar phenotype (Figure 35A, B).

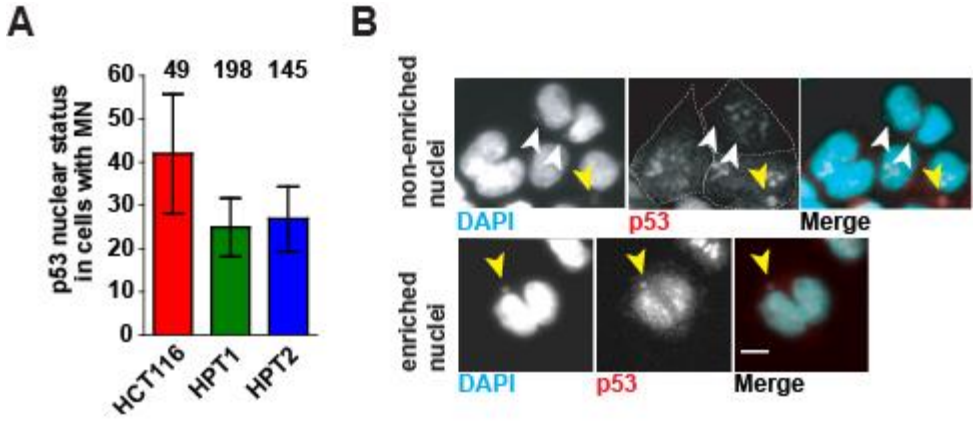

Figure 35. p53 enrichment in the nucleus after micronucleation in HCT116 and posttetraploids. (A) Accumulation of p53 in the major nuclei of cells forming micronuclei in HCT116 and in the PTs. Mean and SEM of four experiments. Numbers above indicate the number of total cells with micronuclei analyzed per cell line. (B) Examples of p53 accumulation in the nuclei and micronuclei of the micronucleating cells, bar 10 μm. Yellow and white arrowheads indicate the micronuclei with and without p53 enrichment, respectively.

Next, we analyzed p53 pathway using transcriptional analysis in posttetraploids. Pathway analysis allows identification of the pathways underrepresented or overrepresented in the given microarray-based mRNA analysis dataset after mapping mRNA of the genes to known pathways. Accordingly, if the mRNAs of genes assigned to a certain pathway are underrepresented in the dataset, the pathway is classified as downregulated. Using this approach, we observed p53 pathway deregulation in posttetraploids (Figure 36). In particular, a key p53 inhibitor Mdm2 is upregulated that might potentially cause direct p53 inhibition. Accordingly, the expression of several genes, regulated by p53 is altered. For example, we observed a prominent upregulation of p21. As well, many genes involved in apoptotic pathway are upregulated. The p53 pathway deregulation may be at least partially responsible for increased tolerance to mitotic errors; however, molecular mechanisms leading to this tolerance remain to be investigated.

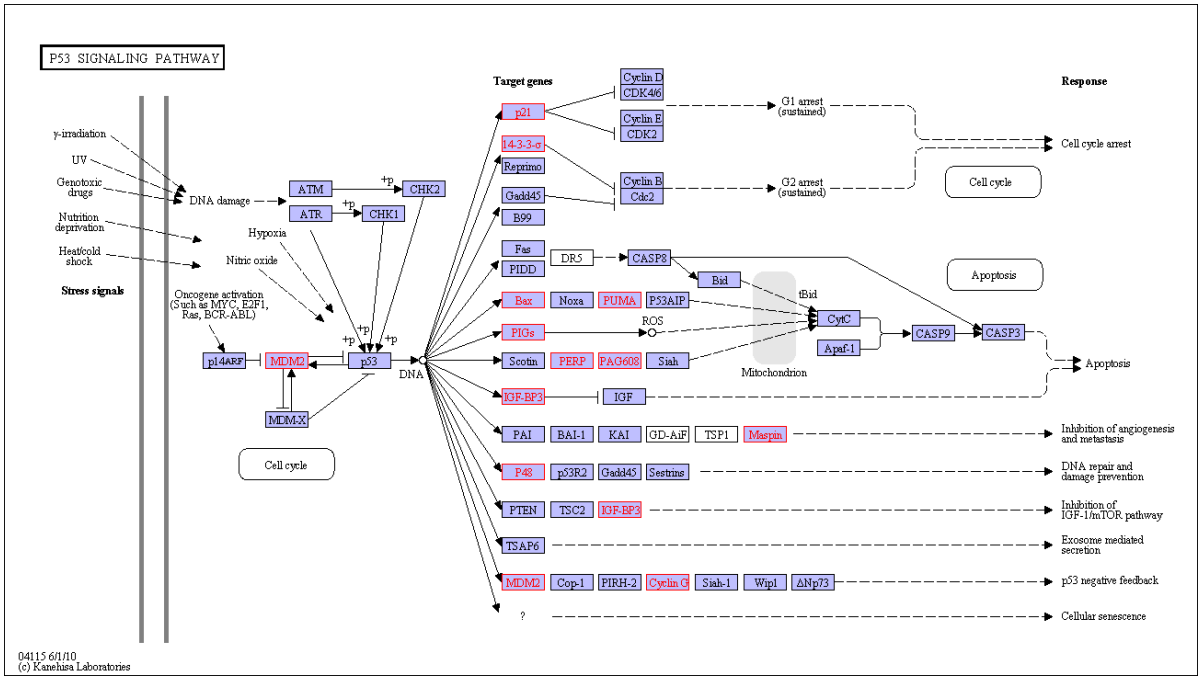

Figure 36. p53 pathway deregulation in posttetraploids.

Upregulated genes are marked in red. Image was provided by Milena Dürrbaum.

Taken together, the PT cell lines can escape a cell cycle arrest after mitotic errors more frequently than both HCT116 diploid and tetraploid progenitor cell lines. An increased tolerance to chromosome segregation errors is often achieved by modifications *upstream* of p53, suggesting that the activation of the p53 pathway after mitotic errors is specifically attenuated in PT cells.

Discussion

A large body of evidence supports the hypothesis that transient tetraploidy leads to formation of chromosomally unstable progeny as proposed previously (Shackney et al., 1989; Storchova and Pellman, 2004). Hitherto, the molecular mechanisms triggering CIN after tetraploidization remained poorly understood. This dissertation provides the comprehensive analysis of chromosomally unstable progenies arising from individual human tetraploid p53-positive cells. The study outlines the molecular mechanisms contributing to the chromosomal instability in posttetraploids. First mechanism is downregulation of several mitotic kinesins, in particular, Kif18A, and associated changes in spindle geometry allowing erroneous mitosis. Second mechanism is increased tolerance to these errors on both mitotic and post-mitotic levels. On mitotic level the tolerance manifests itself as cell division despite tensionless attachments. On post-mitotic level it is observed as less frequent cell cycle arrest and death after mitotic errors. Together, these alterations support the propagation of CIN state and might contribute to CIN in cancer.

Tetraploidization drives chromosomal instability independently of the p53 status.

Multiple lines of evidence suggest that tetraploidy can lead to numerical and structural karyotypic variability of the progeny (Kaneko and Knudson, 2000; Levine et al., 1991a; Levine et al., 1991b; Reid et al., 1996). This fact was further directly shown by several studies (Baia et al., 2008; Fujiwara et al., 2005; Ganem et al., 2009; Hognas et al., 2012; Lv et al., 2012; Sansregret et al., 2011; Vitale et al., 2010). The data presented in this study supports the previously reported observations. Indeed, after six weeks of propagation in culture, the posttetraploid cells displayed a broad variety of karyotypes. Observed karyotypes ranged from near-diploidy to near-tetraploidy, as well as median chromosome numbers varied between different posttetraploids. Therefore, transient passage through tetraploid state leads to variable aneuploidy.

Previously it was shown that HCT116 cells display variable aneuploidy upon securin knockout, but after several passages these cells become chromosomally stable (Pfleghaar et al., 2005). Remarkably, in posttetraploids karyotypic variability was not

eliminated upon further passaging. Even upon propagation for 12 and for 36 additional passages, the karyotype variability remained high in the posttetraploids in contrast to progenitor diploid cells. The observed CIN in posttetraploid cells is not accompanied by p53 inactivation: upon induction of DNA damage the p53 levels increase. Therefore, this work provides not only the evidence that posttetraploid cells can become chromosomally unstable, but also directly shows their p53 proficiency (at least in response to DNA damage induction) and nevertheless CIN. This stands in contrast to many previous reports describing either early cell cycle arrest and death of p53-positive tetraploids (Fujiwara et al., 2005) or proliferation in chromosomally stable state after tetraploidization (Ho et al., 2010; Vitale et al., 2010). However, the results obtained in the present study cannot be directly compared with these reports. First, in the two studies murine fibroblasts or mammary epithelial cells were used as the progenitor cell line (Fujiwara et al., 2005; Ho et al., 2010), thus, murine to human cells variations cannot be completely ruled out. Second, the method of tetraploid cell generation might be critical for further proliferation in posttetraploid state. In the present study, cytokinesis inhibition was used as a method to produce tetraploid cells – an alternative to mitotic slippage in the presence of high concentrations of MT-depolymerizing drug nocodazole over the course of 48 h (Vitale et al., 2010). Potentially, the behavior of posttetraploid progeny can vary depending whether mitosis or cytokinesis was affected upon generation of tetraploids. This explanation can be supported by an observation that prolonged mitotic arrest using antimitotic drugs can cause increased DNA damage and affect the karyotype (Dalton et al., 2007) and potentially lead to the selection of the fittest cells that survive such an insult as prolonged mitotic block. In contrast to that, canonical DNA damage is not increased after cytokinesis failure-based tetraploidization (Kuffer et al., 2013). Finally, in the work of Fujiwara and co-authors, p53-positive tetraploid cells were analyzed only for a short period of time – for 96 hours post-formation. As the analysis of the survival of cells after tetraploidization has been carried out on population level using flow cytometry and for a short period of time (comparing to six weeks post-generation), one cannot completely rule out the possibility, that some survivor cells can emerge and give chromosomally unstable progenies.

A few reports describe aneuploidy and CIN in p53-proficient cells. One report describes deregulation of Notch pathway and overexpression of Hes1 as triggers of tetraploidy and CIN (Baia et al., 2008); of note, it is possible that not tetraploidization, but overexpression of Hes1 *per se* could trigger CIN. Using our strategy for pathway analysis, we could not identify any deregulation of Notch pathway; neither we observed deregulation of HES1 gene. Thus, deregulation of Notch pathway does not appear to play a role in CIN in posttetraploids in the presented study. In the study from Sansregret et al. overexpression of transcription factor CUX1 caused aneuploidy in the tetraploid progeny (Sansregret et al., 2011). The authors propose that prolongation of mitosis caused by CUX1 overexpression allows longer mitosis and a higher chance of extra centrosome clustering. As analyzed posttetraploid cells do not possess extra centrosomes, and the mitosis is not prolonged in posttetraploids, this scenario cannot take place in posttetraploid cells presented in my work. Importantly, in both studies the p53 status of the tetraploid progeny was not directly investigated, thus leaving the opportunity of p53 pathway attenuation. In this context, our results display evidence that the p53 pathway is not inactivated in posttetraploids.

Study from David Pellman's laboratory showed that p53-negative tetraploid progeny arising after cytokinesis failure demonstrated an increase in gross chromosomal rearrangements (Fujiwara et al., 2005). The authors report presence of double-minute chromosomes, dicentric chromosomes and non-reciprocal translocations with the median of two rearrangements per cell. The translocations normally form as a consequence of chromosome breakage and fusions (Gisselsson et al., 2000). I observed that nearly all analyzed posttetraploid cell contained constitutive chromosome translocations that were present in the original diploid cell line (only the translocations were analyzed in the presented study). The posttetraploids displayed some increase in the frequency of sporadic chromosome translocations in comparison to diploid cells. Remarkably, this increase was not dramatic: specifically, the amount of translocations in posttetraploids did not exceed one sporadic translocation per cell, if at all. It is difficult to directly compare the differences in the frequency of the chromosomal structural rearrangements between tetraploid cells, described in Fujiwara et al. study and possttetraploids, described in my work because of several reasons. First, not all aberrations were analyzed in the presented

study, second, in Fujiwara et al. study the authors analyzed murine cells, and finally, the rearrangements in Fujiwara et al. study were from cells taken from arising tumors in contrast to the cells analyzed in my study. However, overall, the frequency of the sporadic structural chromosomal aberrations appears to be lower in posttetraploids from my work. It might be that p53 presence in posttetraploids is important to prevent accumulation of chromosome aberrations, although, the exact mechanisms remain understudied.

A body of evidence suggested that tetraploidization can not only promote CIN, but be associated with tumorigenesis (Fujiwara et al., 2005; Lv et al., 2012; reviewed in Storchova and Pellman, 2004). Although this study did not address directly whether posttetraploids can accelerate tumorigenesis *in vivo* I identified some features of unstable cancer cells that are shared in analyzed posttetraploids. First, similarly as many characterized chromosomally unstable cancers (Storchova and Kuffer, 2008), analyzed posttetraploids have near-triploid to near-tetraploid karyotype. Second, a remarkable feature of tumor cells, that smaller chromosomes are more frequently lost in comparison with bigger ones (Duijf et al., 2012), was detected in HPT1 (but not HPT2). Third, a prominent nuclear blebbing and micronucleation were observed at least in HPTs. This observation is consistent with the data from David Gisselsson and colleagues who identified similar abnormalities in several chromosomally unstable malignant tissues and suggested that abnormal nuclear shape may indicate CIN (Gisselsson et al., 2001). Altogether, posttetraploid progeny shows several features of chromosomally unstable cancer cells.

In summary, my findings show that tetraploidization can lead to CIN in posttetraploid progeny in p53 proficient cells. The presence of functional p53 appears not to be sufficient to suppress observed CIN, as obtained posttetraploid cells proliferate and accumulate aneuploidy despite p53 presence.

Erroneous mitosis is a source of CIN.

Defective mitosis is a frequent cause of CIN. Consistently with karyotyping results, chromosome missegregation was elevated in posttetraploid cells. In particular, posttetraploids display an increase in the frequency of lagging chromosomes. Anaphase lagging may serve as an indirect evidence of elevated merotelic

attachment frequency (Cimini et al., 2001). Merotelic attachments, when at least one sister kinetochore is attached to both spindle poles, are not recognized by the SAC, and have been postulated as the major mechanisms of CIN in cancer cells (Cimini et al., 2001; reviewed in Gregan et al., 2011). Therefore, an increase in merotely, even in presence of functional SAC, will lead to chromosome missegregation and aneuploidy. Some evidence suggests that the merotelically attached laggards frequently segregate to a “correct” daughter cell (Thompson and Compton, 2011). However, even if segregated to a proper daughter cell, the former laggards form micronuclei that often undergo defective replication and accumulate DNA double-strand breaks in the subsequent interphase (Crasta et al., 2012). This can potentially cause fragmented chromosomes in the following mitosis. Accordingly, chromosomes without detectable centromere were observed as a lagging chromosome lacking a CREST signal (acentromeric lagging) in the high-resolution analysis of mitotic errors (Supplementary Table 2). Of note, the laggards, containing the CREST signal could also be chromosome parts containing centromeres and cannot be precisely classified as whole chromosome laggards due to the limitations of implemented assays. Further study involving both centromere and telomere co-staining is required to answer the question whether laggards can be classified as whole chromosome or chromosome fragment laggards. Alternatively, lagging chromosomes can originate in the same mitosis through a conflict of pulling forces that can potentially break double-stranded DNA of the merotelically attached chromosome (Guerrero, Martinez et al. 2010) and leave the chromosome parts lagging behind. Taking together, increased occurrence of lagging chromosomes in posttetraploids is likely a manifestation of an increase in the frequency of merotelic attachments.

Another mitotic defect prominently observed in posttetraploids, is occurrence of anaphase bridges. Numerous reasons can cause anaphase bridging: perturbed DNA replication by replication fork barrier or other replication defects (Chan et al., 2009; Sofueva et al., 2011), defective homology-directed DNA repair (Acilan et al., 2007; Laulier et al., 2011), delayed sister chromatid decatenation (Wang et al., 2008a) or telomere dysfunction (van Steensel et al., 1998). Similarly to lagging chromosomes, anaphase bridges often break in mitosis and result in micronucleation; these micronuclei contain defective nuclear pore complexes and show deregulated gene transcription (Hoffelder et al., 2004). Although we did not investigate the contribution

of DNA replication and repair defects to the CIN in the posttetraploids, we observed downregulation of both DNA replication and repair pathways (Dürrbaum et al, in preparation) that might correlate with an increase in mitotic defects in posttetraploids. However, the direct mechanistic link and causal relationship between defective mitosis and DNA replication and repair in posttetraploids has to be studied in greater detail.

Altogether, a broad variety of mitotic errors can be observed in posttetraploid cell lines. Potentially, merotelic kinetochore attachment and defective DNA replication may be responsible for persistent chromosome missegregation in these cells.

Supernumerary centrosomes are not the sole source of CIN in posttetraploid cells.

Supernumerary centrosomes have been since a long time suspected to be the major source of CIN (translated and annotated in Boveri, 2008). In fact, cells of many unstable cancers, both solid and hematopoetic, contained amplified centrosomes (Chan, 2011; Ghadimi et al., 2000; Lingle et al., 2002; Pihan et al., 1998). Mutations and deregulation in plethora of both oncogenes and tumor suppressors can cause centrosome overamplification in cancers (Fukasawa, 2007). Another straightforward route to obtain multiple centrosomes is cytokinesis failure. In the interphase following cytokinesis failure both centrosomes get duplicated, thus producing four centrosomes causing multipolarity in the next mitosis. Therefore, multiple centrosomes were considered to be the most obvious reason to cause aneuploidy in the cells after induced tetraploidization.

Indeed, the fact that formation of multipolar spindle, followed by abnormal mitosis and cytokinesis, leads to chromosome segregation errors and severe aneuploidy was proposed already by T. Boveri in the beginning of last century (translated and annotated in Boveri, 2008). However, multipolar mitosis often results in cell cycle arrest and in death of the progeny (Ganem et al., 2009). As expected, we observed massive cell cycle arrest and death following early consecutive tetraploid mitoses (present study; Kuffer et al., 2013). Accordingly, the cells containing multiple centrosomes are eliminated from the total population after several rounds of mitoses. We observed that the frequency of multipolar division in posttetraploids was very low six week after the transient tetraploidy. Potentially, the reduction in anaphase

multipolarity is important to reduce the severity of chromosome missegregation and maintain nearly normal chromosome complement.

Many cancer cells with multiple centrosomes develop a strategy to reduce anaphase multipolarity by clustering the supernumerary centrosomes (Ganem et al., 2009; Kwon et al., 2008; Quintyne et al., 2005; Ring et al., 1982; Saunders, 2005; Silkworth et al., 2009). In this case, either all four centrosomes obtained after first tetraploid interphase can cluster pairwise thus producing a pseudo-bipolar spindle, or only two from four are clustering, thus forming a tripolar spindle. Importantly, even the formation of pseudo-bipolar spindle through centrosome clustering does not guarantee faithful chromosome segregation. Mounting evidence suggests that clustering prior to the anaphase onset can cause merotely and manifest itself in frequent occurrence of lagging chromosomes in anaphase (Ganem et al., 2009; Silkworth et al., 2009).

Therefore, it is plausible to speculate that maintaining the extra centrosomes is disadvantageous since it affects the genome stability. Cells that have reduced the centrosome numbers early might gain growth advantage. Data supporting this view were obtained in two laboratories. First, several rounds of induced cytokinesis block in proliferating p53-proficient cells does not lead to centrosome amplification (Krzywicka-Racka and Sluder, 2011). Second, upon extended passaging tetraploid cells lose their extra centrosomes; moreover, loss of the extra centrosomes correlated with the decrease in appearance of chromosomes lagging in anaphase (Ganem et al., 2009). Accordingly to the above presented data, only minor fraction of analyzed posttetraploid cells contained more than two centrosomes. We also observed that the amount of total mitotic errors was reduced with the reduction of centrosome numbers in posttetraploids in comparison with the newly formed tetraploid cells. Strikingly, chromosome missegregation in posttetraploids was not completely eliminated, but decreased comparing to the newly formed tetraploids. This is in contrast to the reported data from David Pellman's laboratory. This discrepancy can be caused by several reasons. First, in the work from David Pellman's laboratory the authors knocked down p53 to allow progression through the first tetraploid mitoses in otherwise non-proliferating tetraploid cells; this knockdown appeared not to be necessary in our case. The inhibition of p53, even transient, might affect chromosome stability. Second, the cells obtained in our laboratory were

passaged over the course of six weeks to allow growth of a cell population out of single individual cell. This potentially can allow achievement of additional changes causing CIN. In contrast to that, the authors from David Pellman's laboratory generated tetraploids by sequential FACS sorting of a total population after induced cytokinesis failure to obtain tetraploids with two centrosomes. Therefore, differences in the selection of tetraploid cells can potentially affect the behaviour of the cells after tetraploidization.

In summary, posttetraploid cell lines reduced their centrosome numbers to maintain robust spindle bipolarity. Thus, the high levels of chromosome missegregation in posttetraploids cannot be attributed solely to the presence of extra centrosomes.

Sister chromatid cohesion is not altered in posttetraploids.

Defects in the sister chromatid cohesion can lead to defective chromosome segregation and CIN (Barber et al., 2008; Hoque and Ishikawa, 2002; Sonoda et al., 2001). Interestingly, defects in the sister chromatid cohesion was reported for yeast tetraploids (Storchova et al., 2006). Whole transcriptome analysis showed that the mRNA levels of one of the subunits of cohesin (Smc3) is consistently decreased in both HPTs. Downregulation of Smc3 was reported to contribute to CIN in an unexpected manner – affecting centrosome number duplication and causing multipolarity (Ghiselli, 2006). This mechanism is unlikely to take place in posttetraploids, since we did not observe any substantial centrosome number amplification. Downregulation of Smc3 was also reported to cause sister chromatid cohesion defect and lead to CIN (Barber et al., 2008). In posttetraploid cells, sister chromatid cohesion does not appear to be altered: neither prominent primary constriction gaps were observed in these cells, nor the distance between sister kinetochores was strongly increased. Possibly, downregulation of Smc3 might limit cohesin complex formation and affect establishment of a proper sister chromatid cohesion without visible defects using assays implemented in the present work. Whether Smc3 downregulation alone is contributing to CIN, and if yes, sufficient to trigger CIN, however, remains to be studied in more detail.

Altered levels of mitotic kinesins change the spindle geometry and enhance the frequency of segregation errors.

In recent years a great attention has been drawn to the role of altered MT dynamics in CIN. Several studies have suggested that increased stabilization of MTs affects the KT-MT attachment error correction rate, thus leading to a higher chance of persistence of incorrect attachments (Bakhoum et al., 2009a; Bakhoum et al., 2009b). This scenario can take place upon downregulation of some mitotic kinesins with depolymerase function or dampening MT polymerization, thus causing slower MT dynamics at the kinetochore (Bakhoum et al., 2009b; Choi and McCollum, 2012; Manning et al., 2007). For example, a decrease of Kif2C/MCAK can enhance the stabilization of incorrect attachments (Bakhoum et al., 2009a). Not only excessive stabilization of MTs and thus slower KT-MT attachment error correction rate can lead to chromosome missegregation, but also high dynamic instability of the KT-MT interaction can manifest itself in CIN. The latter has been reported for deletion of kinesin Kif10/CENPE in murine cells: chromosome segregation fidelity was compromised due to defective KT-MT interactions (Putkey et al., 2002). Similarly, loss of centromeric CENP-F leads to unstable MT capture at the kinetochore and chromosome missegregation (Bomont et al., 2005). Together, the maintenance of proper MT dynamics at the kinetochores appears to be very important for faithful chromosome segregation.

In the presented study, recurrent changes were identified in the expression levels of several mitotic kinesins. However, many of the changes of the expression levels were not confirmed by immunoblotting for all analyzed kinesins. For example, the changes were not confirmed for Kif2C/MCAK and in some posttetraploid cell lines for Kif15. Remarkably, a plus-end MT depolymerase kinesin Kif18A is downregulated in nearly all analyzed PTs and this was confirmed also by immunoblotting. According to the concentration-dependent model of Kif18A action, downregulation of Kif18A can lead to a decrease of depolymerization at the MT plus-end. Thus, the rate of KT-MT attachment error correction at the kinetochore might be reduced and cause subsequent chromosome missegregation.

RNAi depletion of Kif18A was reported to impair chromosome congression, increase the spindle length, decrease the tension on sister kinetochores and activate Mad2-dependent SAC response (Mayr et al., 2007; Stumpff et al., 2012). The spindle length and accordingly, the width, are significantly increased in PT cell lines. However, I did not detect any congression defects in posttetraploid cells. Moreover,

no SAC activation has been observed, as the time from the nuclear envelope breakdown to the onset of anaphase was not increased in the posttetraploids. This phenotype might be explained by the fact that Kif18A levels are only moderately decreased and the remaining protein amount suffices for proper chromosome congression. Alternatively, concurrent changes in levels of other kinesins might compensate for the congression defect. For example, the RNAi-mediated depletion of Kif18A leads to long spindles and abnormal metaphase plate formation; additional co-depletion of Kif4A results in normal chromosome congression, but the spindle remains longer (Stumpff, Wagenbach et al. 2012). Accordingly, the levels of both Kif18A and Kif4A are partially decreased in HPT1 and HPT2, which might enable the increased spindle length without a strong defect of the metaphase plate. Remarkably, mRNA levels of Kif18A are slightly higher in HPT1 than in HPT2, and conversely, levels of Kif4A are slightly higher in HPT2 than in HPT1. Thus one possibility might be that the nearly equal “sum level” of both downregulated kinesins leads to the same phenotypic outcome in both HPTs: similar increase in MT length, absence of the deffect in metaphase plate formation and similar level of mitotic errors.

The altered spindle geometry – increased spindle width and length – likely helps to accommodate higher chromosome numbers of posttetraploid progeny. Eukaryotic cells can scale up the spindle length and width to embrace more chromatin, as larger chromatin mass leads to an increase in microtubule length and formation of longer spindles *in vitro* (Dinarina et al., 2009). Similarly, the spindle length in allotetraploid *Xenopus laevis* is increased in comparison to its diploid relative *Xenopus tropicalis*, owing to the lower activity of a microtubule-severing protein katanin (Loughlin et al., 2011). Of note, besides Kif18A and Kif4A that affect spindle length, the transcription of a microtubule severing protein fidgetin (FIGNL1) is also decreased in both HPT1 and HPT2 (Table 2). Although the function of fidgetin in human mitosis is not fully understood, its downregulation in posttetraploid cells might have the same effect as the inhibition of katanin in tetraploid *X. laevis*. Thus, downregulation of Kif18A, together with Kif4A and potentially FIGNL1, might allow MT elongation and thus segregation of larger DNA mass.

This latter hypothesis is supported by the fact that Kif18A protein levels are dramatically reduced already in the newly formed tetraploids. Notably, the decrease

in protein levels for Kif18A in newly formed tetraploids is unlikely due to the cell death. At the time of the sample collection (24 h from DCD release) the majority of cells are in G2 of the interphase after the 1st tetraploid mitosis and almost no cell death was observed at that time using live cell imaging. However, as the expression of Kif18A gene is cell-cycle regulated and it peaks at G2/M phases (Mayr et al., 2007; Zhang et al., 2010), it can be that the decrease in Kif18A levels at 24 h after the release from DCD can be attributed to observed cell cycle arrest (around 50% of the newly formed tetraploids are arrested by this time) and thus absence of Kif18A gene expression. To investigate whether the decrease in Kif18A levels in newly formed tetraploids is due to lack of the gene expression, it is required to define at what cell cycle stage do tetraploid cells arrest: whether the arrest takes place in G1 after the 1st tetraploid mitosis or further in G2. In the latter case, Kif18A gene should already be transcribed and expressed, and the observed levels are thus not diminished due to cell cycle arrest-mediated lack of gene expression If that holds true, then we can speculate that newly formed tetraploids, because they possess double the amount of DNA in comparison to diploids, have a particular requirement for increased length and width of the mitotic spindle. In turn, allowing the segregation of a larger DNA mass comes at the cost of CIN: newly formed tetraploids and their posttetraploid derivatives display chromosome missegregation, albeit to a different level. Remarkably, in RPT4, the only one of all PT cell lines where the Kif18A levels were not decreased, the chromosome numbers are closer to diploid level (median equals 46). Likely, as RPT4 reduced the number of chromosomes, the decreased Kif18A levels might no longer be essential for the spindle formation. However, it should be noted that the causal relationship remains elusive as the mechanisms of Kif18A regulation are not well understood. Together, Kif18A downregulation might be sufficient to keep chromosome missegregation in the posttetraploids. Nevertheless, it does not exclude additional mechanisms that can further contribute to CIN in posttetraploids.

Interestingly, spindle length does not get accommodated in *S. cerevisiae* polyploids, however, spindle width does (Storchova et al., 2006). Thus, the spindle angle is dramatically increased in tetraploid yeast cells in comparison to progenitor haploids. This geometry was suggested to be the reason in the erroneous mitosis of yeast tetraploids, as it allows a higher frequency of syntelic attachments. In human

posttetraploid cells the increase in a spindle length is proportionally lower than the corresponding increase in the width. It manifests itself not only in longer MTs, but also in in larger spindle angle. Given the multiple KT-MT attachment sites per kinetochore in human cells, both syntelic and merotelic attachments can be formed with a higher probability in posttetraploid cells. This increase in syntely and merotely might contribute to CIN in human posttetraploids, consistently to a proposed model in *S. cerevisiae*.

A decrease in Kif18A levels can alter the stoichiometry in binding between Kif18A and its interaction partners playing important roles in mitosis, such as Survivin (BIRC5), Kif2C/MCAK, BubR1, Cdc8, Ndc80, Cdc20, Clasp1, CenpN, CenpA, CenpE, even if the levels of the latter are not affected *per se*. For example, these proteins have described roles in chromosome passenger complex, KT-MT attachment error correction, mitotic checkpoint, centromere organization. Potentially an alteration in the protein-protein interaction stoichiometry between Kif18A and these proteins can alter the mitotic progression and cause chromosome missegregation; this represents an attractive direction for further investigation.

Taken together, we propose the following model of microtubule dynamics alteration in posttetraploids, associated, in particular, with Kif18A downregulation. The microtubule motor activities are specifically modulated in posttetraploid cells likely contributing to mitotic progression. First, alterations in mitotic motors change spindle geometry to segregate higher chromosome numbers. Second, geometry changes are associated with moderate chromosome missegregation. Potentially, Kif18A downregulation provides a selective advantage for posttetraploid cell proliferation. In this scenario, the proliferation might come at the costs of CIN.

To further validate this model future research is required. First, it remains unclear whether restoration of Kif18A protein levels can restore MT length closer to the length in diploid cells (i.e., to shorten the MTs) and if yes, whether this MT length change will rescue chromosome missegregation. Second, it remains to be understood, what mechanisms cause Kif18A downregulation as early as already in newly formed tetraploids and whether increased DNA mass is causal of Kif18A downregulation to allow formation of longer MTs. An alternative possibility is that Kif18A is decreased due to some other reason independent on larger chromosome

mass and this change allows longer spindles and associated chromosome segregation errors. Finally, it remains an open question, whether Kif18A downregulation alone is responsible for CIN in posttetraploid cells. This possibility is rather unlikely, as continual chromosome missegregation triggers chromosome copy number imbalance, and likely, imbalance in mitotic regulators, KT and MT proteins. In turn, these events can maintain the deregulation of KT-MT dynamics, thus forming a positive feedback loop for persistent chromosome missegregation. This model is consistent with a previously proposed model that even slightly destabilized aneuploid genome can become very labile with time (Matzke et al., 2003).

Increased tolerance to mitotic errors contributes to CIN in posttetraploid cells.

Malfunction of cell cycle checkpoints may represent a potential source of chromosome missegregation and CIN. In particular, defective spindle assembly checkpoint (SAC) can lead to aneuploidy (Cahill et al., 1998; Hanks et al., 2004; Kops et al., 2005; Michel et al., 2001; Musio et al., 2003; Ryan et al., 2012; Sotillo et al., 2007). SAC function can be tested using the mitotic poisons affecting MT dynamics. For example, nocodazole in low nanomolar concentrations was reported to cause decreased MT turnover (Vasquez et al., 1997) that perturbs KT-MT interactions. In turn, the SAC is activated and the time from nuclear envelope breakdown to the onset of anaphase is, accordingly, prolonged. I tested the SAC response using both low (0.5 ng/ml, nanomolar range) concentration of nocodazole, as well as high (200 ng/ml) concentration that arrests cells in metaphase. SAC was activated in response to both partial and complete MT depolymerization by nocodazole in posttetraploids: the posttetraploid cells prolonged the time in metaphase similarly as diploids. Remarkably, chromosome misalignment caused by low concentration of nocodazole halt the anaphase progression in both diploids and posttetraploids, similarly to previous reports on antimitotic drug effects on the majority of CIN cancer cells (Blajeski et al., 2002; Gascoigne and Taylor, 2008; Lee et al., 2004). Furthermore, prolonged mitotic arrest response is consistent with available data on both MIN and CIN cancer cells, showing a robust SAC activation upon treatment with high nocodazole concentration (Tighe et al., 2001).

Notably, even low concentration of nocodazole treatment is a severe insult to cell

fitness and subsequent proliferation. Not only chromosome missegregation dramatically increases in both diploids and posttetraploids, but also the majority of missegregating posttetraploid cells arrest or die in the following interphase. These facts confirm that the effect of nocodazole on posttetraploid cells is very strong and is sufficient to affect cell viability. We hypothesized that testing the activation of the SAC by the strategy that does not affect MTs dynamics, but still increase the frequency of incorrect attachments, might help to reveal possible SAC alterations.

In order to address this latter possibility, SAC activation was further tested upon treatment with Kif11/Eg5 inhibitor VS-83, an analog of monastrol (Mayer et al., 1999) that causes monopolar spindle formation. In this scenario, MTs retain their dynamic properties, i.e. the depolymerization and polymerization rate are likely not altered. Instead, syntelic and merotelic non-bioriented attachments are formed, rendering sister chromatids attached to MTs in a tensionless attachment. The biorientation and proper chromosome attachments are not achieved as long as the inhibitor is present. Thus, SAC-proficient cells should halt the anaphase onset in this case and eventually slip out of mitosis. My data indicates that posttetraploid cells are able to progress through mitosis despite the presence of tensionless attachments, i.e. divide their chromosomes into two (and sometimes more than two) daughter nuclei. This feature was observed in both analyzed HPTs and RPT1. Careful analysis excluded the possibility that posttetraploid cells are more resistant to this inhibitor, as the bipolar spindle frequency was only slightly increased in posttetraploids in comparison to diploids. A few mutually not excluding possibilities can be considered. First possibility is that posttetraploids cannot recognize tensionless attachments because of a specific defect in SAC. To address this possibility, to date, I analyzed the mRNA levels of the SAC genes (~80 entries) and could identify only one recurrent change in both HPT1 and HPT2 that could explain the observed phenotype: a strong downregulation of a kinetochore-associated mitotic checkpoint protein KNTC1. Its inactivation was shown to cause aberrant mitosis in human and *D. melanogaster* cells (Basto et al., 2000; Chan et al., 2000). More data about the SAC protein levels and activity in PTs will be required to answer the question of SAC functionality in these cells. As cells dividing chromosomes prolong time from NE breakdown to onset of anaphase, although this time period is shorter than from NE breakdown to mitotic slippage in slipping cells, it suggests a second possibility. The possibility is

that SAC might get activated in response to tensionless attachments, but cannot be maintained for long. Generally, the possibility of weakened SAC is a matter of a debate in the field. Some data supports the view that even a single unattached kinetochore is sufficient to activate SAC and to halt the anaphase onset (Rieder et al., 1994). Other findings indicate that SAC can be weakened, i.e. cannot be maintained for long due to inefficient recruitment and/or mutations in SAC factors (Weaver and Cleveland, 2005). Our data about the SAC activation and maintenance in posttetraploid cells in response to tensionless attachments rather supports the latter view and suggests a specific SAC weakening in the posttetraploids.

The third considered possibility is that posttetraploids can in fact recognize tensionless attachments, but cannot properly correct them. Potentially, inefficient error correction at the kinetochore may occur due to insufficient Kif18A and thus slower MT depolymerization at the kinetochores. Finally, the increased frequency of division in the presence of tensionless attachments in posttetraploids can be associated with cumulative effects of both weakened SAC and defective error correction. In this context, downregulation of Kif18A contributes to inefficient error correction at the kinetochores and, additionally, weakened SAC allows the division despite the malattachments. Thus, defective SAC in posttetraploids might provide an additional explanation to the lack of mitotic arrest, observed by Kif18A RNAi-mediated depletion alone in the work from Thomas Mayer laboratory (Mayr et al., 2007), and further proliferation in CIN state.

The lack of postmitotic arrest in the following G1 can also contribute to increased chromosomal instability observed in posttetraploid cell lines. Both human diploid cells as well as the majority of newly formed tetraploid cells enter a permanent p53-dependent arrest and often die after chromosome missegregation (Andreassen et al., 2001; Ganem and Pellman, 2007; Thompson and Compton, 2010; Vitale et al., 2010). Our observations on diploid and tetraploid cells support these findings (this study; Kuffer et al., 2013). However, posttetraploid cells arrest and die with a significantly lower frequency after bipolar erroneous mitoses in contrast to their progenitor cell lines. These findings indicate that not only the mitosis *per se* is affected in posttetraploids, but also the *downstream* cell cycle arrest pathways might be attenuated.

The observed arrest in the progenitor diploid and newly formed tetraploid cell lines is mediated through p53 (Kuffer et al., 2013). In interphase following chromosome missegregation, phosphorylated p53 gets stabilized and accumulates in the nucleus (Thompson and Compton, 2010). I hypothesized that if p53 activation is defective, it might fail to accumulate in the nucleus. Indeed, less prominent p53 enrichment in the main nuclei after chromosome missegregation was observed in posttetraploids in comparison to diploids. The data suggests that the activation of the p53 after mitotic errors might be impaired in posttetraploid cells. Furthermore, we identified p53 pathway deregulation using gene expression data on posttetraploid cells. This deregulation may at least partially be responsible for altered response to defective mitosis. Taken together, p53 response to chromosome missegregation is attenuated in posttetraploids. We propose that cells with attenuated p53 response might proliferate better despite chromosome missegregation.

The data from Duane Compton's laboratory demonstrated that p53-dependent cell cycle arrest after chromosome missegregation is executed through a *downstream* target of p53 – p21 (Thompson and Compton, 2010). A remarkable increase has been observed in the expression levels of the CDKN1A gene encoding p21. Although the reasons of this phenomenon are unclear, potential scenario could be that the concurrent increase in p21 might allow selective proliferation of only moderately missegregating cells. However, the role of p21 deregulation in the proliferation of posttetraploids was not directly investigated and requires further study.

A large body of evidence suggests that moderate levels of CIN are better compatible with extended survival, in contrast with high CIN levels (Watanabe et al., 2012). Our findings are in line with this proposal. In a stark contrast to newly formed tetraploids (Fujiwara et al., 2005; Ho et al., 2010; Kuffer et al., 2013), posttetraploid cells reduce the levels of chromosome missegregation to a moderate, yet higher than diploids, level, and efficiently proliferate. This hypothesis was further corroborated by the report that artificial increase in chromosome missegregation can act as an efficient strategy in eliminating tumor cells (Janssen et al., 2009). In agreement with this report, increasing the chromosome missegregation in posttetraploids by low concentrations of nocodazole triggers cell cycle arrest and subsequent death.

The presented analysis of progeny arising from individual human tetraploid cells suggests that CIN results from alterations in two major mechanisms accordingly to a following model. First, downregulation of one of key mitotic kinesins, Kif18A, leads to altered spindle geometry to allow segregation of large DNA mass and increased rates of chromosome segregation errors. Second, an altered response to defective attachments and p53 pathway attenuation allows posttetraploids to tolerate increase in chromosome missegregation. The identified changes characterize a route that might be relevant for formation of cancer cells with complex near-tri and near-tetraploid karyotypes. The expression of kinesins in tumor cells is often abnormal, and kinesins are becoming an alternative for cancer therapy (Huszar et al., 2009). Notably, overexpression of Kif18A was reported to be associated with tumorigenesis, particularly colon and breast carcinogenesis (Nagahara et al., 2011; Zhang et al., 2010). Further research has to be carried out in order to understand whether downregulation of Kif18A could also promote tumorigenesis. As Kif18A downregulation is linked to abnormal mitotic progression, it is plausible to speculate that lack of mitotic arrest (either due to defect in SAC or only partial downregulation of Kif18A) allows progression with mitotic errors and accumulation of aneuploidy. Further research on the role of microtubule dynamics and motor activity in CIN cells, as well as SAC function will be important for the understanding of the role of kinesins and contribution of SAC weakening in CIN and tumorigenesis.

Supplementary Information

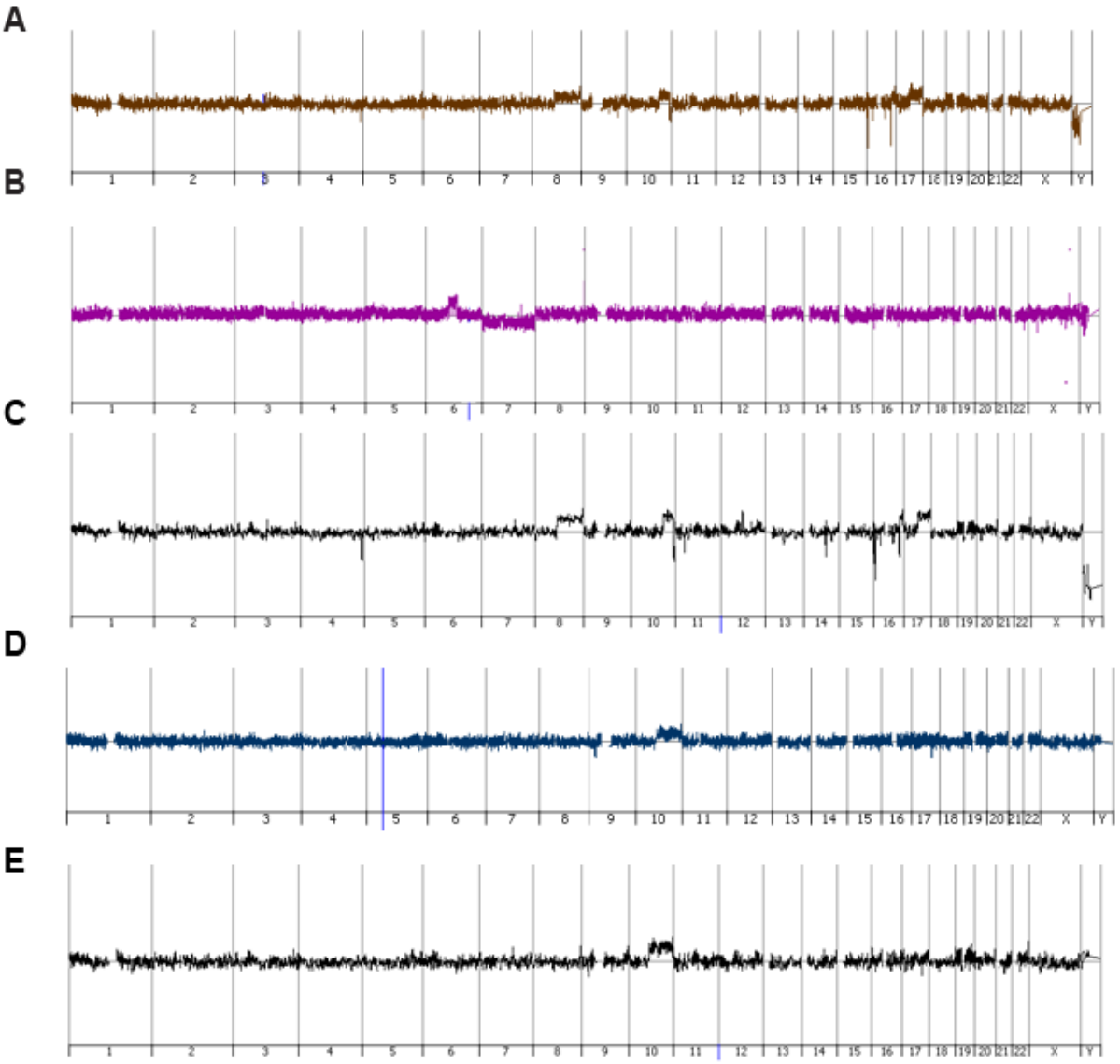

Supplementary Figure 1. aCGH of HCT116 and RPE1 and their posttetraploid derivatives.
aCGH of (A) HCT116, (B) HPT1, (C) HPT2, (C) RPE1 (here aCGH of RPE1 not expressing H2B-GFP is shown), (D) RPT1. (B) HPT1 shows deregulation of chromosome 7. A major part of chromosome 6 is amplified, besides a small amplification present on chromosome X. The graph represents the HPT1 signal normalized to HCT116 signal (HCT116 was used as a reference control for a CGH hybridization) (C) HPT2 shows amplification of major parts of chromosomes 8, 10, 16 and 17 and a deletion of the Y chromosome in comparison to the human reference DNA. (E) RPT1 shows amplification of major parts of chromosome 10 in comparison to the human reference DNA. X-axis indicates the chromosomes, aligned from chromosome 1 to chromosome Y.

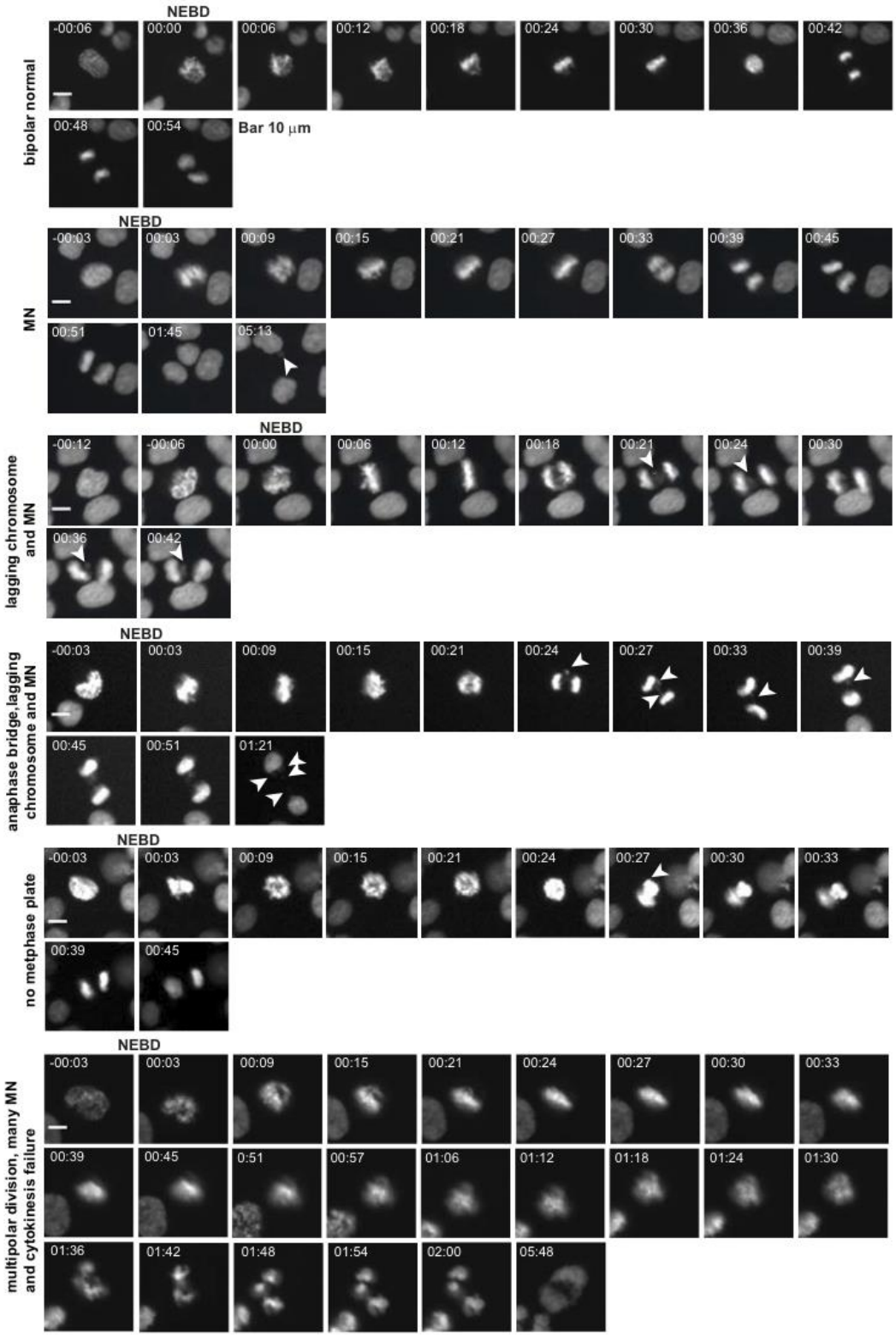

Supplementary Figure 2. Examples of observed chromosome segregation errors in live cell imaging.

Chromatin is visualized by H2B-GFP, time: hh:mm. White arrowheads indicate errors in bipolar mitosis.

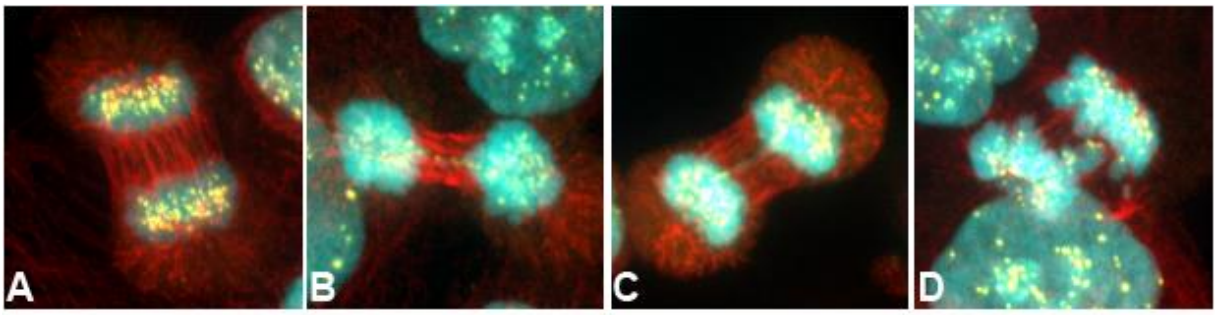

Supplementary Figure 3. Representative images of mitotic errors in HPTs.

(A) No mitotic errors; (B), (C) Anaphase bridges; (D) Anaphase bridges and lagging chromosomes. Staining: DNA Sytox Green (cyan), MTs α-tubulin (red), centromeres (CREST, yellow).

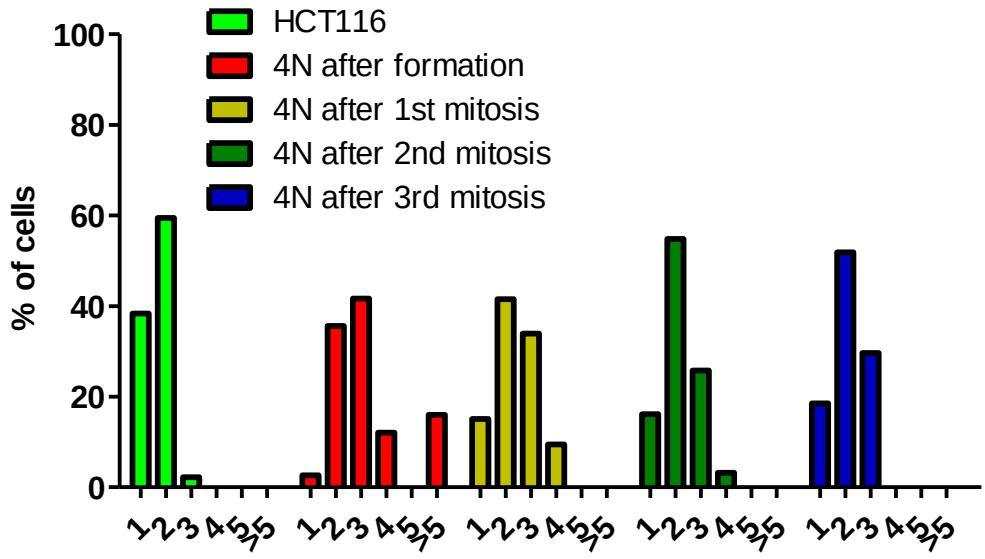

Supplementary Figure 4. Reduction in the centrosome numbers after progression through several consecutive mitoses in newly formed tetraploid cells.

Centrosome numbers in the newly formed tetraploid cells. X-axis: the number of centrosomes. HCT116 - no treatment, 4N after formation – 4 hours, 4N after the first mitosis – 24 hours, 4N after the second mitosis – 48 hours, 4N after the third mitosis – 80 hours after DCD release.

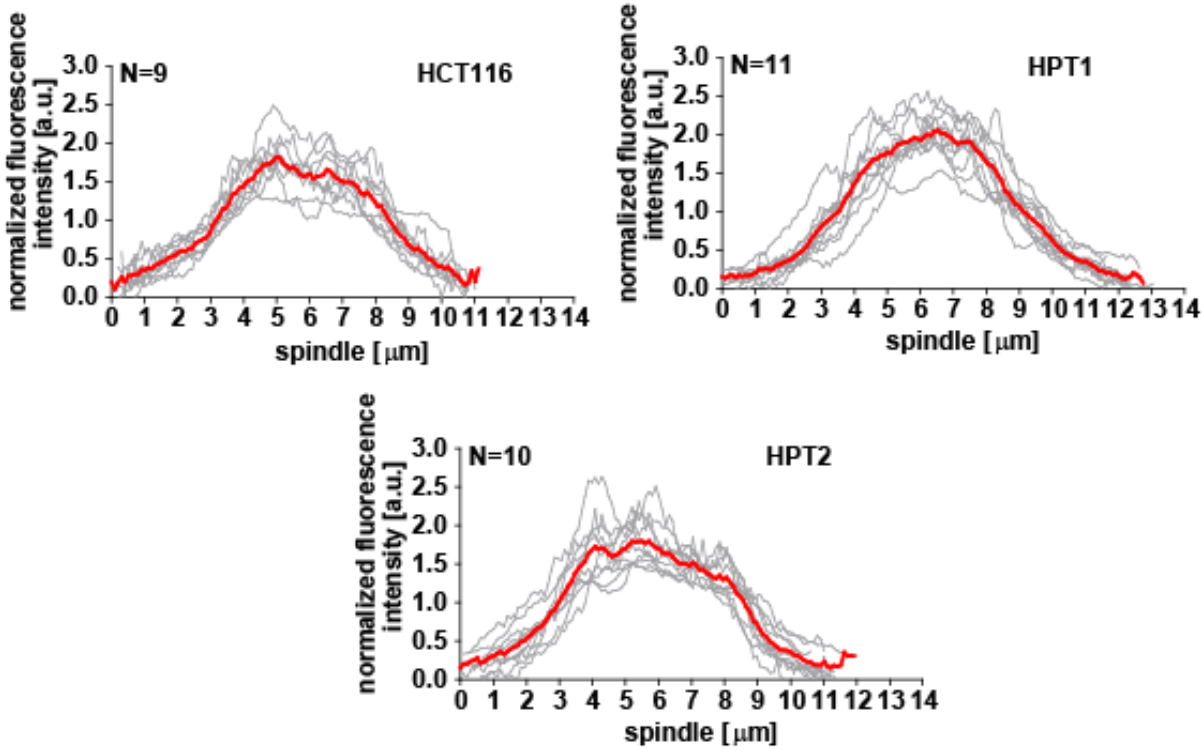

Supplementary Figure 5. The chromosome oscillations are unlikely to be altered in the posttetraploids.

Normalized intensity of the CREST signal along the spindle in HCT116 and its posttetraploid derivatives, mean of measurements for nine to eleven cells per cell line. The mean intensity line is depicted in red; intensity lines for every individual cell are shown in grey. The image analysis was carried out by Dr. Zuzana Storchova.

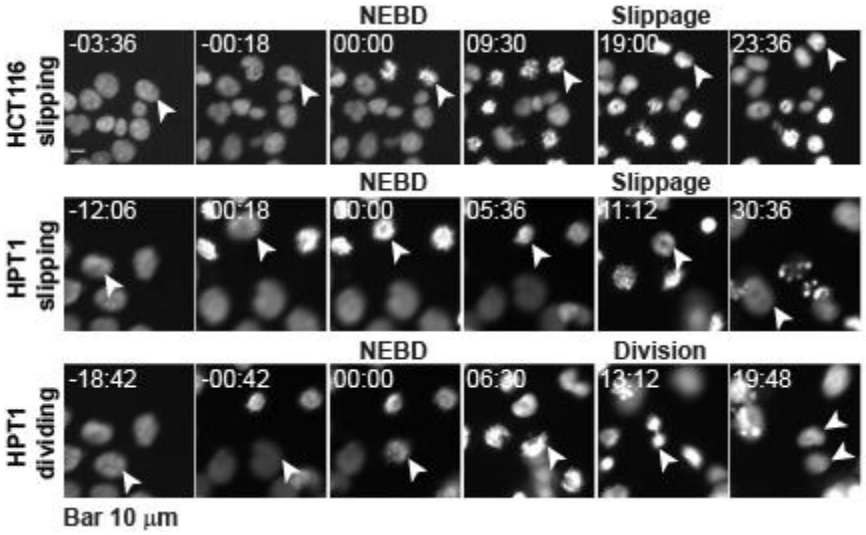

Supplementary Figure 6. Posttetraploid cell lines divide in presence of tensionless microtubule-kinetochore attachments.

Cells arresting and dividing in the presence of VS-83 (live cell imaging), time: hh:mm. White arrowheads indicate the cells followed on the timelapse tiles.

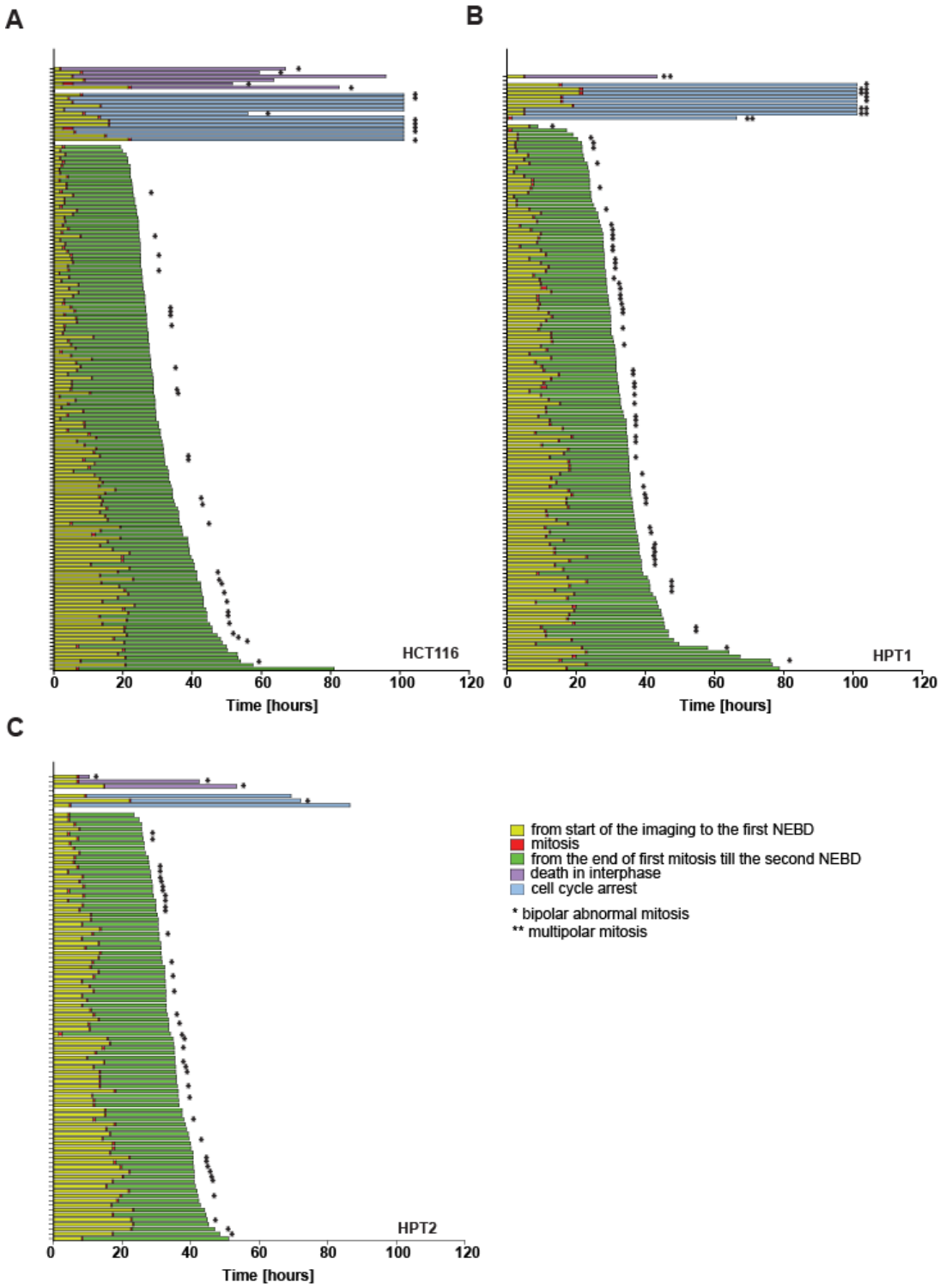

Supplementary Figure 7. Fate analysis of HCT116 and HPTs (one representative experiment out of four).

cell line	mitotic phase	type of error in anaphase, number of observed errors	presence/absence of centromeres in the observed error (description)
HPT1	anaphase	lagging chromosome, 2	3 CREST in the lagging chromosomes
HPT1	anaphase	lagging chromosome, 2	no CREST in the lagging chromosomes, 1 CREST in the part of DNA that is not in the total mass, but does not look like an obvious lagging
HPT1	anaphase	anaphase bridge, 1	stretched CREST signals at both ends of the bridge
HPT1	anaphase	lagging chromosome, 2	no CREST in one lagging chromosome, CREST in the other lagging, CREST in the part of DNA that does not look like an obvious lagging
HPT1	telophase	lagging chromosome, 1, anaphase bridge, 1	no CREST signal in either of errors
HPT1	anaphase	lagging chromosome, 2	no CREST in one lagging chromosome, CREST in the other lagging
HPT1	anaphase	lagging chromosome, 3, anaphase bridge, 2	2 CREST signals in one lagging, no CREST signals in two other ones, non-stretched CREST signals at both ends of the 1st bridge, stretched CREST signals at both ends of the 2nd bridge
HPT1	anaphase	no error	
HPT1	late anaphase	lagging chromosome, 2	CREST in both lagging chromosomes
HPT1	telophase	telophase bridge, 1	CREST signals at both ends of the bridge
HPT1	anaphase	no error	
HPT1	anaphase	lagging chromosome, 1	CREST signal in the lagging chromosome
HPT1	anaphase, might be 3 MTOCs	lagging chromosome, 4	3 CREST in the 1st lagging chromosome, 3 CREST in 2nd lagging chromosome, 1 CREST in the 3rd lagging chromosome, no CREST in the 4th lagging chromosome
HPT1	late anaphase	anaphase bridge	stretched CREST signals at one end of the bridge
HPT1	anaphase	anaphase bridge, 2, lagging chromosome, 1	non-stretched CREST signals at both ends of the 1st bridge, stretched CREST signals at both ends of the 2nd bridge, no CREST in lagging
HPT1	anaphase, might be 3 MTOCs	lagging lateral chromosome, 1	3 CREST in the lagging chromosome

HPT1	late anaphase	anaphase bridge, 1	2 non-stretched CREST signals at both ends (2 on each) of the bridge
HPT1	anaphase	no error	
HPT1	anaphase, might be 3 MTOCs	lagging chromosome, 6	~26 CREST signals in all laggings, except one lateral lagging, at least 2 of them are stretched
HPT1	telophase	lagging chromosome, 2	no CREST in one lagging chromosome, CREST in the other lagging chromosome
HPT1	anaphase	anaphase bridge, 1	no CREST signal in the bridge
HCT 116	anaphase	no error	
HCT 116	telophase	no error	
HCT 116	anaphase	no error	
HCT 116	anaphase	no error	
HCT 116	telophase	no error	
HCT 116	anaphase	no error	
HCT 116	telophase	no error	
HCT 116	anaphase	no error	
HCT 116	anaphase	no error	
HCT 116	anaphase	no error	
HCT 116	anaphase	no error	
HCT 116	anaphase	lagging chromosome, 1	3 CREST signals in the midzone
HCT 116	anaphase	no error	
HCT 116	telophase	lagging chromosome, 2	CREST in both lagging chromosomes
HCT 116	anaphase	no error	
HCT 116	anaphase	no error	
HCT 116	anaphase	lagging chromosome, 1	2 CREST signals in the lagging chromosome
HCT 116	telophase	no error	

HCT 116	anaphase	anaphase bridge, 1	non-stretched CREST signals at both ends of the bridge
HCT 116	anaphase	lagging chromosome, 2	no CREST signals in the lagging chromosome
HCT 116	telophase	no error	
HCT 116	telophase	telophase bridge, 1	stretched CREST signals at both ends of the bridge
HCT 116	telophase	no error	
HCT 116	anaphase	no error	
HPT2	telophase	lagging chromosome, 1	2 big but faint CREST signals in the midzone
HPT2	anaphase	anaphase bridge, 1	1 CREST in the part of DNA that is not in the total mass, but does not look like an obvious lagging
HPT2	telophase	anaphase bridge, 1	non-stretched CREST signals at both ends of the bridge, 2 CREST in the part of DNA that is not in the total mass, but does not look like an obvious lagging
HPT2	telophase	no error	
HPT2	telophase	no error	
HPT2	telophase	no error	
HPT2	anaphase	lagging chromosome, 2	CREST in both lagging chromosomes
HPT2	anaphase	no error	
HPT2	anaphase	no error	
HPT2	anaphase	anaphase bridge, 2	non-stretched CREST signals at both ends of the 1st bridge, stretched CREST signals at both ends of the 2nd bridge
HPT2	telophase	no error	
HPT2	anaphase	lagging chromosome, 1	1 CREST signal in the lagging chromosome
HPT2	telophase	lagging chromosome, 2	1 CREST signal in the 1st lagging chromosome, no CREST in the 2nd (lateral) lagging chromosome
HPT2	anaphase	anaphase bridge, 1, lagging chromosome, 1	non-stretched CREST signals at both ends of the bridge, no CREST in the lagging chromosome
HPT2	anaphase	anaphase bridge, 1	~6 CREST signals in the anaphase bridge
HPT2	telophase	telophase bridge, 1	no CREST signal

HPT2	anaphase	anaphase bridge, 1, lagging chromosome, 1	non-stretched CREST signals at both ends of the bridge, 2 CREST in the lagging chromosome
HPT2	anaphase	no error	

Supplementary Table 1. High resolution imaging analysis of mitotic errors observed in HCT116 and its posttetraploid derivatives.

ratio HPT1/ HCT116 [log_2]	up-/downregulation	ratio HPT2/ HCT116 [log_2]	up-/downregulation	gene names	function
-1.17	down	-0.47		aurkb;aurkb-sv2;AURKB;AIK2;AIM1;ARK2;STK12	**Mitotic error correction**
-1.02	down	0.04		CDCA8;PESCRG3	
-0.75	down	0.10		BIRC5;API4;IAP4	
-0.65		-0.36		INCENP	
-1.18	down	-0.63		CASC5;KIAA1570;KNL1	**Kinetochore**
-0.63		-0.06		MIS12	
-1.35	down	-0.13		CENPA	
-0.35		-0.19		CENPB	
-0.68		-0.43		CENPC1;CENPC;ICEN7;hCG_40345	
-0.48		-0.20		CENPH;ICEN35;hCG_27171	
-1.50	down	-0.10		CENPI;FSHPRH1;ICEN19;LRPR1;RP5-1188J21.1-002;RP5-1188J21.1-003	
-1.31	down	-0.69		CENPE	
-0.68		-0.04		ZW10	
-1.03	down	-0.16		ZWILCH	
-0.37		-0.06		KATNA1;RP1-12G14.1-004;RP1-12G14.1-005	**Severing MAPs**
-1.96	down	-2.43	down	FIGNL1	
-0.12		0.47		SPAST;ADPSP;FSP2;KIAA1083;SPG4	
-0.50		-0.35		STMN1;RP1-125I3.5-004;LAP18;OP18;RP1-125I3.5-006	
-1.08	down	-0.58		HCTP4;TPX2;hCG_38821;HCA90;RP11-243J16.10-002;C20orf1;C20orf2;DIL2;HCA519	**Stabilizing MAPs**
-1.00	down	-0.50		CKAP5;KIAA0097	
-0.38		0.96	up	GPR142;PGR2;KIF19	
-1.43	down	-0.55		KIF11;EG5;KNSL1;TRIP5	
1.24	up	0.73		KIF12;RP11-56P10.3-001;hCG_32518	**Kinesins**
-0.45		-0.03		KIF13A;RBKIN;RP11-500C11.2-003	
0.35		0.81	up	KIF13B;GAKIN;KIAA0639	
-1.00	down	-0.65		KIF14;KIAA0042	
-1.45	down	-0.89	down	KIF15;KLP2;KNSL7	
0.25		0.61		KIF16B;C20orf23;KIAA1590;SNX23;RP5-971B4.1-002	
0.10		-0.51		KIF17;RP11-401M16.8-004;RP11-401M16.8-009;KIAA1405;KIF3X	
-0.91	down	-1.91	down	KIF18A;OK/SW-cl.108	
-1.49	down	-0.87	down	KIF18B	
-0.75		-0.07		KIF1B;KIAA0591;KIAA1448;KIF1Bbeta;RP4-736L20.1-005	
-0.14		0.49		KIF1C;KIAA0706	
-0.87	down	-0.50		KIF20A;RAB6KIFL	
-0.79	down	-0.26		KIF20B;KRMP1;MPHOSPH1	
-0.13		0.16		KIF21A;KIAA1708;KIF2;DKFZp779C159	
-0.33		-0.59		KIF21B;RP11-180A14.4-004;hCG_2027369;KIAA0449	
-1.16	down	-0.52		KIF22;KID;KNSL4;hCG_2039829;A-	

				328A3.5;OBP-1;OBP-2	
-1.23	down	-0.29		KIF23;KNSL5;MKLP1	
-1.21	down	-0.90	down	KIF24;C9orf48	
-0.74		-0.57		KIF26A;KIAA1236	
0.09		0.69		KIF26B	
0.17		0.03		KIF27	
-0.78	down	-0.21		KIF2A;KIF2;KNS2	
-1.20	down	-0.77	down	KIF2C;KNSL6;RP11-269F19.1-004;RP11-269F19.1-003;RP11-269F19.1-006	
-0.37		-0.15		KIF3A;KIF3	
-0.28		0.14		KIF3B;KIAA0359	
0.46		0.01		KIF3C;hCG_21381;DKFZp686G1646	
-1.35	down	-0.80	down	KIF4A;KIF4	
0.04		0.28		KIF5A;NKHC1	
-0.08		0.11		KIF5B;KNS;KNS1;KIF5B-ALK	
0.59		-0.45		KIF5C;KIAA0531;NKHC2;Nbla04137;DKFZp566O183	
-0.17		0.84	up	KIF9	
0.36		0.60		KIFAP3;RP1-190I16.1-002;hCG_38009;RP1-190I16.1-003;KIF3AP;SMAP	
-0.80	down	-0.41		KIFC1;DAQB-126H3.5-002;HSET;KNSL2;DASS-97D12.2-002;XXbac-BPG294E21.2-002	
0.20		0.45		KIFC2;hCG_24018	
-0.83	down	-0.19		KIFC3;hCG_1795607;DKFZp686D23201	
0.91	up	NA		KIF1A;hCG_32293;ATSV;C2orf20	
-0.91	down	-0.31		MAD1L1;tcag7.525;MAD1;TXBP181	**Spindle assembly checkpoint**
-1.12	down	-0.11		MAD2L1;MAD2;hCG_37351	
-0.48		-0.36		MAD2L2;RP3-330O12.4-007;RP3-330O12.4-002;RP3-330O12.4-006;RP3-330O12.4-008;RP3-330O12.4-005;hCG_24776;MAD2B;REV7	
-0.87	down	-0.36		BUB1;BUB1L;hCG_16817	
-1.25	down	-0.49		BUB1B;BUBR1;MAD3L;SSK1	
-0.57		0.20		BUB3	
-1.72	down	-0.96	down	KNTC1;KIAA0166	
-1.29	down	-0.03		KNTC2;hCG_38410;NDC80;HEC;HEC1	
0.32		0.32		LOC392748;tcag7.1276;RPS27;RP11-422P24.3-002;RPS27L;hCG_33491;MPS1;RP11-422P24.3-001;hCG_1746747;hCG_1996850;hCG_2001249	
-0.21		0.05		SMC1A;DXS423E;KIAA0178;SB1.8;SMC1;SMC1L1;RP6-29D12.1-003;DKFZp686L19178	**Sister chromatid cohesion**
-1.11	down	-0.76	down	SMC3;BAM;BMH;CSPG6;SMC3L1	
-0.25		0.34		ELOVL1;SSC1;CGI-88	
-0.17		0.06		STAG2;RP11-517O1.1-007;RP11-517O1.1-020;RP11-517O1.1-017;RP11-517O1.1-011;RP11-517O1.1-014;RP11-517O1.1-013;RP11-517O1.1-002;RP11-517O1.1-006;hCG_15646;SA2;DKFZp781H1753;DKFZp686P168;DKFZp686C21148;DKFZp686P16143;DKFZp686I05169	
-1.70	down	-1.42	down	ESPL1;ESP1;KIAA0165	

-0.59		-0.84	down	TP53;P53;hCG_42016;p53	**Cell cycle regulation**
-0.03		0.06		APC;DP2.5;APC variant protein	
-0.64		-0.07		CCNB1;CCNB	
-0.83	down	-0.46		CDC20	
0.19		0.69		MDM2;mdm2;MDM2 isoform N1_40;MDM2 isoform KB9	
-0.25		-0.37		MDM4;MDMX;RP11-430C7.1-006;RP11-430C7.1-007;RP11-430C7.1-009	
-0.29		0.25		RB1	
-1.62	down	-0.75		BRCA1;RNF53	
-1.42	down	-0.68		BRCA2;FACD;FANCD1	
-0.04		-0.20		MYC;hCG_15917;BHLHE39;c-myc	
-0.62		-0.18		RANBP1;hCG_17886	
-1.11	down	-0.35		FOXM1;FKHL16;HFH11;MPP2;WIN;hCG_1731745	
0.74		0.17		CDH1;hCG_28201;CDHE;UVO	
-0.35		0.16		CCND1;BCL1;PRAD1;hCG_2016647;cyclin D1	
-0.85	down	-0.70		CCNE1;CCNE	
0.32		0.31		ATM;DKFZp781A0353	
1.27	up	2.39	up	CDKN1A;CAP20;CDKN1;CIP1;MDA6;PIC1;SDI1;WAF1;hCG_15367	

Supplementary Table 2. mRNA levels of the CIN-associated genes.

Ratio HPT/HCT116 [log_2] – log_2 of the ratio of respective HPT/HCT116 for mRNA data for every individual gene entry. The median of three biological replicates for each gene entry was used. Up-/downregulation – log_2 of the ratio is more or equals 0.75 (up) or less or equals -0.75 (down). Note, that some genes cannot be classified to the only group (e.g., some entries can be classified in both spindle assembly checkpoint

and kinetochore).

Materials and Methods

1. Materials

1.1. Cell lines.

HCT116, RPE1-hTERT cell lines and their derivatives were used in the study. HCT116 is a human colorectal carcinoma cell line, purchased from ATCC (No. CCL-247, LGC Standards GMBH, Wesel, Germany). H2B-GFP-expressing HCT116 cell line, established by Christian Kuffer, was used in this work. In brief, the cell line was generated by lipofection with FugeneHD (Roche, Mannheim, Germany) with pBOS-H2BGFP construct (BD Pharmingen, Heidelberg, Germany) according to manufacturer's protocol; further, transfected cells were cultured in selection medium on blasticidin (6 µg/ml, Alexis Biochemicals, Lausen, Switzerland), individual clones were screened for H2B-GFP expression before use in this project. HCT116 cell line was also passaged for additional 36 passages (duration of approximately three months) in order to obtain late passage HCT116 36p cell line. 2N CP4 cell line was established by Silvia Stingele using single-cell purification, followed by a clonal expansion of HCT116. RPE1 hTERT is an immortalized by telomerase expression human retinal pigment epithelium cell line; hTERT-RPE1, expressing H2B-GFP, used in the present work, was a generous gift from Dr. Stephen Taylor (The University of Manchester, UK). Throughout the study both HCT116 and RPE1 hTERT H2B-GFP-expressing cell lines were referred to as HCT116 and RPE1, respectively.

1.2. Primary antibodies.

The following primary antibodies were used in the study. Table 1 lists the species used to obtain antibodies, the respective dilutions and commercial and non-commercial sources of the antibodies.

antibody	species	dilution	source	catalogue number
anti-p53	mouse	1:1000	Santa Cruz, Heidelberg, Germany	(DO-1): sc-126
anti-p53	rabbit	1:500	Cell Signaling, Frankfurt am Main,	#9282

			Germany	
anti-α-actinin	mouse	1:500	Santa Cruz	(H-2): sc-17829
anti-GAPDH	goat	1:1000	Abcam, Cambridge, UK	ab9483
anti-GAPDH	goat	1:1000	Cell Signaling, Frankfurt am Main, Germany	14C10
anti-Kif15	rabbit	1:1000	Dr. Thomas Mayer, University of Konstanz, Germany	-
anti-Kif18A	rabbit	1:500	Dr. Thomas Mayer, University of Konstanz, Germany	-
anti-α-tubulin	mouse	1:500	Sigma, Taufkirchen, Germany	T6199
anti-γ-tubulin	rabbit	1:1000	Abcam	ab84355
anti-γ-tubulin	mouse	1:1000	Abcam	ab11316
anti-CREST	human	1:1000	Immunovision, Springdale, USA	HCT-0100

Table 3. Primary antibodies used throughout the study.

1.3. Sodium dodecyl sulfate-polyacrylamide (SDS-PAGE) gel electrophoresis and immunoblotting materials.

Mini-PROTEAN TGX (Tris-Glycine eXtended) 4–15% gradient and Any KD precast gels (BioRad, Munich, Germany) were used for the SDS-PAGE. Following buffers were used for SDS-PAGE and subsequent immunoblotting:

- RIPA lysis buffer (pH 7.5): 50 mM HEPES, 150 mM NaCl, 1.5 mM $MgCl_2$, 1 mM EGTA, 10% glycerol, 1% TritonX-100, 100 mM NaF, 10 mM $Na_4P_2O_7$, protease inhibitor cocktail.
- Lämmli buffer: 62.5 mM Tris/HCl pH 6.8, 2% (w/v) glycerol, 0.002% (w/v) bromphenole blue, 2.5% β-mercaptoethanol.
- Lower SDS buffer (pH 8.8): 1.5 M Tris-HCl, 0.4% (w/v) SDS.

- Upper SDS buffer (pH 6.8): 0.5 M Tris-HCl, 0.4% (w/v) SDS.
- SDS-PAGE running buffer: 25 mM Tris/HCl, 200 mM glycine, 0.1% (w/v) SDS.
- Immunoblotting transfer buffer: 25 mM Tris/HCl, 1.44% (w/v) glycerol, 20% methanol.
- TBST (pH 7.5): 50 mM Tris, 150 mM NaCl.
- Blocking buffer: 5% (w/v) skim milk powder, TBST.

1.4. Other materials.

- 20x SSC (pH 7.0): 3 M NaCl, 300 mM $C_3H_5O(COO)_3Na_3$.
- PBS (pH 7.5): 137 mM NaCl, 2.7 mM KCl, 10 mM Na_4HPO_4, 2 mM KH_2PO_4.
- PBST (pH 7.5): PBS (pH 7.5), 0.1% Tween20.
- Pepsin solution: 50µl Pepsin, 1ml 1N HCl, 99ml dH_2O.

All other materials are described in the appropriate methods sections.

2. Methods

2.1. Cryopreservation and cultivation of cells.

Cells were preserved in a freezing solution containing 90% fetal calf serum (FCS, Gibco, Karlsruhe, Germany) and 10% DMSO as a cryoprotector with minimal cell concentration 10^6 cells/ml. For short term storage, vials containing cells were preserved at -80°C in a freezer; long-term preservation was carried out in liquid nitrogen. To thaw the cells, the vials were gently agitated for 5 min in a 37°C water bath. Further, cells were pelleted, resuspended in a fresh culture medium and plated on a 10-cm cell culture plates. Cell culture was established for experimental use after two to four days in culture. Both HCT116 and RPE1 cells, and their derivatives were cultured in Dulbecco's modified medium (DMEM, Gibco, Karlsruhe, Germany), supplemented with heat-inactivated 10% FCS and 1% PenStrep (50 IU/ml penicillin and 50 µg/ml streptomycin, PAA, Pasching, Austria) at 37°C in a humidified atmosphere with 5% CO_2.

Cell splitting was performed three times per week. In brief, cells were washed with PBS, treated with trypsin-EDTA (PAA, Pasching, Austria) for 5 min at 37°C until complete detachment from the dish and subsequently dispensed into 1:5-1:10 ratios in 10 ml growth medium. Cells in the log-phase of growth (60-75% confluency) were used for the experiments. Prior seeding for the experiments, cells were counted on Beckman Coulter Z1 cell counter (Beckman Coulter, Munich, Germany) and diluted

with a cell culture medium in order to obtain the necessary concentrations. Generally, depending on required density and the cell line type (lower cell count requirement for RPE1 and higher for HCT116), 25000 or 50000 cells/ml density was used for imaging experiments,

2.2. Generation of posttetraploid cell lines.

HCT116 and RPE1 cells were treated with 0.75 µM of actomyosin inhibitor dihydrocytochalasin D (DCD, Sigma, Taufkirchen, Germany) for 18 hours. Cells were then rinsed three times with PBS, harvested and counted, then placed into a drug-free medium and subcloned by limiting dilution on 96-well plates with the dilution rate 0.5 cell per well. Tetraploid RPE1 H2B-GFP cells were grown on 96-well plates coated with gelatin (Merck Biosciences, Darmstadt, Germany). After six weeks expansion in culture, individual subclones were harvested for flow cytometry to measure the DNA content. In brief, cells were fixed in 70% ice-cold ethanol and stained with the 50 µg/ml of DNA-intercalating reagent propidium iodide (PI, Sigma, Taufkirchen, Germany) in a sodium citrate solution containing RNAse A (Sigma, Taufkirchen, Germany). The DNA content was measured using BD FACS Calibur (Becton Dickinson, Heidelberg, Germany). The stocks of subclones with confirmed near-tetraploid DNA content termed posttetraploid derivatives (PTs) were frozen down at -80°C and in the liquid nitrogen. To minimize the effect of additional genetic variations between PT cell lines, all aneuploid cell lines underwent minimal passages and were analyzed at the same passage.

Late passages of two posttetraploid cell lines (HPT1 and HPT2) were obtained by culturing the respective cell lines for 12 (approximately one month) and 36 (approximately three months) additional passages.

2.3. Determination of non-viable cells in culture.

Cells in culture were treated with 50 µg/ml PI in DMEM for 10 minutes, washed with PBS, trypsinized and immediately submitted to flow cytometry (FACS Calibur, BD Biosciences). All solutions contained PI at the same concentration. The data acquisition was carried out using CellQuest Pro (BD Biosciences) software. Data was analyzed using FlowJo (Tree Star Inc., Ashland, USA) and Prism software (GraphPad Software Inc., La Jolla, USA).

2.4. Protein biochemistry methods.

2.4.1. Cell lysis and protein concentration measurement.

Pelleted cells were resuspended using RIPA lysis buffer with protease inhibitor cocktail (Pefabloc SC, Roth, Karlsruhe, Germany), incubated for 10 min on ice, ultrasound sonicated in a waterbath for 15 min; total cell lysate was then spun down at 13600 rpm for 10 minutes at 4°C on a table-top microcentrifuge (Eppendorf, Hamburg, Germany). Part of the supernatant was transferred to Eppendorf tubes for storage at -80°C and part used for downstream applications in immunoblotting. Protein concentration was measured in quadruplicates using Bradford dye on SmartSpec 3000 spectrophotometer (both, BioRad, Munich, Germany) at 595 nm wavelength and the median of the measurements was further used. Subsequently, protein levels were adjusted in all samples by adding required volume of lysis buffer, resuspended in 4x Lämmli buffer with 2.5% β-mercaptoethanol and boiled at 95°C for 5 min.

2.4.2. SDS-PAGE and immunoblotting.

Processed total cell lysates were separated by SDS-PAGE; protein size was estimated using PrecisionPlus All Blue or PrecisionPlus Kaleidoscope protein markers (both BioRad, Munich, Germany). Separated proteins were then transferred to a methanol-activated polyvinylidene difluoride membrane (PVDF, Roche, Mannheim, Germany) using wet transfer Mini-PROTEAN II electrophoresis system (BioRad, Munich, Germany). Membranes were blocked in 5% skim milk (Fluka, Taufkirchen, Germany) in Tris-buffered saline with 0.05% Tween20 (TBST), decorated with respective primary antibodies diluted in blocking solution overnight at 4°C with gentle agitation. Further, the membranes were rinsed for 30 min with TBST with a triple buffer exchange, incubated with HRP-conjugated secondary antibodies (R&D Systems), followed by triple TBST wash, chemiluminescence using ECLplus kit and detection either on ECL hyperfilm (GE Healthcare), on X-ray hyperfilm processor MI-5 (Medical Index, Bad Rappenau, Germany) or using Fujifilm Luminescent Image Analyzer (LAS-3000 Lite) system (Fujifilm, Düsseldorf, Germany). Protein band quantification was carried out using ImageJ (National Institutes of Health, http://rsb.info.nih.gov/ij/).

2.5. Microscopy.

Long-term live cell timelapse data were recorded on an inverted Zeiss Observer.Z1 microscope (Visitron Systems) equipped with a humidified chamber (EMBLEM, Heidelberg, Germany) at 37°C, 40% humidity and in the atmosphere of 5% CO_2 using CoolSNAP HQ2 camera (Photometrics, Roper Scientific, Ottobrunn, Germany); Plan Neofluar 20x, or 10x magnification air objective NA 1.0 (Zeiss, Jena, Germany); epifluorescent X-Cite 120 Series lamp (EXFO, Lumen Dynamics Group Inc., Mississauga, Canada); using GFP filter and differential interference contrast (DIC) in cell culture medium; further referred to as Visitron Systems microscope.

Imaging of fixed cells was carried out on Marianas SDC system comprising inverted Zeiss Observer.Z1 microscope, Plan Apochromat 63x magnification oil objective, 40x magnification air objective or 20x magnification air objective, equipped with epifluorescent X-Cite 120 Series lamp; 473, 561 and 660 nm lasers (LaserStack, Intelligent Imaging Innovations, Inc., Göttingen, Germany); spinning disc head (Yokogawa, Herrsching, Germany); CoolSNAP-HQ2 and CoolSNAP-EZ CCD cameras (Photometrics, Intelligent Imaging Innovations, Inc., Göttingen, Germany); further referred to as 3I microscope. Imaging conditions for each experiment are specified in respective method sections.

2.5.1. Live cell imaging.

2.5.1.1. Live imaging of untreated cells and cells treated with mitotic poisons.

The cells were seeded on glass-bottomed 96-black well plates two days prior to imaging. For SAC analysis, cells were treated with either: a) low (0.5 ng/ml) or high concentration of nocodazole (200 ng/ml) (Sigma, Taufkirchen, Germany) or b) high concentration of VS-83 (20 µM for HCT116 and 10 µM for RPE1; VS-83 was kindly provided by Dr. T. Mayer) prior to imaging. Subsequently, the plate was sealed with parafilm to avoid evaporation of the medium and imaged with Visitron Systems microscope. Image acquisition was performed with MetaMorph 7.1 software (Meta Imaging Series Environment, Molecular Devices, Ismaning, Germany) with GFP (50-60 ms exposure) and DIC (10 ms exposure). For HCT116 live imaging, a timelapse of three minutes was used for duration of 24 hours. Subsequently, the timelapse was

changed to nine minutes till the end of imaging equaling 96 hours. RPE1 and its derivatives were imaged for 50 hours with three-minute timelapse using 20x air objective. For the mitotic slippage analysis in a presence of nocodazole or VS-83, cells were imaged for 96 hours with six minute timelapse. Image analysis was performed using ImageJ and Slidebook 5 software (Intelligent Imaging Innovations, Inc., Göttingen, Germany); statistical analysis was carried out using Prism software.

2.5.1.2. RNA interference followed by live imaging.

Kinesin HSET (KIFC1) was depleted by RNAi. Fresh tetraploid cells were generated 18 hours prior the start of imaging as described in 2.5.1.1. ON-TARGET plus SMARTpool KIFC1 siRNA (L-004958-00-0005, Dharmacon, Thermo Scientific, Lafayette, USA) and scrambled RNAi as a negative control (Ambion, Dresden, Germany) were used at 12 nM concentration. Transfection procedures were performed using Oligofectamine (Invitrogen, Karlsruhe, Germany) according to the manufacturer's protocol on a glass-bottomed 96-black well plates (Greiner Bio-One, Frickenhausen, Germany), two days prior the start of imaging. Cells were visualized imaged on a Visitron Systems microscope for 72 hours using MetaMorph 7.1 software with a six minute timelapse using 10x magnification air objective. The polarity of mitosis was assessed using ImageJ software, statistical analysis was carried out using Prism software.

2.5.2. Determination of the chromosome copy number and chromosomal structural aberrations in cells.

2.5.2.1. Chromosome spreads (standard karyotyping).

Cells were treated with 50 ng/ml of a microtubule-depolymerizing drug, colchicine (Serva, Heidelberg, Germany) for 4.5 hours, collected and pelleted using table-top centrifuge, swollen in 75 mM KCl (Roth, Karlsruhe, Germany) in a 37°C waterbath for 15 minutes, fixed with Carnoy solution with a triple exchange of the fixative/centrifuging cycles (ice-cold 75% methanol and 25% acetic acid; both, Sigma, Taufkirchen, Germany) and spread on a wet glass slide with a glass Pasteur pipette. The slides were subsequently dried on a 42°C heat block (VWR, Darmstadt, Germany) covered with wet Kim Wipes paper tissue for approximately 5 minutes and stained with Giemsa dye (Fluka, Taufkirchen, Germany) for chromosome

visualization. Chromosome spreads were imaged and analyzed on a 3I microscope using brightfield and DIC using Slidebook 5 software.

2.5.2.2. Fluorescence *in situ* hybridization (FISH) on centromeric region.

Centromeric FISH was carried out using satellite enumeration probes against centromeric regions of specific chromosomes (1, 3, 7, and 12) conjugated either to a red or a green fluorophore according to manufacturer's protocol (Cytocell, Cambridge, UK). In brief, cells were processed as described in 2.5.2.1, obtained cell suspension was dropped on dry glass slide, dehydrated in ethanol (Sigma, Taufkirchen, Germany) concentration series (70%, 85%, 100%), washed with 2x SSC, allowed to air dry. Further, cellular DNA was denatured on a hot plate (72°C), hybridized overnight with the prewarmed at 37°C probes in hybridization buffer (Cytocell, Cambridge, UK) sealed with rubber cement at 37°C in the dark. Subsequently, slides were washed in 2xSSC at 75°C, and then briefly rinsed in 1xSSC at the room temperature and allowed to air dry. DNA was counterstained with DAPI (Cytocell, Cambridge, UK), and the cover slips were mounted on slides using antifade solution (Cytocell, Cambridge, UK). Images were acquired with the 3I microscope using 63x magnification objective with Texas Red, FITC and DAPI filters. 0.5 µm optical sections in the z-axis were collected and subsequently projected into a single z-projection for the analysis. The acquisition and analysis were performed by visual inspection by two independent observers using Slidebook 5 software.

2.5.2.3. Whole chromosome multicolor FISH (mFISH)

mFISH was carried out in collaboration with Dr. Stefan Müller at the Institute of Human Genetics, University Hospital, Ludwig-Maximilians-University, Munich. The cell suspension was prepared as described in 2.5.2.1 (colchicine concentration was increased to 400 ng/ml). DNA probes (24XCyte Human Multicolor FISH Probe Kit, MetaSystems, Altlussheim, Germany) were denatured at 72°C for 7 minutes, then, incubated in 37°C water bath for 30 min to pre-anneal probes. Fixed cells were dropped on a cleaned slide, allowed to air dry. Metaphase slides were pepsinized in order to eliminate cytoplasmic proteins, incubate in a coplin jar for 2 min at 37°C (depending on the amount of cytoplasm, time can be increased to 5 min), further, rinsed twice for 7 min each time in 1xPBS, dehydrated in 70%, 90%, 100% EtOH

series, 3 min each. Finally, the slides were baked at 61.4°C for 1 h on a hot plate. Metaphase slides were denatured at 72°C for 1min 30 sec in 70% Formamide/2xSSC, pH 7.0, dehydrated in 70% (-20°C), 90% (-20°C), 100% (RT) EtOH series, 3 min each.

Hybridization *in situ* was carried out as following. 4 µl probe was applied on a slide in the drop area, covered with 15x15 mm coverslip, sealed with rubber cement and incubated in a dark chamber overnight (~20 h) at 37°C. Subsequently, rubber cement was removed, coverslip was removed by soaking the slide in 4XSSCT (4 X SSC with 0.2% Tween 20). Slides were washed 3x5min in 0.1xSSC at 62°C, incubated in 4xSSCT at RT for 1 min.

One of the DNA probes was conjugated with biotin, thus required detection with streptavidin-Alexa Fluor 488 (Molecular Probes). Each slide was covered with 1ml blocking solution (3% BSA/4x SSCT, BSA solution was covered with parafilm on metaphase spread to avoid drying) and incubated for 18 min at 37°C, then rinsed in 4xSSCT at RT, and incubated with the antibody diluted in 1% BSA/4x SSCT (150-200 µl of antibody working solution was added to slide, covered with 24x50 mm coverslip, and incubated in a dark chamber for 45 min at 37°C). Finally, the slides were washed twice each time 7 min in 4xSSCT at 42°C, mounted in Vectashield Antifade solution (4',6 diamidino-2-phenylindole, Vector laboratories H-1200, Axxora/Alexis, Lörrach, Germany) with DAPI and cover with 24x60 mm coverslip sealed with a nail polish.

The spreads were analyzed on the Zeiss Observer.Z1 microscope, Plan Apochromat 63x magnification oil objective in DAPI, CFP, GFP, Cy3, Texas Red and Cy5 channels. The analysis was carried out using Adobe Photoshop (Adobe Systems, San Jose, USA) for visual inspection of the images; statistical analysis was performed using MS Excel (Microsoft) and Prism.

2.5.3. Mitotic error analyses in fixed cells.

2.5.3.1. Mitotic abnormalities scoring in anaphase and early telophase.

Cells were grown on glass-bottomed 96-black well plates, briefly washed with PBST, fixed with 100% methanol for 10 min at -20°C, washed three times with phosphate-

buffered saline with 0.05% Tween20 (PBST). DNA was stained with SYTOX Green Nucleic Acid dye (Molecular Probes, Invitrogen, Karlsruhe, Germany) with added RNAse. Imaging was carried out on Visitron Systems microscope using GFP and DIC filters and 20x magnification objective with Slidebook 5. Lagging DNA mass and anaphase bridges were scored in anaphases and early telophases by visual inspection of the images.

2.5.3.2. Micronucleation test.

Cells were seeded on glass-bottomed 96-black well plates two days prior to fixation, treated with DCD for 18 hours in order to mark those cells that underwent a single mitosis before the fixation. Cells that underwent mitosis during the DCD treatment become binucleated, and only they were scored in the analysis. Cells were washed with PBS, fixed with 100% methanol for 10 min at -20°C, followed by triple PBS wash and stained with DAPI (1 μg/ml; Roth, Karlsruhe, Germany). For the p53 nuclear enrichment staining, the cells were blocked following the fixation using 5% FCS/PBS solution with addition of 0.5% TritonX100 (Roth, Karlsruhe, Germany), incubated overnight with anti-p53 antibody (1:500, Cell Signaling), washed with 400 mM NaCl and subsequently twice in PBST, detected with DyLight 594-conjugated antibody (all DyLight antibodies: Thermo Fisher Scientific Inc.). DAPI was used as DNA counterstain. Cells were finally washed in 400 mM NaCl and twice in PBST. Acquisition and analysis were performed using Slidebook 5 with 3I microscope, 20x magnification objective. The percentage of binucleated cells containing micronucleus as well as p53 status in the nuclei and micronuclei were determined.

2.5.4. Immunofluorescent staining.

2.5.4.1. Mitotic spindle staining.

Cells were grown on glass-bottomed 96-black well plates and treated with MG132 10 μM (Calbiochem, Darmstadt, Germany) for 3 hours prior fixation. Cells were briefly washed with PBS, fixed with 100% methanol for 10 min at -20°C, washed three times with PBS, blocked with using 5% FCS/PBS solution with addition of 0.5% Triton X100, incubated overnight with anti-α-tubulin (1:500, Sigma) and anti-γ-tubulin antibody (1:1000, Santa Cruz), washed with 400 mM NaCl and subsequently twice in PBST, detected with DyLight 594- and DyLight 649-conjugated antibodies. DNA was stained with SYTOX Green with added RNAse. Cells were finally washed in 400 mM

NaCl and twice in PBST. The imaging was carried out on the 3I microscope with 63x magnification objective and 0.5 µm optical sections in the z-axis subsequently projected into a single z-projection (for spindle parameters measurement), or with 40x air single optical plane (for VS-83 sensitivity test); 473 nm, 561 nm and 660 nm argon lasers were used. Spindle parameter measurements were carried out using Slidebook 5; only the cells having both opposite spindle poles present in the same optical plane were scored for the spindle parameter measurements.

2.5.4.2. Staining for interkinetochore distance, kinetochore distribution measurements and high-resolution mitotic error visualization.

The cells were processed similarly as described for mitotic spindle immunofluorescence and stained with anti-α-tubulin (1:500, Sigma) and anti-CREST (1:1000, Immunovision) antibodies visualized by anti-human Alexa Fluor 647 (1:1000, Invitrogen) and anti-mouse DyLight 594-conjugated secondary antibodies. The imaging was carried out on the 3I microscope with 63x magnification oil objective with 0.5 µm optical sections in the z- axis using 473 nm, 561 nm and 660 nm argon lasers and analyzed using Slidebook 5. Interkinetochore distances were measured on pairs of sister kinetochores CREST signal within the same optical section. Kinetochore distribution measurements were carried out as three independent measurements of the line intensity of CREST signal per mitotic cell; the signal was corrected for the background intensity and averaged per cell. Mitotic errors were analyzed by visual inspection of the 3D captures.

2.5.4.3. Centrosome staining.

Cells were seeded two days prior the imaging on glass-bottomed 96-black well plates, fixed with 4% formaldehyde (Fluka, Taufkirchen, Germany), followed by dehydration with 100% methanol for 10 min at -20°C**,** blocking in 1% bovine albumin in PBS (BSA/PBS) solution and staining with anti-γ-tubulin antibody (1:1000, Abcam) detected with DyLight 649-conjugated antibody (Thermo Fisher Scientific Inc.). The mitotic “wave” timing for centrosome counting in newly formed tetraploid cells was determined previously using live cell imaging of the cells over 96 h. Images were acquired with the 3I microscope, 473 nm and 660 nm argon lasers and DIC. The

acquisition and analysis were performed using Slidebook 5; 0.5 µm optical sections in the z-axis were collected and subsequently projected into a single z-projection.

2.6. High-throughput methods.

2.6.1. Array comparative genomic hybridization (aCGH).

Genomic DNA for aCGH analysis was extracted using a Qiagen Gentra Puregene Kit (Qiagen, Hilden, Germany) according to manufacturer´s protocol. gDNA concentration and DNA absorbance ratio (260nm/280nm) were recorded for all samples using NanoDrop ND-1000 UV-VIS Spectrophotometer (PeqLab, Erlangen, Germany). The aCGH analysis was performed by IMGM laboratories GmbH, Martinsried, Germany. In short, hybridizations were carried out on Agilent SurePrint G3 Human Genome CGH Microarrays 2x400K (HPT1/HCT116) or on Agilent Human Genome CGH Microarrays 4x44K (HPT2/internal reference and HCT116/internal reference) Agilent Human Genome CGH Microarray in combination with a Two-Color-based hybridization protocol. The digested gDNA samples were directly labeled with exo-Klenow fragments and random primers by incorporation of Cy-5 dUTP (2'-deoxyuridine 5'-triphosphate) for the experimental samples and Cy-3 dUTP for the reference samples (Genomic DNA Enzymatic Labeling Kit, Agilent Technologies) according to IMGM laboratories guidelines. After purification, each experimental sample was combined with its respective reference sample, hybridized on respective arrays; signals on the microarrays were detected on Scan Control 8.4.1 Software (Agilent Technologies) on the Agilent DNA Microarray Scanner and extracted from the images using Feature Extraction 10.5.1.1 Software (Agilent Technologies). Raw microarray data were normalized by background subtraction, expected average subtraction and division by estimated variance by IMGM laboratories. Subsequent analysis was carried out on $\log_2$ of the ratios (HPT1/HCT116 and HPT2/HCT116) using Perseus software (version 1.2.6.16, http://maxquant.org/downloads.htm; part of the MaxQuant Software Package) and R (http://www.r-project.org/).

2.6.2. mRNA microarray-based gene expression analysis.

mRNA was purified using a Qiagen mRNeasy mini kit. Genome-wide expression profiling was conducted by IMGM laboratories GmbH. In summary, RNA concentration and purity were determined by the NanoDrop ND-1000; RNA integrity

was analyzed by capillary electrophoresis on 2100 Bioanalyzer (Agilent Technology). Total RNA samples were spiked with *in vitro* synthesized polyadenlyated transcripts (One-Color RNA Spike-In Mix, Agilent Technologies) for internal labeling control. 500 ng total RNA were used for reverse transcription. Labeled cDNA was hybridized at 65°C for 17 hours on Agilent SurePrint G3 Human GE Microarray (8x60K) according to a One-Color-based hybridization protocol. The microarrays were washed with Gene Expression Wash Buffers (Agilent Technologies) and dried in acetonitrile (Sigma). The fluorescent signal intensities were detected with an Agilent DNA Microarray Scanner and the data was extracted using Feature Extraction 10.5.1 Software (Agilent Technologies). Raw data were normalized by background substraction. Bioinformatics analysis of the microarray data was performed using Perseus, R and Excel (MS Office). Log_2 ratios HPT/HCT116 were calculated for each individual entry. Unpaired Student t-test was performed on signal intensities ratios, with correction for multiple testing. Both local and frequent FDR were calculated with the *fdrtool* software package in R; FDR cutoff was set as 0.01. Entries not satisfying the FDR cutoff are noted and nevertheless discussed in the work.

The data will be deposited in NCBI's Gene Expression Omnibus database and will be accessible through assigned GEO Series accession number (GSE47830) upon corresponding manuscript acceptance:
http://www.ncbi.nlm.nih.gov/geo/query/acc.cgi?token=dzqjzayqemioivy&acc=GSE47830
Individual candidate analysis was carried out using public STRING database (database of known protein interactions, http://string-db.org/). Pathway analysis was carried out using KEGG (Kyoto Encyclopedia of Genes and Genomes) database (http://www.genome.jp/kegg/kegg1.html).

2.7. Statistical analysis.

All statistical analysis was carried out using MS Excel, GraphPad Prism and R. Numbers of replicates, individual data points, as well as meaning of statistical error bars are specified in the figure legends. The statistical significance of the observed differences was verified by an unpaired Student t-test when the Gaussian distribution can be assumed; otherwise, by a Mann-Whitney test. The comparison of non-

Gaussian distributions where the equal variances could not be assumed was carried out using Mood's median test.

2.8. Image processing.

Image processing was performed using Slidebook 5, ImageJ, Adobe Photoshop and Adobe Illustrator CS2 (Adobe Systems, San Jose, USA).

Figure list

References

Acilan, C., Potter, D.M., and Saunders, W.S. (2007). DNA repair pathways involved in anaphase bridge formation. Genes Chromosomes Cancer *46*, 522-531.

Adams, R.R., Maiato, H., Earnshaw, W.C., and Carmena, M. (2001). Essential roles of Drosophila inner centromere protein (INCENP) and aurora B in histone H3 phosphorylation, metaphase chromosome alignment, kinetochore disjunction, and chromosome segregation. J Cell Biol *153*, 865-880.

Aguirre-Portoles, C., Bird, A.W., Hyman, A., Canamero, M., Perez de Castro, I., and Malumbres, M. (2012). Tpx2 controls spindle integrity, genome stability, and tumor development. Cancer Res *72*, 1518-1528.

Albertin, W., and Marullo, P. (2012). Polyploidy in fungi: evolution after whole-genome duplication. Proc Biol Sci *279*, 2497-2509.

Aleza, P., Froelicher, Y., Schwarz, S., Agusti, M., Hernandez, M., Juarez, J., Luro, F., Morillon, R., Navarro, L., and Ollitrault, P. (2011). Tetraploidization events by chromosome doubling of nucellar cells are frequent in apomictic citrus and are dependent on genotype and environment. Ann Bot *108*, 37-50.

Ambrose, J.C., Li, W., Marcus, A., Ma, H., and Cyr, R. (2005). A minus-end-directed kinesin with plus-end tracking protein activity is involved in spindle morphogenesis. Mol Biol Cell *16*, 1584-1592.

Anderson, G.R., Stoler, D.L., and Brenner, B.M. (2001). Cancer: the evolved consequence of a destabilized genome. Bioessays *23*, 1037-1046.

Andreassen, P.R., Lohez, O.D., Lacroix, F.B., and Margolis, R.L. (2001). Tetraploid state induces p53-dependent arrest of nontransformed mammalian cells in G1. Mol Biol Cell *12*, 1315-1328.

Andrews, P.D., Ovechkina, Y., Morrice, N., Wagenbach, M., Duncan, K., Wordeman, L., and Swedlow, J.R. (2004). Aurora B regulates MCAK at the mitotic centromere. Dev Cell *6*, 253-268.

Antonio, C., Ferby, I., Wilhelm, H., Jones, M., Karsenti, E., Nebreda, A.R., and Vernos, I. (2000). Xkid, a chromokinesin required for chromosome alignment on the metaphase plate. Cell *102*, 425-435.

Asteriti, I.A., Rensen, W.M., Lindon, C., Lavia, P., and Guarguaglini, G. (2010). The Aurora-A/TPX2 complex: a novel oncogenic holoenzyme? Biochim Biophys Acta *1806*, 230-239.

Badciong, J.C., and Haas, A.L. (2002). MdmX is a RING finger ubiquitin ligase capable of synergistically enhancing Mdm2 ubiquitination. J Biol Chem *277*, 49668-49675.

Baia, G.S., Stifani, S., Kimura, E.T., McDermott, M.W., Pieper, R.O., and Lal, A. (2008). Notch activation is associated with tetraploidy and enhanced chromosomal instability in meningiomas. Neoplasia *10*, 604-612.

Bakhoum, S.F., and Compton, D.A. (2012). Chromosomal instability and cancer: a complex relationship with therapeutic potential. J Clin Invest *122*, 1138-1143.

Bakhoum, S.F., Genovese, G., and Compton, D.A. (2009a). Deviant kinetochore microtubule dynamics underlie chromosomal instability. Curr Biol *19*, 1937-1942.

Bakhoum, S.F., Thompson, S.L., Manning, A.L., and Compton, D.A. (2009b). Genome stability is ensured by temporal control of kinetochore-microtubule dynamics. Nat Cell Biol *11*, 27-35.

Barber, T.D., McManus, K., Yuen, K.W., Reis, M., Parmigiani, G., Shen, D., Barrett, I., Nouhi, Y., Spencer, F., Markowitz, S.*, et al.* (2008). Chromatid cohesion defects may underlie chromosome instability in human colorectal cancers. Proc Natl Acad Sci U S A *105*, 3443-3448.

Barboza, J.A., Liu, G., Ju, Z., El-Naggar, A.K., and Lozano, G. (2006). p21 delays tumor onset by preservation of chromosomal stability. Proc Natl Acad Sci U S A *103*, 19842-19847.

Barr, A.R., and Gergely, F. (2008). MCAK-independent functions of ch-Tog/XMAP215 in microtubule plus-end dynamics. Mol Cell Biol *28*, 7199-7211.

Basto, R., Brunk, K., Vinadogrova, T., Peel, N., Franz, A., Khodjakov, A., and Raff, J.W. (2008). Centrosome amplification can initiate tumorigenesis in flies. Cell *133*, 1032-1042.

Basto, R., Gomes, R., and Karess, R.E. (2000). Rough deal and Zw10 are required for the metaphase checkpoint in Drosophila. Nat Cell Biol *2*, 939-943.

Blajeski, A.L., Phan, V.A., Kottke, T.J., and Kaufmann, S.H. (2002). G(1) and G(2) cell-cycle arrest following microtubule depolymerization in human breast cancer cells. J Clin Invest *110*, 91-99.

Bomont, P., Maddox, P., Shah, J.V., Desai, A.B., and Cleveland, D.W. (2005). Unstable microtubule capture at kinetochores depleted of the centromere-associated protein CENP-F. Embo J *24*, 3927-3939.

Booth, D.G., Hood, F.E., Prior, I.A., and Royle, S.J. (2011). A TACC3/ch-TOG/clathrin complex stabilises kinetochore fibres by inter-microtubule bridging. Embo J *30*, 906-919.

Borel, F., Lohez, O.D., Lacroix, F.B., and Margolis, R.L. (2002). Multiple centrosomes arise from tetraploidy checkpoint failure and mitotic centrosome clusters in p53 and RB pocket protein-compromised cells. Proc Natl Acad Sci U S A *99*, 9819-9824.

Boveri, T. (2008). Concerning the origin of malignant tumours by Theodor Boveri. Translated and annotated by Henry Harris. J Cell Sci *121 Suppl 1*, 1-84.

Brinkley, B.R. (2001). Managing the centrosome numbers game: from chaos to stability in cancer cell division. Trends Cell Biol *11*, 18-21.

Brito, D.A., and Rieder, C.L. (2009). The ability to survive mitosis in the presence of microtubule poisons differs significantly between human nontransformed (RPE-1) and cancer (U2OS, HeLa) cells. Cell Motil Cytoskeleton *66*, 437-447.

Brosh, R., and Rotter, V. (2009). When mutants gain new powers: news from the mutant p53 field. Nat Rev Cancer *9*, 701-713.

Brown, K.D., Wood, K.W., and Cleveland, D.W. (1996). The kinesin-like protein CENP-E is kinetochore-associated throughout poleward chromosome segregation during anaphase-A. J Cell Sci *109 (Pt 5)*, 961-969.

Bunz, F., Fauth, C., Speicher, M.R., Dutriaux, A., Sedivy, J.M., Kinzler, K.W., Vogelstein, B., and Lengauer, C. (2002). Targeted inactivation of p53 in human cells does not result in aneuploidy. Cancer Res *62*, 1129-1133.

Burds, A.A., Lutum, A.S., and Sorger, P.K. (2005). Generating chromosome instability through the simultaneous deletion of Mad2 and p53. Proc Natl Acad Sci U S A *102*, 11296-11301.

Cahill, D.P., Lengauer, C., Yu, J., Riggins, G.J., Willson, J.K., Markowitz, S.D., Kinzler, K.W., and Vogelstein, B. (1998). Mutations of mitotic checkpoint genes in human cancers. Nature *392*, 300-303.

Cai, S., Weaver, L.N., Ems-McClung, S.C., and Walczak, C.E. (2009). Kinesin-14 family proteins HSET/XCTK2 control spindle length by cross-linking and sliding microtubules. Mol Biol Cell *20*, 1348-1359.

Caldwell, C.M., Green, R.A., and Kaplan, K.B. (2007). APC mutations lead to cytokinetic failures in vitro and tetraploid genotypes in Min mice. J Cell Biol *178*, 1109-1120.

Carroll, P.E., Okuda, M., Horn, H.F., Biddinger, P., Stambrook, P.J., Gleich, L.L., Li, Y.Q., Tarapore, P., and Fukasawa, K. (1999). Centrosome hyperamplification in human cancer: chromosome instability induced by p53 mutation and/or Mdm2 overexpression. Oncogene *18*, 1935-1944.

Carter, S.L., Eklund, A.C., Kohane, I.S., Harris, L.N., and Szallasi, Z. (2006). A signature of chromosomal instability inferred from gene expression profiles predicts clinical outcome in multiple human cancers. Nat Genet *38*, 1043-1048.

Casimiro, M.C., Crosariol, M., Loro, E., Ertel, A., Yu, Z., Dampier, W., Saria, E.A., Papanikolaou, A., Stanek, T.J., Li, Z.*, et al.* (2012). ChIP sequencing of cyclin D1 reveals a transcriptional role in chromosomal instability in mice. J Clin Invest *122*, 833-843.

Casimiro, M.C., and Pestell, R.G. (2012). Cyclin d1 induces chromosomal instability. Oncotarget *3*, 224-225.

Cassimeris, L. (2002). The oncoprotein 18/stathmin family of microtubule destabilizers. Curr Opin Cell Biol *14*, 18-24.

Chan, G.K., Jablonski, S.A., Starr, D.A., Goldberg, M.L., and Yen, T.J. (2000). Human Zw10 and ROD are mitotic checkpoint proteins that bind to kinetochores. Nat Cell Biol *2*, 944-947.

Chan, J.Y. (2011). A clinical overview of centrosome amplification in human cancers. Int J Biol Sci *7*, 1122-1144.

Chan, K.L., Palmai-Pallag, T., Ying, S., and Hickson, I.D. (2009). Replication stress induces sister-chromatid bridging at fragile site loci in mitosis. Nat Cell Biol *11*, 753-760.

Charrasse, S., Mazel, M., Taviaux, S., Berta, P., Chow, T., and Larroque, C. (1995). Characterization of the cDNA and pattern of expression of a new gene over-expressed in human hepatomas and colonic tumors. Eur J Biochem *234*, 406-413.

Cheeseman, I.M., Anderson, S., Jwa, M., Green, E.M., Kang, J., Yates, J.R., 3rd, Chan, C.S., Drubin, D.G., and Barnes, G. (2002). Phospho-regulation of kinetochore-microtubule attachments by the Aurora kinase Ipl1p. Cell *111*, 163-172.

Choi, S.H., and McCollum, D. (2012). A role for metaphase spindle elongation forces in correction of merotelic kinetochore attachments. Curr Biol *22*, 225-230.

Cimini, D., Howell, B., Maddox, P., Khodjakov, A., Degrassi, F., and Salmon, E.D. (2001). Merotelic kinetochore orientation is a major mechanism of aneuploidy in mitotic mammalian tissue cells. J Cell Biol *153*, 517-527.

Cimini, D., Moree, B., Canman, J.C., and Salmon, E.D. (2003). Merotelic kinetochore orientation occurs frequently during early mitosis in mammalian tissue cells and error correction is achieved by two different mechanisms. J Cell Sci *116*, 4213-4225.

Cochran, J.C., Gatial, J.E., 3rd, Kapoor, T.M., and Gilbert, S.P. (2005). Monastrol inhibition of the mitotic kinesin Eg5. J Biol Chem *280*, 12658-12667.

Compton, D.A. (2000). Spindle assembly in animal cells. Annu Rev Biochem *69*, 95-114.

Connell, J.W., Lindon, C., Luzio, J.P., and Reid, E. (2009). Spastin couples microtubule severing to membrane traffic in completion of cytokinesis and secretion. Traffic *10*, 42-56.

Crasta, K., Ganem, N.J., Dagher, R., Lantermann, A.B., Ivanova, E.V., Pan, Y., Nezi, L., Protopopov, A., Chowdhury, D., and Pellman, D. (2012). DNA breaks and chromosome pulverization from errors in mitosis. Nature *482*, 53-58.

Dalton, W.B., Nandan, M.O., Moore, R.T., and Yang, V.W. (2007). Human cancer cells commonly acquire DNA damage during mitotic arrest. Cancer Res *67*, 11487-11492.

Deitch, A.D., Miller, G.J., and deVere White, R.W. (1993). Significance of abnormal diploid DNA histograms in localized prostate cancer and adjacent benign prostatic tissue. Cancer *72*, 1692-1700.

DeLuca, J.G., Moree, B., Hickey, J.M., Kilmartin, J.V., and Salmon, E.D. (2002). hNuf2 inhibition blocks stable kinetochore-microtubule attachment and induces mitotic cell death in HeLa cells. J Cell Biol *159*, 549-555.

Dinarina, A., Pugieux, C., Corral, M.M., Loose, M., Spatz, J., Karsenti, E., and Nedelec, F. (2009). Chromatin shapes the mitotic spindle. Cell *138*, 502-513.

Donehower, L.A., Godley, L.A., Aldaz, C.M., Pyle, R., Shi, Y.P., Pinkel, D., Gray, J., Bradley, A., Medina, D., and Varmus, H.E. (1995). Deficiency of p53 accelerates mammary tumorigenesis in Wnt-1 transgenic mice and promotes chromosomal instability. Genes Dev *9*, 882-895.

Dorsett, D. (2011). Cohesin: genomic insights into controlling gene transcription and development. Curr Opin Genet Dev *21*, 199-206.

Doxsey, S. (2001). Re-evaluating centrosome function. Nat Rev Mol Cell Biol *2*, 688-698.

Draviam, V.M., Shapiro, I., Aldridge, B., and Sorger, P.K. (2006). Misorientation and reduced stretching of aligned sister kinetochores promote chromosome missegregation in EB1- or APC-depleted cells. Embo J *25*, 2814-2827.

Du, Y., English, C.A., and Ohi, R. (2010). The kinesin-8 Kif18A dampens microtubule plus-end dynamics. Curr Biol *20*, 374-380.

Duelli, D., and Lazebnik, Y. (2007). Cell-to-cell fusion as a link between viruses and cancer. Nat Rev Cancer *7*, 968-976.

Duesberg, P., and Li, R. (2003). Multistep carcinogenesis: a chain reaction of aneuploidizations. Cell Cycle *2*, 202-210.

Duesberg, P., Stindl, R., and Hehlmann, R. (2000). Explaining the high mutation rates of cancer cells to drug and multidrug resistance by chromosome reassortments that are catalyzed by aneuploidy. Proc Natl Acad Sci U S A *97*, 14295-14300.

Duijf, P.H., Schultz, N., and Benezra, R. (2012). Cancer cells preferentially lose small chromosomes. Int J Cancer.

Dutrillaux, B., Gerbault-Seureau, M., Remvikos, Y., Zafrani, B., and Prieur, M. (1991). Breast cancer genetic evolution: I. Data from cytogenetics and DNA content. Breast Cancer Res Treat *19*, 245-255.

Fujiwara, T., Bandi, M., Nitta, M., Ivanova, E.V., Bronson, R.T., and Pellman, D. (2005). Cytokinesis failure generating tetraploids promotes tumorigenesis in p53-null cells. Nature *437*, 1043-1047.

Fukasawa, K. (2007). Oncogenes and tumour suppressors take on centrosomes. Nat Rev Cancer *7*, 911-924.

Galipeau, P.C., Cowan, D.S., Sanchez, C.A., Barrett, M.T., Emond, M.J., Levine, D.S., Rabinovitch, P.S., and Reid, B.J. (1996). 17p (p53) allelic losses, 4N (G2/tetraploid) populations, and progression to aneuploidy in Barrett's esophagus. Proc Natl Acad Sci U S A *93*, 7081-7084.

Gallardo, M.H., Bickham, J.W., Honeycutt, R.L., Ojeda, R.A., and Kohler, N. (1999). Discovery of tetraploidy in a mammal. Nature *401*, 341.

Gandhi, R., Bonaccorsi, S., Wentworth, D., Doxsey, S., Gatti, M., and Pereira, A. (2004). The Drosophila kinesin-like protein KLP67A is essential for mitotic and male meiotic spindle assembly. Mol Biol Cell *15*, 121-131.

Ganem, N.J., and Compton, D.A. (2004). The KinI kinesin Kif2a is required for bipolar spindle assembly through a functional relationship with MCAK. J Cell Biol *166*, 473-478.

Ganem, N.J., Godinho, S.A., and Pellman, D. (2009). A mechanism linking extra centrosomes to chromosomal instability. Nature *460*, 278-282.

Ganem, N.J., and Pellman, D. (2007). Limiting the proliferation of polyploid cells. Cell *131*, 437-440.

Gascoigne, K.E., and Taylor, S.S. (2008). Cancer cells display profound intra- and interline variation following prolonged exposure to antimitotic drugs. Cancer Cell *14*, 111-122.

Gassmann, R., Carvalho, A., Henzing, A.J., Ruchaud, S., Hudson, D.F., Honda, R., Nigg, E.A., Gerloff, D.L., and Earnshaw, W.C. (2004). Borealin: a novel chromosomal passenger required for stability of the bipolar mitotic spindle. J Cell Biol *166*, 179-191.

Gergely, F., Draviam, V.M., and Raff, J.W. (2003). The ch-TOG/XMAP215 protein is essential for spindle pole organization in human somatic cells. Genes Dev *17*, 336-341.

Ghadimi, B.M., Sackett, D.L., Difilippantonio, M.J., Schrock, E., Neumann, T., Jauho, A., Auer, G., and Ried, T. (2000). Centrosome amplification and instability occurs exclusively in aneuploid, but not in diploid colorectal cancer cell lines, and correlates with numerical chromosomal aberrations. Genes Chromosomes Cancer *27*, 183-190.

Ghiselli, G. (2006). SMC3 knockdown triggers genomic instability and p53-dependent apoptosis in human and zebrafish cells. Mol Cancer *5*, 52.

Giet, R., Petretti, C., and Prigent, C. (2005). Aurora kinases, aneuploidy and cancer, a coincidence or a real link? Trends Cell Biol *15*, 241-250.

Gisselsson, D. (2011). Mechanisms of whole chromosome gains in tumors--many answers to a simple question. Cytogenet Genome Res *133*, 190-201.

Gisselsson, D., Bjork, J., Hoglund, M., Mertens, F., Dal Cin, P., Akerman, M., and Mandahl, N. (2001). Abnormal nuclear shape in solid tumors reflects mitotic instability. Am J Pathol *158*, 199-206.

Gisselsson, D., Hakanson, U., Stoller, P., Marti, D., Jin, Y., Rosengren, A.H., Stewenius, Y., Kahl, F., and Panagopoulos, I. (2008). When the genome plays dice: circumvention of the spindle assembly checkpoint and near-random chromosome segregation in multipolar cancer cell mitoses. PLoS One *3*, e1871.

Gisselsson, D., Jin, Y., Lindgren, D., Persson, J., Gisselsson, L., Hanks, S., Sehic, D., Mengelbier, L.H., Ora, I., Rahman, N.*, et al.* (2010). Generation of trisomies in cancer cells by multipolar mitosis and incomplete cytokinesis. Proc Natl Acad Sci U S A *107*, 20489-20493.

Gisselsson, D., Pettersson, L., Hoglund, M., Heidenblad, M., Gorunova, L., Wiegant, J., Mertens, F., Dal Cin, P., Mitelman, F., and Mandahl, N. (2000). Chromosomal breakage-fusion-bridge events cause genetic intratumor heterogeneity. Proc Natl Acad Sci U S A *97*, 5357-5362.

Gordon, D.J., Resio, B., and Pellman, D. (2012). Causes and consequences of aneuploidy in cancer. Nat Rev Genet *13*, 189-203.

Goshima, G., Wollman, R., Stuurman, N., Scholey, J.M., and Vale, R.D. (2005). Length control of the metaphase spindle. Curr Biol *15*, 1979-1988.

Gregan, J., Polakova, S., Zhang, L., Tolic-Norrelykke, I.M., and Cimini, D. (2011). Merotelic kinetochore attachment: causes and effects. Trends Cell Biol *21*, 374-381.

Guerrero, A.A., Martinez, A.C., and van Wely, K.H. (2010). Merotelic attachments and non-homologous end joining are the basis of chromosomal instability. Cell Div *5*, 13.

Guidotti, J.E., Bregerie, O., Robert, A., Debey, P., Brechot, C., and Desdouets, C. (2003). Liver cell polyploidization: a pivotal role for binuclear hepatocytes. J Biol Chem *278*, 19095-19101.

Gupta, M.L., Jr., Carvalho, P., Roof, D.M., and Pellman, D. (2006). Plus end-specific depolymerase activity of Kip3, a kinesin-8 protein, explains its role in positioning the yeast mitotic spindle. Nat Cell Biol *8*, 913-923.

Hanks, S., Coleman, K., Reid, S., Plaja, A., Firth, H., Fitzpatrick, D., Kidd, A., Mehes, K., Nash, R., Robin, N.*, et al.* (2004). Constitutional aneuploidy and cancer predisposition caused by biallelic mutations in BUB1B. Nat Genet *36*, 1159-1161.

Hardy, P.A., and Zacharias, H. (2005). Reappraisal of the Hansemann-Boveri hypothesis on the origin of tumors. Cell Biol Int *29*, 983-992.

Haruki, N., Harano, T., Masuda, A., Kiyono, T., Takahashi, T., Tatematsu, Y., Shimizu, S., Mitsudomi, T., Konishi, H., Osada, H.*, et al.* (2001). Persistent increase in chromosome instability in lung cancer: possible indirect involvement of p53 inactivation. Am J Pathol *159*, 1345-1352.

Hegarat, N., Smith, E., Nayak, G., Takeda, S., Eyers, P.A., and Hochegger, H. (2011). Aurora A and Aurora B jointly coordinate chromosome segregation and anaphase microtubule dynamics. J Cell Biol *195*, 1103-1113.

Hernando, E., Nahle, Z., Juan, G., Diaz-Rodriguez, E., Alaminos, M., Hemann, M., Michel, L., Mittal, V., Gerald, W., Benezra, R.*, et al.* (2004). Rb inactivation promotes genomic instability by uncoupling cell cycle progression from mitotic control. Nature *430*, 797-802.

Hirokawa, N., Noda, Y., Tanaka, Y., and Niwa, S. (2009). Kinesin superfamily motor proteins and intracellular transport. Nat Rev Mol Cell Biol *10*, 682-696.

Ho, C.C., Hau, P.M., Marxer, M., and Poon, R.Y. (2010). The requirement of p53 for maintaining chromosomal stability during tetraploidization. Oncotarget *1*, 583-595.

Hoffelder, D.R., Luo, L., Burke, N.A., Watkins, S.C., Gollin, S.M., and Saunders, W.S. (2004). Resolution of anaphase bridges in cancer cells. Chromosoma *112*, 389-397.

Hognas, G., Tuomi, S., Veltel, S., Mattila, E., Murumagi, A., Edgren, H., Kallioniemi, O., and Ivaska, J. (2012). Cytokinesis failure due to derailed integrin traffic induces aneuploidy and oncogenic transformation in vitro and in vivo. Oncogene *31*, 3597-3606.

Hoque, M.T., and Ishikawa, F. (2002). Cohesin defects lead to premature sister chromatid separation, kinetochore dysfunction, and spindle-assembly checkpoint activation. J Biol Chem *277*, 42306-42314.

Huang, Y., Yao, Y., Xu, H.Z., Wang, Z.G., Lu, L., and Dai, W. (2009a). Defects in chromosome congression and mitotic progression in KIF18A-deficient cells are partly mediated through impaired functions of CENP-E. Cell Cycle *8*, 2643-2649.

Huang, Y.F., Chang, M.D., and Shieh, S.Y. (2009b). TTK/hMps1 mediates the p53-dependent postmitotic checkpoint by phosphorylating p53 at Thr18. Mol Cell Biol *29*, 2935-2944.

Huszar, D., Theoclitou, M.E., Skolnik, J., and Herbst, R. (2009). Kinesin motor proteins as targets for cancer therapy. Cancer Metastasis Rev *28*, 197-208.

Hyman, A.A., and Karsenti, E. (1996). Morphogenetic properties of microtubules and mitotic spindle assembly. Cell *84*, 401-410.

Ikui, A.E., Yang, C.P., Matsumoto, T., and Horwitz, S.B. (2005). Low concentrations of taxol cause mitotic delay followed by premature dissociation of p55CDC from Mad2 and BubR1 and abrogation of the spindle checkpoint, leading to aneuploidy. Cell Cycle *4*, 1385-1388.

Iwaizumi, M., Shinmura, K., Mori, H., Yamada, H., Suzuki, M., Kitayama, Y., Igarashi, H., Nakamura, T., Suzuki, H., Watanabe, Y.*, et al.* (2009). Human Sgo1

downregulation leads to chromosomal instability in colorectal cancer. Gut *58*, 249-260.

Jallepalli, P.V., Waizenegger, I.C., Bunz, F., Langer, S., Speicher, M.R., Peters, J.M., Kinzler, K.W., Vogelstein, B., and Lengauer, C. (2001). Securin is required for chromosomal stability in human cells. Cell *105*, 445-457.

Janssen, A., Kops, G.J., and Medema, R.H. (2009). Elevating the frequency of chromosome mis-segregation as a strategy to kill tumor cells. Proc Natl Acad Sci U S A *106*, 19108-19113.

Janssen, A., van der Burg, M., Szuhai, K., Kops, G.J., and Medema, R.H. (2011). Chromosome segregation errors as a cause of DNA damage and structural chromosome aberrations. Science *333*, 1895-1898.

Jeganathan, K., Malureanu, L., Baker, D.J., Abraham, S.C., and van Deursen, J.M. (2007). Bub1 mediates cell death in response to chromosome missegregation and acts to suppress spontaneous tumorigenesis. J Cell Biol *179*, 255-267.

Jordan, M.A., Thrower, D., and Wilson, L. (1992). Effects of vinblastine, podophyllotoxin and nocodazole on mitotic spindles. Implications for the role of microtubule dynamics in mitosis. J Cell Sci *102 (Pt 3)*, 401-416.

Joseph, J., Liu, S.T., Jablonski, S.A., Yen, T.J., and Dasso, M. (2004). The RanGAP1-RanBP2 complex is essential for microtubule-kinetochore interactions in vivo. Curr Biol *14*, 611-617.

Joukov, V., Groen, A.C., Prokhorova, T., Gerson, R., White, E., Rodriguez, A., Walter, J.C., and Livingston, D.M. (2006). The BRCA1/BARD1 heterodimer modulates ran-dependent mitotic spindle assembly. Cell *127*, 539-552.

Kabeche, L., and Compton, D.A. (2012). Checkpoint-independent stabilization of kinetochore-microtubule attachments by Mad2 in human cells. Curr Biol *22*, 638-644.

Kaneko, Y., and Knudson, A.G. (2000). Mechanism and relevance of ploidy in neuroblastoma. Genes Chromosomes Cancer *29*, 89-95.

Kaplan, K.B., Burds, A.A., Swedlow, J.R., Bekir, S.S., Sorger, P.K., and Nathke, I.S. (2001). A role for the Adenomatous Polyposis Coli protein in chromosome segregation. Nat Cell Biol *3*, 429-432.

Kapoor, T.M., Lampson, M.A., Hergert, P., Cameron, L., Cimini, D., Salmon, E.D., McEwen, B.F., and Khodjakov, A. (2006). Chromosomes can congress to the metaphase plate before biorientation. Science *311*, 388-391.

Kapoor, T.M., Mayer, T.U., Coughlin, M.L., and Mitchison, T.J. (2000). Probing spindle assembly mechanisms with monastrol, a small molecule inhibitor of the mitotic kinesin, Eg5. J Cell Biol *150*, 975-988.

Katayama, H., Ota, T., Jisaki, F., Ueda, Y., Tanaka, T., Odashima, S., Suzuki, F., Terada, Y., and Tatsuka, M. (1999). Mitotic kinase expression and colorectal cancer progression. J Natl Cancer Inst *91*, 1160-1162.

Kim, N., and Song, K. (2013). KIFC1 is essential for bipolar spindle formation and genomic stability in the primary human fibroblast IMR-90 cell. Cell Struct Funct.

Kirkland, J.A., Stanley, M.A., and Cellier, K.M. (1967). Comparative study of histologic and chromosomal abnormalities in cervical neoplasia. Cancer *20*, 1934-1952.

Kline, S.L., Cheeseman, I.M., Hori, T., Fukagawa, T., and Desai, A. (2006). The human Mis12 complex is required for kinetochore assembly and proper chromosome segregation. J Cell Biol *173*, 9-17.

Ko, M.A., Rosario, C.O., Hudson, J.W., Kulkarni, S., Pollett, A., Dennis, J.W., and Swallow, C.J. (2005). Plk4 haploinsufficiency causes mitotic infidelity and carcinogenesis. Nat Genet *37*, 883-888.

Kops, G.J., Foltz, D.R., and Cleveland, D.W. (2004). Lethality to human cancer cells through massive chromosome loss by inhibition of the mitotic checkpoint. Proc Natl Acad Sci U S A *101*, 8699-8704.

Kops, G.J., Weaver, B.A., and Cleveland, D.W. (2005). On the road to cancer: aneuploidy and the mitotic checkpoint. Nat Rev Cancer *5*, 773-785.

Krzywicka-Racka, A., and Sluder, G. (2011). Repeated cleavage failure does not establish centrosome amplification in untransformed human cells. J Cell Biol *194*, 199-207.

Kufer, T.A., Sillje, H.H., Korner, R., Gruss, O.J., Meraldi, P., and Nigg, E.A. (2002). Human TPX2 is required for targeting Aurora-A kinase to the spindle. J Cell Biol *158*, 617-623.

Kuffer, C., Kuznetsova, A.Y., and Storchova, Z. (2013). Abnormal mitosis triggers p53-dependent cell cycle arrest in human tetraploid cells. Chromosoma.

Kurasawa, Y., Earnshaw, W.C., Mochizuki, Y., Dohmae, N., and Todokoro, K. (2004). Essential roles of KIF4 and its binding partner PRC1 in organized central spindle midzone formation. Embo J *23*, 3237-3248.

Kwon, M., Godinho, S.A., Chandhok, N.S., Ganem, N.J., Azioune, A., Thery, M., and Pellman, D. (2008). Mechanisms to suppress multipolar divisions in cancer cells with extra centrosomes. Genes Dev *22*, 2189-2203.

Laan, L., Pavin, N., Husson, J., Romet-Lemonne, G., van Duijn, M., Lopez, M.P., Vale, R.D., Julicher, F., Reck-Peterson, S.L., and Dogterom, M. (2012). Cortical dynein controls microtubule dynamics to generate pulling forces that position microtubule asters. Cell *148*, 502-514.

Laoukili, J., Kooistra, M.R., Bras, A., Kauw, J., Kerkhoven, R.M., Morrison, A., Clevers, H., and Medema, R.H. (2005). FoxM1 is required for execution of the mitotic programme and chromosome stability. Nat Cell Biol *7*, 126-136.

Laulier, C., Cheng, A., and Stark, J.M. (2011). The relative efficiency of homology-directed repair has distinct effects on proper anaphase chromosome separation. Nucleic Acids Res *39*, 5935-5944.

Lawrence, C.J., Dawe, R.K., Christie, K.R., Cleveland, D.W., Dawson, S.C., Endow, S.A., Goldstein, L.S., Goodson, H.V., Hirokawa, N., Howard, J.*, et al.* (2004). A standardized kinesin nomenclature. J Cell Biol *167*, 19-22.

Lee, E.A., Keutmann, M.K., Dowling, M.L., Harris, E., Chan, G., and Kao, G.D. (2004). Inactivation of the mitotic checkpoint as a determinant of the efficacy of microtubule-targeted drugs in killing human cancer cells. Mol Cancer Ther *3*, 661-669.

Lee, H.O., Davidson, J.M., and Duronio, R.J. (2009a). Endoreplication: polyploidy with purpose. Genes Dev *23*, 2461-2477.

Lee, Y.H., Oh, B.K., Yoo, J.E., Yoon, S.M., Choi, J., Kim, K.S., and Park, Y.N. (2009b). Chromosomal instability, telomere shortening, and inactivation of p21(WAF1/CIP1) in dysplastic nodules of hepatitis B virus-associated multistep hepatocarcinogenesis. Mod Pathol *22*, 1121-1131.

Lengauer, C., Kinzler, K.W., and Vogelstein, B. (1997). Genetic instability in colorectal cancers. Nature *386*, 623-627.

Lengauer, C., Kinzler, K.W., and Vogelstein, B. (1998). Genetic instabilities in human cancers. Nature *396*, 643-649.

Levesque, A.A., and Compton, D.A. (2001). The chromokinesin Kid is necessary for chromosome arm orientation and oscillation, but not congression, on mitotic spindles. J Cell Biol *154*, 1135-1146.

Levine, D.S., Rabinovitch, P.S., Haggitt, R.C., Blount, P.L., Dean, P.J., Rubin, C.E., and Reid, B.J. (1991a). Distribution of aneuploid cell populations in ulcerative colitis with dysplasia or cancer. Gastroenterology *101*, 1198-1210.

Levine, D.S., Sanchez, C.A., Rabinovitch, P.S., and Reid, B.J. (1991b). Formation of the tetraploid intermediate is associated with the development of cells with more than four centrioles in the elastase-simian virus 40 tumor antigen transgenic mouse model of pancreatic cancer. Proc Natl Acad Sci U S A *88*, 6427-6431.

Lin, Z.Z., Jeng, Y.M., Hu, F.C., Pan, H.W., Tsao, H.W., Lai, P.L., Lee, P.H., Cheng, A.L., and Hsu, H.C. (2010). Significance of Aurora B overexpression in hepatocellular carcinoma. Aurora B Overexpression in HCC. BMC Cancer *10*, 461.

Lingle, W.L., Barrett, S.L., Negron, V.C., D'Assoro, A.B., Boeneman, K., Liu, W., Whitehead, C.M., Reynolds, C., and Salisbury, J.L. (2002). Centrosome amplification drives chromosomal instability in breast tumor development. Proc Natl Acad Sci U S A *99*, 1978-1983.

Liu, D., Vader, G., Vromans, M.J., Lampson, M.A., and Lens, S.M. (2009). Sensing chromosome bi-orientation by spatial separation of aurora B kinase from kinetochore substrates. Science *323*, 1350-1353.

Liu, J., and Onuchic, J.N. (2006). A driving and coupling "Pac-Man" mechanism for chromosome poleward translocation in anaphase A. Proc Natl Acad Sci U S A *103*, 18432-18437.

Livingstone, L.R., White, A., Sprouse, J., Livanos, E., Jacks, T., and Tlsty, T.D. (1992). Altered cell cycle arrest and gene amplification potential accompany loss of wild-type p53. Cell *70*, 923-935.

Loughlin, R., Wilbur, J.D., McNally, F.J., Nedelec, F.J., and Heald, R. (2011). Katanin contributes to interspecies spindle length scaling in Xenopus. Cell *147*, 1397-1407.

Lv, L., Zhang, T., Yi, Q., Huang, Y., Wang, Z., Hou, H., Zhang, H., Zheng, W., Hao, Q., Guo, Z*., et al.* (2012). Tetraploid cells from cytokinesis failure induce aneuploidy and spontaneous transformation of mouse ovarian surface epithelial cells. Cell Cycle *11*, 2864-2875.

Maiato, H., DeLuca, J., Salmon, E.D., and Earnshaw, W.C. (2004). The dynamic kinetochore-microtubule interface. J Cell Sci *117*, 5461-5477.

Manning, A.L., Ganem, N.J., Bakhoum, S.F., Wagenbach, M., Wordeman, L., and Compton, D.A. (2007). The kinesin-13 proteins Kif2a, Kif2b, and Kif2c/MCAK have distinct roles during mitosis in human cells. Mol Biol Cell *18*, 2970-2979.

Manning, A.L., Longworth, M.S., and Dyson, N.J. (2010). Loss of pRB causes centromere dysfunction and chromosomal instability. Genes Dev *24*, 1364-1376.

Margolis, R.L., Lohez, O.D., and Andreassen, P.R. (2003). G1 tetraploidy checkpoint and the suppression of tumorigenesis. J Cell Biochem *88*, 673-683.

Martin-Lluesma, S., Stucke, V.M., and Nigg, E.A. (2002). Role of Hec1 in spindle checkpoint signaling and kinetochore recruitment of Mad1/Mad2. Science *297*, 2267-2270.

Marxer, M., Foucar, C.E., Man, W.Y., Chen, Y., Ma, H.T., and Poon, R.Y. (2012). Tetraploidization increases sensitivity to Aurora B kinase inhibition. Cell Cycle *11*, 2567-2577.

Masramon, L., Ribas, M., Cifuentes, P., Arribas, R., Garcia, F., Egozcue, J., Peinado, M.A., and Miro, R. (2000). Cytogenetic characterization of two colon cell lines by using conventional G-banding, comparative genomic hybridization, and whole chromosome painting. Cancer Genet Cytogenet *121*, 17-21.

Masterson, J. (1994). Stomatal size in fossil plants: evidence for polyploidy in majority of angiosperms. Science *264*, 421-424.

Matijasevic, Z., Steinman, H.A., Hoover, K., and Jones, S.N. (2008). MdmX promotes bipolar mitosis to suppress transformation and tumorigenesis in p53-deficient cells and mice. Mol Cell Biol *28*, 1265-1273.

Matsuura, S., Ito, E., Tauchi, H., Komatsu, K., Ikeuchi, T., and Kajii, T. (2000). Chromosomal instability syndrome of total premature chromatid separation with mosaic variegated aneuploidy is defective in mitotic-spindle checkpoint. Am J Hum Genet *67*, 483-486.

Matzke, M.A., Mette, M.F., Kanno, T., and Matzke, A.J. (2003). Does the intrinsic instability of aneuploid genomes have a causal role in cancer? Trends Genet *19*, 253-256.

Mayer, T.U., Kapoor, T.M., Haggarty, S.J., King, R.W., Schreiber, S.L., and Mitchison, T.J. (1999). Small molecule inhibitor of mitotic spindle bipolarity identified in a phenotype-based screen. Science *286*, 971-974.

Mayer, V.W., and Aguilera, A. (1990). High levels of chromosome instability in polyploids of Saccharomyces cerevisiae. Mutat Res *231*, 177-186.

Mayr, M.I., Hummer, S., Bormann, J., Gruner, T., Adio, S., Woehlke, G., and Mayer, T.U. (2007). The human kinesin Kif18A is a motile microtubule depolymerase essential for chromosome congression. Curr Biol *17*, 488-498.

Mazumdar, M., Lee, J.H., Sengupta, K., Ried, T., Rane, S., and Misteli, T. (2006). Tumor formation via loss of a molecular motor protein. Curr Biol *16*, 1559-1564.

Mazumdar, M., and Misteli, T. (2005). Chromokinesins: multitalented players in mitosis. Trends Cell Biol *15*, 349-355.

Mazumdar, M., Sundareshan, S., and Misteli, T. (2004). Human chromokinesin KIF4A functions in chromosome condensation and segregation. J Cell Biol *166*, 613-620.

Menssen, A., Epanchintsev, A., Lodygin, D., Rezaei, N., Jung, P., Verdoodt, B., Diebold, J., and Hermeking, H. (2007). c-MYC delays prometaphase by direct transactivation of MAD2 and BubR1: identification of mechanisms underlying c-MYC-induced DNA damage and chromosomal instability. Cell Cycle *6*, 339-352.

Michaelis, C., Ciosk, R., and Nasmyth, K. (1997). Cohesins: chromosomal proteins that prevent premature separation of sister chromatids. Cell *91*, 35-45.

Michel, L.S., Liberal, V., Chatterjee, A., Kirchwegger, R., Pasche, B., Gerald, W., Dobles, M., Sorger, P.K., Murty, V.V., and Benezra, R. (2001). MAD2 haplo-insufficiency causes premature anaphase and chromosome instability in mammalian cells. Nature *409*, 355-359.

Mikule, K., Delaval, B., Kaldis, P., Jurcyzk, A., Hergert, P., and Doxsey, S. (2007). Loss of centrosome integrity induces p38-p53-p21-dependent G1-S arrest. Nat Cell Biol *9*, 160-170.

Mimori-Kiyosue, Y., and Tsukita, S. (2003). "Search-and-capture" of microtubules through plus-end-binding proteins (+TIPs). J Biochem *134*, 321-326.

Mitchison, T., and Kirschner, M. (1984). Dynamic instability of microtubule growth. Nature *312*, 237-242.

Miyoshi, Y., Iwao, K., Ikeda, N., Egawa, C., and Noguchi, S. (2002). Acceleration of chromosomal instability of BRCA1-associated hereditary breast cancers by p53 abnormality. Breast J *8*, 77-80.

Moll, U.M., and Petrenko, O. (2003). The MDM2-p53 interaction. Mol Cancer Res *1*, 1001-1008.

Montgomery, B.T., Nativ, O., Blute, M.L., Farrow, G.M., Myers, R.P., Zincke, H., Therneau, T.M., and Lieber, M.M. (1990). Stage B prostate adenocarcinoma. Flow cytometric nuclear DNA ploidy analysis. Arch Surg *125*, 327-331.

Moore, A., and Wordeman, L. (2004). The mechanism, function and regulation of depolymerizing kinesins during mitosis. Trends Cell Biol *14*, 537-546.

Morrison, C., Vagnarelli, P., Sonoda, E., Takeda, S., and Earnshaw, W.C. (2003). Sister chromatid cohesion and genome stability in vertebrate cells. Biochem Soc Trans *31*, 263-265.

Mulder, A.M., Glavis-Bloom, A., Moores, C.A., Wagenbach, M., Carragher, B., Wordeman, L., and Milligan, R.A. (2009). A new model for binding of kinesin 13 to curved microtubule protofilaments. J Cell Biol *185*, 51-57.

Muller, C., Gross, D., Sarli, V., Gartner, M., Giannis, A., Bernhardt, G., and Buschauer, A. (2007). Inhibitors of kinesin Eg5: antiproliferative activity of monastrol analogues against human glioblastoma cells. Cancer Chemother Pharmacol *59*, 157-164.

Murphy, T.D. (2003). Drosophila skpA, a component of SCF ubiquitin ligases, regulates centrosome duplication independently of cyclin E accumulation. J Cell Sci *116*, 2321-2332.

Musacchio, A., and Salmon, E.D. (2007). The spindle-assembly checkpoint in space and time. Nat Rev Mol Cell Biol *8*, 379-393.

Musio, A., Montagna, C., Zambroni, D., Indino, E., Barbieri, O., Citti, L., Villa, A., Ried, T., and Vezzoni, P. (2003). Inhibition of BUB1 results in genomic instability and

anchorage-independent growth of normal human fibroblasts. Cancer Res *63*, 2855-2863.

Mussman, J.G., Horn, H.F., Carroll, P.E., Okuda, M., Tarapore, P., Donehower, L.A., and Fukasawa, K. (2000). Synergistic induction of centrosome hyperamplification by loss of p53 and cyclin E overexpression. Oncogene *19*, 1635-1646.

Nagahara, M., Nishida, N., Iwatsuki, M., Ishimaru, S., Mimori, K., Tanaka, F., Nakagawa, T., Sato, T., Sugihara, K., Hoon, D.S.*, et al.* (2011). Kinesin 18A expression: clinical relevance to colorectal cancer progression. Int J Cancer *129*, 2543-2552.

Nakamura, Y., Takaira, M., Sato, E., Kawano, K., Miyoshi, O., and Niikawa, N. (2003). A tetraploid liveborn neonate: cytogenetic and autopsy findings. Arch Pathol Lab Med *127*, 1612-1614.

Nakayama, K., Nagahama, H., Minamishima, Y.A., Matsumoto, M., Nakamichi, I., Kitagawa, K., Shirane, M., Tsunematsu, R., Tsukiyama, T., Ishida, N.*, et al.* (2000). Targeted disruption of Skp2 results in accumulation of cyclin E and p27(Kip1), polyploidy and centrosome overduplication. Embo J *19*, 2069-2081.

Nguyen, H.G., Makitalo, M., Yang, D., Chinnappan, D., St Hilaire, C., and Ravid, K. (2009). Deregulated Aurora-B induced tetraploidy promotes tumorigenesis. Faseb J *23*, 2741-2748.

Nicklas, R.B., and Ward, S.C. (1994). Elements of error correction in mitosis: microtubule capture, release, and tension. J Cell Biol *126*, 1241-1253.

Nigg, E.A. (2002). Centrosome aberrations: cause or consequence of cancer progression? Nat Rev Cancer *2*, 815-825.

Niikura, Y., Ohta, S., Vandenbeldt, K.J., Abdulle, R., McEwen, B.F., and Kitagawa, K. (2006). 17-AAG, an Hsp90 inhibitor, causes kinetochore defects: a novel mechanism by which 17-AAG inhibits cell proliferation. Oncogene *25*, 4133-4146.

Normand, G., and King, R.W. (2010). Understanding cytokinesis failure. Adv Exp Med Biol *676*, 27-55.

Olaharski, A.J., Sotelo, R., Solorza-Luna, G., Gonsebatt, M.E., Guzman, P., Mohar, A., and Eastmond, D.A. (2006). Tetraploidy and chromosomal instability are early events during cervical carcinogenesis. Carcinogenesis *27*, 337-343.

Ornitz, D.M., Hammer, R.E., Messing, A., Palmiter, R.D., and Brinster, R.L. (1987). Pancreatic neoplasia induced by SV40 T-antigen expression in acinar cells of transgenic mice. Science *238*, 188-193.

Oromendia, A.B., Dodgson, S.E., and Amon, A. (2012). Aneuploidy causes proteotoxic stress in yeast. Genes Dev *26*, 2696-2708.

Ota, T., Suto, S., Katayama, H., Han, Z.B., Suzuki, F., Maeda, M., Tanino, M., Terada, Y., and Tatsuka, M. (2002). Increased mitotic phosphorylation of histone H3 attributable to AIM-1/Aurora-B overexpression contributes to chromosome number instability. Cancer Res *62*, 5168-5177.

Otto, S.P., and Whitton, J. (2000). Polyploid incidence and evolution. Annu Rev Genet *34*, 401-437.

Pampalona, J., Frias, C., Genesca, A., and Tusell, L. (2012). Progressive telomere dysfunction causes cytokinesis failure and leads to the accumulation of polyploid cells. PLoS Genet *8*, e1002679.

Peris, L., Wagenbach, M., Lafanechere, L., Brocard, J., Moore, A.T., Kozielski, F., Job, D., Wordeman, L., and Andrieux, A. (2009). Motor-dependent microtubule disassembly driven by tubulin tyrosination. J Cell Biol *185*, 1159-1166.

Peters, J.M., and Nishiyama, T. (2012). Sister Chromatid Cohesion. Cold Spring Harb Perspect Biol.

Pfau, S.J., and Amon, A. (2012). Chromosomal instability and aneuploidy in cancer: from yeast to man. EMBO Rep *13*, 515-527.

Pfleghaar, K., Heubes, S., Cox, J., Stemmann, O., and Speicher, M.R. (2005). Securin is not required for chromosomal stability in human cells. PLoS Biol *3*, e416.

Pihan, G.A., Purohit, A., Wallace, J., Knecht, H., Woda, B., Quesenberry, P., and Doxsey, S.J. (1998). Centrosome defects and genetic instability in malignant tumors. Cancer Res *58*, 3974-3985.

Popova, T., Manie, E., Rieunier, G., Caux-Moncoutier, V., Tirapo, C., Dubois, T., Delattre, O., Sigal-Zafrani, B., Bollet, M., Longy, M.*, et al.* (2012). Ploidy and Large-Scale Genomic Instability Consistently Identify Basal-like Breast Carcinomas with BRCA1/2 Inactivation. Cancer Res *72*, 5454-5462.

Putkey, F.R., Cramer, T., Morphew, M.K., Silk, A.D., Johnson, R.S., McIntosh, J.R., and Cleveland, D.W. (2002). Unstable kinetochore-microtubule capture and chromosomal instability following deletion of CENP-E. Dev Cell *3*, 351-365.

Quintyne, N.J., Reing, J.E., Hoffelder, D.R., Gollin, S.M., and Saunders, W.S. (2005). Spindle multipolarity is prevented by centrosomal clustering. Science *307*, 127-129.

Reid, B.J., Barrett, M.T., Galipeau, P.C., Sanchez, C.A., Neshat, K., Cowan, D.S., and Levine, D.S. (1996). Barrett's esophagus: ordering the events that lead to cancer. Eur J Cancer Prev *5 Suppl 2*, 57-65.

Ricke, R.M., Jeganathan, K.B., and van Deursen, J.M. (2011). Bub1 overexpression induces aneuploidy and tumor formation through Aurora B kinase hyperactivation. J Cell Biol *193*, 1049-1064.

Ricke, R.M., van Ree, J.H., and van Deursen, J.M. (2008). Whole chromosome instability and cancer: a complex relationship. Trends Genet *24*, 457-466.

Rieder, C.L., Cole, R.W., Khodjakov, A., and Sluder, G. (1995). The checkpoint delaying anaphase in response to chromosome monoorientation is mediated by an inhibitory signal produced by unattached kinetochores. J Cell Biol *130*, 941-948.

Rieder, C.L., and Maiato, H. (2004). Stuck in division or passing through: what happens when cells cannot satisfy the spindle assembly checkpoint. Dev Cell *7*, 637-651.

Rieder, C.L., Schultz, A., Cole, R., and Sluder, G. (1994). Anaphase onset in vertebrate somatic cells is controlled by a checkpoint that monitors sister kinetochore attachment to the spindle. J Cell Biol *127*, 1301-1310.

Ring, D., Hubble, R., and Kirschner, M. (1982). Mitosis in a cell with multiple centrioles. J Cell Biol *94*, 549-556.

Rischitor, P.E., Konzack, S., and Fischer, R. (2004). The Kip3-like kinesin KipB moves along microtubules and determines spindle position during synchronized mitoses in Aspergillus nidulans hyphae. Eukaryot Cell *3*, 632-645.

Rivlin, N., Brosh, R., Oren, M., and Rotter, V. (2011). Mutations in the p53 Tumor Suppressor Gene: Important Milestones at the Various Steps of Tumorigenesis. Genes Cancer *2*, 466-474.

Roll-Mecak, A., and McNally, F.J. (2010). Microtubule-severing enzymes. Curr Opin Cell Biol *22*, 96-103.

Roll-Mecak, A., and Vale, R.D. (2008). Structural basis of microtubule severing by the hereditary spastic paraplegia protein spastin. Nature *451*, 363-367.

Ruchaud, S., Carmena, M., and Earnshaw, W.C. (2007). Chromosomal passengers: conducting cell division. Nat Rev Mol Cell Biol *8*, 798-812.

Ryan, S.D., Britigan, E.M., Zasadil, L.M., Witte, K., Audhya, A., Roopra, A., and Weaver, B.A. (2012). Up-regulation of the mitotic checkpoint component Mad1 causes chromosomal instability and resistance to microtubule poisons. Proc Natl Acad Sci U S A *109*, E2205-2214.

Salina, D., Enarson, P., Rattner, J.B., and Burke, B. (2003). Nup358 integrates nuclear envelope breakdown with kinetochore assembly. J Cell Biol *162*, 991-1001.

Salisbury, J.L., Whitehead, C.M., Lingle, W.L., and Barrett, S.L. (1999). Centrosomes and cancer. Biol Cell *91*, 451-460.

Sansregret, L., Vadnais, C., Livingstone, J., Kwiatkowski, N., Awan, A., Cadieux, C., Leduy, L., Hallett, M.T., and Nepveu, A. (2011). Cut homeobox 1 causes chromosomal instability by promoting bipolar division after cytokinesis failure. Proc Natl Acad Sci U S A *108*, 1949-1954.

Satge, D., Sommelet, D., Geneix, A., Nishi, M., Malet, P., and Vekemans, M. (1998). A tumor profile in Down syndrome. Am J Med Genet *78*, 207-216.

Saunders, W. (2005). Centrosomal amplification and spindle multipolarity in cancer cells. Semin Cancer Biol *15*, 25-32.

Sawin, K.E., LeGuellec, K., Philippe, M., and Mitchison, T.J. (1992). Mitotic spindle organization by a plus-end-directed microtubule motor. Nature *359*, 540-543.

Saxton, W.M., Stemple, D.L., Leslie, R.J., Salmon, E.D., Zavortink, M., and McIntosh, J.R. (1984). Tubulin dynamics in cultured mammalian cells. J Cell Biol *99*, 2175-2186.

Schvartzman, J.M., Duijf, P.H., Sotillo, R., Coker, C., and Benezra, R. (2011). Mad2 is a critical mediator of the chromosome instability observed upon Rb and p53 pathway inhibition. Cancer Cell *19*, 701-714.

Shackney, S.E., Berg, G., Simon, S.R., Cohen, J., Amina, S., Pommersheim, W., Yakulis, R., Wang, S., Uhl, M., Smith, C.A.*, et al.* (1995). Origins and clinical implications of aneuploidy in early bladder cancer. Cytometry *22*, 307-316.

Shackney, S.E., and Silverman, J.F. (2003). Molecular evolutionary patterns in breast cancer. Adv Anat Pathol *10*, 278-290.

Shackney, S.E., Smith, C.A., Miller, B.W., Burholt, D.R., Murtha, K., Giles, H.R., Ketterer, D.M., and Pollice, A.A. (1989). Model for the genetic evolution of human solid tumors. Cancer Res *49*, 3344-3354.

Shah, J.V., Botvinick, E., Bonday, Z., Furnari, F., Berns, M., and Cleveland, D.W. (2004). Dynamics of centromere and kinetochore proteins; implications for checkpoint signaling and silencing. Curr Biol *14*, 942-952.

Sharp, D.J., Rogers, G.C., and Scholey, J.M. (2000). Microtubule motors in mitosis. Nature *407*, 41-47.

Sheltzer, J.M., Blank, H.M., Pfau, S.J., Tange, Y., George, B.M., Humpton, T.J., Brito, I.L., Hiraoka, Y., Niwa, O., and Amon, A. (2011). Aneuploidy drives genomic instability in yeast. Science *333*, 1026-1030.

Sheltzer, J.M., Torres, E.M., Dunham, M.J., and Amon, A. (2012). Transcriptional consequences of aneuploidy. Proc Natl Acad Sci U S A *109*, 12644-12649.

Shen, K.C., Heng, H., Wang, Y., Lu, S., Liu, G., Deng, C.X., Brooks, S.C., and Wang, Y.A. (2005). ATM and p21 cooperate to suppress aneuploidy and subsequent tumor development. Cancer Res *65*, 8747-8753.

Shepard, J.L., Amatruda, J.F., Finkelstein, D., Ziai, J., Finley, K.R., Stern, H.M., Chiang, K., Hersey, C., Barut, B., Freeman, J.L.*, et al.* (2007). A mutation in separase causes genome instability and increased susceptibility to epithelial cancer. Genes Dev *21*, 55-59.

Shi, Q., and King, R.W. (2005). Chromosome nondisjunction yields tetraploid rather than aneuploid cells in human cell lines. Nature *437*, 1038-1042.

Shin, H.J., Baek, K.H., Jeon, A.H., Park, M.T., Lee, S.J., Kang, C.M., Lee, H.S., Yoo, S.H., Chung, D.H., Sung, Y.C.*, et al.* (2003). Dual roles of human BubR1, a mitotic checkpoint kinase, in the monitoring of chromosomal instability. Cancer Cell *4*, 483-497.

Shrestha, S., Wilmeth, L.J., Eyer, J., and Shuster, C.B. (2012). PRC1 controls spindle polarization and recruitment of cytokinetic factors during monopolar cytokinesis. Mol Biol Cell *23*, 1196-1207.

Silkworth, W.T., Nardi, I.K., Scholl, L.M., and Cimini, D. (2009). Multipolar spindle pole coalescence is a major source of kinetochore mis-attachment and chromosome mis-segregation in cancer cells. PLoS One *4*, e6564.

Smith, S.L., Bowers, N.L., Betticher, D.C., Gautschi, O., Ratschiller, D., Hoban, P.R., Booton, R., Santibanez-Koref, M.F., and Heighway, J. (2005). Overexpression of aurora B kinase (AURKB) in primary non-small cell lung carcinoma is frequent, generally driven from one allele, and correlates with the level of genetic instability. Br J Cancer *93*, 719-729.

Sofueva, S., Osman, F., Lorenz, A., Steinacher, R., Castagnetti, S., Ledesma, J., and Whitby, M.C. (2011). Ultrafine anaphase bridges, broken DNA and illegitimate recombination induced by a replication fork barrier. Nucleic Acids Res *39*, 6568-6584.

Solomon, D.A., Kim, T., Diaz-Martinez, L.A., Fair, J., Elkahloun, A.G., Harris, B.T., Toretsky, J.A., Rosenberg, S.A., Shukla, N., Ladanyi, M.*, et al.* (2011). Mutational inactivation of STAG2 causes aneuploidy in human cancer. Science *333*, 1039-1043.

Sonoda, E., Matsusaka, T., Morrison, C., Vagnarelli, P., Hoshi, O., Ushiki, T., Nojima, K., Fukagawa, T., Waizenegger, I.C., Peters, J.M., *et al.* (2001). Scc1/Rad21/Mcd1 is required for sister chromatid cohesion and kinetochore function in vertebrate cells. Dev Cell *1*, 759-770.

Sotillo, R., Hernando, E., Diaz-Rodriguez, E., Teruya-Feldstein, J., Cordon-Cardo, C., Lowe, S.W., and Benezra, R. (2007). Mad2 overexpression promotes aneuploidy and tumorigenesis in mice. Cancer Cell *11*, 9-23.

Spruck, C.H., Won, K.A., and Reed, S.I. (1999). Deregulated cyclin E induces chromosome instability. Nature *401*, 297-300.

Stefanova, I., Jenderny, J., Kaminsky, E., Mannhardt, A., Meinecke, P., Grozdanova, L., and Gillessen-Kaesbach, G. (2010). Mosaic and complete tetraploidy in live-born infants: two new patients and review of the literature. Clin Dysmorphol *19*, 123-127.

Stingele, S., Stoehr, G., Peplowska, K., Cox, J., Mann, M., and Storchova, Z. (2012). Global analysis of genome, transcriptome and proteome reveals the response to aneuploidy in human cells. Mol Syst Biol *8*, 608.

Storchova, Z., Breneman, A., Cande, J., Dunn, J., Burbank, K., O'Toole, E., and Pellman, D. (2006). Genome-wide genetic analysis of polyploidy in yeast. Nature *443*, 541-547.

Storchova, Z., and Kuffer, C. (2008). The consequences of tetraploidy and aneuploidy. J Cell Sci *121*, 3859-3866.

Storchova, Z., and Pellman, D. (2004). From polyploidy to aneuploidy, genome instability and cancer. Nat Rev Mol Cell Biol *5*, 45-54.

Straight, A.F., and Field, C.M. (2000). Microtubules, membranes and cytokinesis. Curr Biol *10*, R760-770.

Straight, A.F., Sedat, J.W., and Murray, A.W. (1998). Time-lapse microscopy reveals unique roles for kinesins during anaphase in budding yeast. J Cell Biol *143*, 687-694.

Stumpff, J., Du, Y., English, C.A., Maliga, Z., Wagenbach, M., Asbury, C.L., Wordeman, L., and Ohi, R. (2011). A tethering mechanism controls the processivity and kinetochore-microtubule plus-end enrichment of the kinesin-8 Kif18A. Mol Cell *43*, 764-775.

Stumpff, J., von Dassow, G., Wagenbach, M., Asbury, C., and Wordeman, L. (2008). The kinesin-8 motor Kif18A suppresses kinetochore movements to control mitotic chromosome alignment. Dev Cell *14*, 252-262.

Stumpff, J., Wagenbach, M., Franck, A., Asbury, C.L., and Wordeman, L. (2012). Kif18A and chromokinesins confine centromere movements via microtubule growth suppression and spatial control of kinetochore tension. Dev Cell *22*, 1017-1029.

Su, X., Ohi, R., and Pellman, D. (2012). Move in for the kill: motile microtubule regulators. Trends Cell Biol *22*, 567-575.

Su, X., Qiu, W., Gupta, M.L., Jr., Pereira-Leal, J.B., Reck-Peterson, S.L., and Pellman, D. (2011). Mechanisms underlying the dual-mode regulation of microtubule dynamics by Kip3/kinesin-8. Mol Cell *43*, 751-763.

Tanaka, K., Mukae, N., Dewar, H., van Breugel, M., James, E.K., Prescott, A.R., Antony, C., and Tanaka, T.U. (2005). Molecular mechanisms of kinetochore capture by spindle microtubules. Nature *434*, 987-994.

Tanaka, T., Fuchs, J., Loidl, J., and Nasmyth, K. (2000). Cohesin ensures bipolar attachment of microtubules to sister centromeres and resists their precocious separation. Nat Cell Biol *2*, 492-499.

Tanaka, T., Mori, H., Takahashi, M., and Williams, G.M. (1984). DNA content of hyperplastic and neoplastic acinar cell lesions in rat and human pancreas. J Exp Pathol *1*, 315-326.

Tanenbaum, M.E., Macurek, L., Janssen, A., Geers, E.F., Alvarez-Fernandez, M., and Medema, R.H. (2009). Kif15 cooperates with eg5 to promote bipolar spindle assembly. Curr Biol *19*, 1703-1711.

Tedeschi, A., Ciciarello, M., Mangiacasale, R., Roscioli, E., Rensen, W.M., and Lavia, P. (2007). RANBP1 localizes a subset of mitotic regulatory factors on spindle microtubules and regulates chromosome segregation in human cells. J Cell Sci *120*, 3748-3761.

Teh, M.T., Gemenetzidis, E., Chaplin, T., Young, B.D., and Philpott, M.P. (2010). Upregulation of FOXM1 induces genomic instability in human epidermal keratinocytes. Mol Cancer *9*, 45.

Thompson, S.L., Bakhoum, S.F., and Compton, D.A. (2010). Mechanisms of chromosomal instability. Curr Biol *20*, R285-295.

Thompson, S.L., and Compton, D.A. (2008). Examining the link between chromosomal instability and aneuploidy in human cells. J Cell Biol *180*, 665-672.

Thompson, S.L., and Compton, D.A. (2010). Proliferation of aneuploid human cells is limited by a p53-dependent mechanism. J Cell Biol *188*, 369-381.

Thompson, S.L., and Compton, D.A. (2011). Chromosome missegregation in human cells arises through specific types of kinetochore-microtubule attachment errors. Proc Natl Acad Sci U S A *108*, 17974-17978.

Tighe, A., Johnson, V.L., Albertella, M., and Taylor, S.S. (2001). Aneuploid colon cancer cells have a robust spindle checkpoint. EMBO Rep *2*, 609-614.

Tirnauer, J.S., Canman, J.C., Salmon, E.D., and Mitchison, T.J. (2002). EB1 targets to kinetochores with attached, polymerizing microtubules. Mol Biol Cell *13*, 4308-4316.

Uetake, Y., and Sluder, G. (2004). Cell cycle progression after cleavage failure: mammalian somatic cells do not possess a "tetraploidy checkpoint". J Cell Biol *165*, 609-615.

Vader, G., Medema, R.H., and Lens, S.M. (2006). The chromosomal passenger complex: guiding Aurora-B through mitosis. J Cell Biol *173*, 833-837.

Van de Peer, Y., Maere, S., and Meyer, A. (2009). The evolutionary significance of ancient genome duplications. Nat Rev Genet *10*, 725-732.

van Steensel, B., Smogorzewska, A., and de Lange, T. (1998). TRF2 protects human telomeres from end-to-end fusions. Cell *92*, 401-413.

Vanneste, D., Takagi, M., Imamoto, N., and Vernos, I. (2009). The role of Hklp2 in the stabilization and maintenance of spindle bipolarity. Curr Biol *19*, 1712-1717.

Varga, V., Leduc, C., Bormuth, V., Diez, S., and Howard, J. (2009). Kinesin-8 motors act cooperatively to mediate length-dependent microtubule depolymerization. Cell *138*, 1174-1183.

Varley, J.M. (2003). Germline TP53 mutations and Li-Fraumeni syndrome. Hum Mutat *21*, 313-320.

Vasquez, R.J., Howell, B., Yvon, A.M., Wadsworth, P., and Cassimeris, L. (1997). Nanomolar concentrations of nocodazole alter microtubule dynamic instability in vivo and in vitro. Mol Biol Cell *8*, 973-985.

Vischioni, B., Oudejans, J.J., Vos, W., Rodriguez, J.A., and Giaccone, G. (2006). Frequent overexpression of aurora B kinase, a novel drug target, in non-small cell lung carcinoma patients. Mol Cancer Ther *5*, 2905-2913.

Vitale, I., Senovilla, L., Galluzzi, L., Criollo, A., Vivet, S., Castedo, M., and Kroemer, G. (2008). Chk1 inhibition activates p53 through p38 MAPK in tetraploid cancer cells. Cell Cycle *7*, 1956-1961.

Vitale, I., Senovilla, L., Jemaa, M., Michaud, M., Galluzzi, L., Kepp, O., Nanty, L., Criollo, A., Rello-Varona, S., Manic, G.*, et al.* (2010). Multipolar mitosis of tetraploid cells: inhibition by p53 and dependency on Mos. Embo J *29*, 1272-1284.

Wade, M., and Wahl, G.M. (2009). Targeting Mdm2 and Mdmx in cancer therapy: better living through medicinal chemistry? Mol Cancer Res *7*, 1-11.

Walther, A., Houlston, R., and Tomlinson, I. (2008). Association between chromosomal instability and prognosis in colorectal cancer: a meta-analysis. Gut *57*, 941-950.

Wang, L.H., Schwarzbraun, T., Speicher, M.R., and Nigg, E.A. (2008a). Persistence of DNA threads in human anaphase cells suggests late completion of sister chromatid decatenation. Chromosoma *117*, 123-135.

Wang, P., Greiner, T.C., Lushnikova, T., and Eischen, C.M. (2006). Decreased Mdm2 expression inhibits tumor development induced by loss of ARF. Oncogene *25*, 3708-3718.

Wang, P., Lushnikova, T., Odvody, J., Greiner, T.C., Jones, S.N., and Eischen, C.M. (2008b). Elevated Mdm2 expression induces chromosomal instability and confers a survival and growth advantage to B cells. Oncogene *27*, 1590-1598.

Watanabe, T., Kobunai, T., Yamamoto, Y., Matsuda, K., Ishihara, S., Nozawa, K., Yamada, H., Hayama, T., Inoue, E., Tamura, J.*, et al.* (2012). Chromosomal instability (CIN) phenotype, CIN high or CIN low, predicts survival for colorectal cancer. J Clin Oncol *30*, 2256-2264.

Weaver, B.A., and Cleveland, D.W. (2005). Decoding the links between mitosis, cancer, and chemotherapy: The mitotic checkpoint, adaptation, and cell death. Cancer Cell *8*, 7-12.

Welburn, J.P., Vleugel, M., Liu, D., Yates, J.R., 3rd, Lampson, M.A., Fukagawa, T., and Cheeseman, I.M. (2010). Aurora B phosphorylates spatially distinct targets to differentially regulate the kinetochore-microtubule interface. Mol Cell *38*, 383-392.

West, R.R., Malmstrom, T., Troxell, C.L., and McIntosh, J.R. (2001). Two related kinesins, klp5+ and klp6+, foster microtubule disassembly and are required for meiosis in fission yeast. Mol Biol Cell *12*, 3919-3932.

Williams, B.R., Prabhu, V.R., Hunter, K.E., Glazier, C.M., Whittaker, C.A., Housman, D.E., and Amon, A. (2008). Aneuploidy affects proliferation and spontaneous immortalization in mammalian cells. Science *322*, 703-709.

Willmarth, N.E., Albertson, D.G., and Ethier, S.P. (2004). Chromosomal instability and lack of cyclin E regulation in hCdc4 mutant human breast cancer cells. Breast Cancer Res *6*, R531-539.

Wirth, K.G., Wutz, G., Kudo, N.R., Desdouets, C., Zetterberg, A., Taghybeeglu, S., Seznec, J., Ducos, G.M., Ricci, R., Firnberg, N.*, et al.* (2006). Separase: a universal trigger for sister chromatid disjunction but not chromosome cycle progression. J Cell Biol *172*, 847-860.

Wong, C., and Stearns, T. (2005). Mammalian cells lack checkpoints for tetraploidy, aberrant centrosome number, and cytokinesis failure. BMC Cell Biol *6*, 6.

Wordeman, L. (2005). Microtubule-depolymerizing kinesins. Curr Opin Cell Biol *17*, 82-88.

Wordeman, L., Wagenbach, M., and von Dassow, G. (2007). MCAK facilitates chromosome movement by promoting kinetochore microtubule turnover. J Cell Biol *179*, 869-879.

Xu, J., Wang, M., Gao, X., Hu, B., Du, Y., Zhou, J., Tian, X., and Huang, X. (2011). Separase phosphosite mutation leads to genome instability and primordial germ cell depletion during oogenesis. PLoS One *6*, e18763.

Yamada, H.Y., Yao, Y., Wang, X., Zhang, Y., Huang, Y., Dai, W., and Rao, C.V. (2012). Haploinsufficiency of SGO1 results in deregulated centrosome dynamics, enhanced chromosomal instability and colon tumorigenesis. Cell Cycle *11*, 479-488.

Yang, Z., Loncarek, J., Khodjakov, A., and Rieder, C.L. (2008). Extra centrosomes and/or chromosomes prolong mitosis in human cells. Nat Cell Biol *10*, 748-751.

Yoon, D.S., Wersto, R.P., Zhou, W., Chrest, F.J., Garrett, E.S., Kwon, T.K., and Gabrielson, E. (2002). Variable levels of chromosomal instability and mitotic spindle checkpoint defects in breast cancer. Am J Pathol *161*, 391-397.

Yu, Y., and Feng, Y.M. (2010). The role of kinesin family proteins in tumorigenesis and progression: potential biomarkers and molecular targets for cancer therapy. Cancer *116*, 5150-5160.

Zhang, C., Zhu, C., Chen, H., Li, L., Guo, L., Jiang, W., and Lu, S.H. (2010). Kif18A is involved in human breast carcinogenesis. Carcinogenesis *31*, 1676-1684.

Zhang, D., Rogers, G.C., Buster, D.W., and Sharp, D.J. (2007). Three microtubule severing enzymes contribute to the "Pacman-flux" machinery that moves chromosomes. J Cell Biol *177*, 231-242.

Zhang, N., Ge, G., Meyer, R., Sethi, S., Basu, D., Pradhan, S., Zhao, Y.J., Li, X.N., Cai, W.W., El-Naggar, A.K.*, et al.* (2008a). Overexpression of Separase induces aneuploidy and mammary tumorigenesis. Proc Natl Acad Sci U S A *105*, 13033-13038.

Zhang, X., Ems-McClung, S.C., and Walczak, C.E. (2008b). Aurora A phosphorylates MCAK to control ran-dependent spindle bipolarity. Mol Biol Cell *19*, 2752-2765.

Zhu, C., Zhao, J., Bibikova, M., Leverson, J.D., Bossy-Wetzel, E., Fan, J.B., Abraham, R.T., and Jiang, W. (2005). Functional analysis of human microtubule-based motor proteins, the kinesins and dyneins, in mitosis/cytokinesis using RNA interference. Mol Biol Cell *16*, 3187-3199.

Zhu, J., Pavelka, N., Bradford, W.D., Rancati, G., and Li, R. (2012). Karyotypic determinants of chromosome instability in aneuploid budding yeast. PLoS Genet *8*, e1002719.

Abbreviations

APC	adenomatous polyposis coli
aCGH	array comparative genomic hybridization
APC/C	anaphase-promoting complex/cyclosome
ATCC	American type culture collection
ATP	adenosin triphosphate
Bub1	budding uninhibited by benzimidazoles 1
BubR1	budding uninhibited by benzimidazoles-related 1
CDK1	cyclin-dependent kinase 1
cDNA	complementary DNA
CIN	chromosomal instability
CPC	chromosome passenger complex
CREST	calcinosis, Raynaud's syndrome, esophageal dysmotility, sclerodactyly, telangiectasia
DCB	dihydrocytochalasin B
DCD	dihydrocytochalasin D
DMEM	Dulbecco's modified Eagle's medium
DRB	doxorubicin
DSB	double-strand break
dUTP	2’-deoxyuridine 5’-triphosphate
FISH	fluorescent *in situ* hybridization
GAPDH	glyceraldehyde triphosphate dehydrogenase
gDNA	genomic DNA
GDP	guanosin diphosphate
GFP	green fluorescent protein
GTP	guanosin triphosphate
H2B	histone 2B
HCT116	human colon cancer cell line
HPT	HCT116-derived posttetraploid cells
INCENP	inner centromere protein
KHC	kinesin heavy chain
KLC	kinesin light chain
KT	kinetochore
MAD	mitotic arrest-deficient
MAP	microtubule-associated protein
MAP kinase	mitogen-activated protein kinase
mFISH	multicolor FISH
MIN	microsatellite instability
MMEC	murine mammary epithelial cells
MN	micronucleus
MOSEC	mouse ovarian surface epithelial cells
MT	microtubule
NE	nuclear envelope
NEBD	nuclear envelope breakdown
NS	not significant

PI	propidium iodide
PT	posttetraploid cells
PVDF	polyvinylidene difluoride membrane
RNAi	RNA interference
RPE1 hTERT	retinal pigment epithelium cell line
RPT	RPE1-derived posttetraploid cells
SAC	spindle assembly checkpoint
SD	standard deviation
SEM	standard error of mean

Acknowledgements

I would like to thank my Ph.D. thesis supervisor Zuzana Storchova, Ph.D. for allowing me to perform research in her group at the Max Planck Institute of Biochemistry. I am heartfelt grateful for her constant support and guidance, advice, patience and open ear as well as for the excellent working conditions in the lab.

I thank Prof. Dr. Stefan Jentsch for being my official doctoral thesis supervisor and representing my advisor at the thesis defense in the Department of Biology, LMU. I also thank Prof. Dr. Peter Becker for kindly accepting to co-referee my work. I am grateful to Prof. Dr. Barbara Conradt and Prof. Dr. Jürgen Soll for being in my thesis committee and Prof. Dr. Ute Vothknecht and Prof. Dr. Angelika Böttger for careful reading and evaluation of my dissertation.

I wish to thank Chris Kuffer for his genuine interest in my Ph.D. thesis project from the very beginning, the openness to answer questions no matter how busy he was, and immeasurable amount of time invested in our endless scientific and non-scientific discussions. Thanks for sharing with me the challenges of the Ph.D. student life.

I would like to express a deep sense of gratitude to many other people I had a chance to work with. I thank Dr. Silvia Stingele for her willingness to answer all the questions, for sharing both the hardest and fun Ph.D. times with me. I thank Milena Dürrbaum for the tremendous amount of work on mRNA analysis; Dr. Karolina Peplowska and Andreas Wallek for their helpful advices and recommendations in various biochemical and non-biochemical questions; Verena Passerini and Neysan Donnelly for great support at the EMBO meeting in Nice and for useful comments on my writing. Tons of thanks go to Aline Campos Sparr, Susanne Gutmann, Sandra Kurz and Giuliana Lott for excellent technical support for the paper manuscript preparation and making time spent in the lab unique and fun. I thank all members of MCB for their suggestions at the lab meetings, especially, Ivan. Also, I would like to thank Gabriele Stöhr from Mann Department for showing me how to work with Perseus and answering my endless flow of questions on aCGH and mRNA data analysis.

I wish express my gratitude to Dr. Thomas Mayer, Prof. Dr. Holger Bastians, Dr. Mohan Gupta, Dr. Silke Hauf, Dr. Steven Bergink for their helpful advice on my project.

I wish to thank our collaborator Dr. Stefan Müller from the Institute of Human Genetics for a great help with mFISH analysis. As well I would like to thank Dr. Gunnar Schotta and Matthias Hahn from the Department of Medicine, LMU for giving me a great opportunity to participate in the Suv4-20 project and learn more about chromatin organization.

My special appreciation goes to Dr. Jean-Paul Armache who was with me despite all rises and falls, staying my close friend in my best and worst times. Thank you for the support and critical comments on this thesis. I am immensely grateful to Nadja Rodionova for being with me during the bloodiest times of the Ph.D. and for all her advice and care. Thanks a lot to Jenia, Ekaterina, Anastasia, Dmitry, Yuri, Victoria, Sofia, Liza and MPI crowd who always had time to discuss projects with me and at the same time enjoy the life outside of science.

At the very end I would like to express my sincere gratitude to my parents Dr. Natalia Kuznetsova, Dr. Yuri Kuznetsov, my sister Anna and my grandparents. Я выражаю Вам глубочайшую благодарность и сердечную признательность за веру в мои силы, помощь на всех этапах моего профессионального и личного пути, терпение и готовность поддержать в любую минуту. Спасибо Вам за то, что Вы были всегда со мной.

In preparation	**Response to aneuploidy in human cells** Milena Dürrbaum, **Anastasia Yurievna Kuznetsova**, Verena Passerini, Silvia Stingele, Gabriele Stöhr, Zuzana Storchova.
2013	**Abnormal mitosis triggers p53-dependent cell cycle arrest in human tetraploid cells** Christian Kuffer, **Anastasia Yurievna Kuznetsova**, Zuzana Storchova. *Chromosoma*. DOI 10.1007/s00412-013-0414-0.
2013	**Suv4-20h2 mediates chromatin compaction and is essential for cohesin recruitment to heterochromatin** Matthias Hahn*, Silvia Dambacher*, Stanimir Dulev, **Anastasia Yurievna Kuznetsova**, Simon Eck, Stefan Wörz, Dennis Sadic, Maike Schulte, Jan-Philipp Mallm, Andreas Maiser, Lothar Schermelleh, Pierre Debs, Harald von Melchner, Heinrich Leonhardt, Karl Rohr, Karsten Rippe, Zuzana Storchova and Gunnar Schotta. (*equal contribution) *Genes Dev*. DOI: 10.1101/gad.210377.112.
2008	**Reactive oxygen species generated in mitochondria induce fragmentation of the mitochondrial reticulum in HeLa cells** Nepryakhina OK, **Kuznetsova AYu**, Lyamzaev KG, Izyumov DS, Pletjushkina OYu, Chernyak BV, Skulachev VP. *Dokl Biol Sci.* 420 (1): 221-223.